

T H E U N I V E R S I T Y O F M I C H I G A N

COLLEGE OF ENGINEERING  
Department of Nuclear Engineering

Technical Report

ENERGY-DEPENDENT NEUTRON TRANSPORT THEORY  
IN THE FAST DOMAIN

Basil Nicolaenko

Paul F. Zweifel, Project Director

ORA Project 01046

supported by:

NATIONAL SCIENCE FOUNDATION  
GRANT NO. GK-1713  
WASHINGTON, D.C.

administered through:

OFFICE OF RESEARCH ADMINISTRATION      ANN ARBOR

February 1968



## TABLE OF CONTENTS

	Page
LIST OF TABLES	vi
LIST OF FIGURES	vii
ABSTRACT	ix
CHAPTER	
I. INTRODUCTION	1
II. NEUTRON TRANSPORT EQUATION WITH INELASTIC SCATTERING AND WITHOUT REGENERATION	11
2.1. Introduction	11
2.2. Introduction of a Synthetic Inelastic Scattering Kernel	13
2.3. Spectral Study of the Synthetic Inelastic Slowing-Down Operator	18
2.4. Introduction and Properties of a New Energy Transformation	27
2.5. Solution of Full-Space and Half-Space Problems	39
2.5.1. Eigenfunctions and Eigenvalues	39
2.5.2. The Set $\{v_i(\lambda)\}$	40
2.5.3. Completeness Theorems	41
2.5.4. Green's Function and Other Applications	42
III. NEUTRON TRANSPORT EQUATION WITH FISSION AND ISOTROPIC SLOWING-DOWN: A METHOD OF SOLUTION	45
3.1. Introduction	45
3.2. Isotropic Elastic Scattering with Fission: Spectral Study of the Corresponding Energy Transfer Operator	46
3.3. Isotropic Inelastic Scattering with Fission: Spectral Study of the Corresponding Energy Transfer Operator	52
3.4. Solution of the Complete Transport Equation: Decomposition into Two Associated Equations	56
3.5. Analytical Expressions of Solutions for Various Boundary Conditions	62
3.5.1. Full-Space Green's Function	64
3.5.2. Albedo Problem	66
3.5.3. Milne Problem	68
3.5.4. Slab Criticality Problem	69

TABLE OF CONTENTS (Continued)

	Page
IV. NEUTRON TRANSPORT EQUATION WITH FISSION AND ANISOTROPIC SCATTERING	71
4.1. Isotropy Versus Anisotropy	71
4.2. A Method of Solution Using Singular Normal Modes	71
4.3. Incompleteness and Completeness of the Normal Modes	77
4.4. Conclusion	84
4.5. Appendix B. Half-Range Completeness Theorem in the Anisotropic Case	85
V. ASYMPTOTIC BEHAVIOR OF THE SLOWING-DOWN TRANSIENTS	91
5.1. Introduction	91
5.2. Introduction of an Energy-Green's Function	91
5.3. Failure of Classical Methods of Asymptotic Evaluation	97
5.4. Exact $\mathcal{M}$ -Inversion of the Energy-Green's Function	102
5.5. Spatial Asymptotic Component of the Energy-Green's Function	107
5.6. Asymptotic Expression for the Green's Function of the Infinite Multiplying Medium	119
VI. THE APPROACH TO EQUILIBRIUM IN THE FAST EXPONENTIAL EXPERIMENT. APPLICATION TO THE ZPR-IV SYSTEMS	124
6.1. An Experimental Challenge: Is Complete Spectral Equilibrium Attained in the Fast Exponential Experiment	124
6.2. Detailed Data on the Fast Exponential Experiment in ZPR-IV Systems	140
6.3. Adjustment of the Theoretical Model to Experimental Conditions and Data in ZPR-IV Systems	150
6.3.1. Introduction	150
6.3.2. Reduction of the Three-Dimensional Transport Equation to a Single-Dimensional One	153
6.3.3. Adjustment of the Parameters in the Theoretical Formula for the Neutron Distribution	165
6.4. Slowing-Down Transients and the Approach to Equilibrium in ZPR-IV Like Systems: A Numerical Study	172
6.4.1. The Computational Procedure	172
6.4.2. Relative Importance of Spatial Transport Transients and Slowing-Down Transients	176



TABLE OF CONTENTS (Concluded)

	Page
6.4.3. Is Equilibrium Reached in the Exponential ZPR-IV Systems?	182
6.4.4. The Behavior of Slowing-Down Transients in the High-Energy Range	185
6.4.5. The Behavior of Slowing-Down Transients in the Low-Energy Range	187
VII. CONCLUSIONS AND DIRECTIONS OF FURTHER WORK	189
APPENDIX A - TO CHAPTER II. EXTENSIONS OF THEOREMS 2.3.1 AND 2.3.4 TO A FUNCTIONAL SPACE $L'$	196
APPENDIX B. HALF-RANGE COMPLETENESS THEOREM IN THE ANISOTROPIC CASE (Section 4.5 in Chapter IV)	200
APPENDIX C - TO CHAPTER VI. ABOUT THE REDUCTION OF THE THREE-DIMENSIONAL TRANSPORT EQUATION TO A SINGLE-DIMENSIONAL ONE	201
APPENDIX D - TO CHAPTER VI. ON AN IMPROVED THEORETICAL FORMULA FOR THE ASYMPTOTIC ENERGY SPECTRUM	206
APPENDIX E - TO CHAPTER VI. TABLES OF CALCULATED VALUES OF $\rho(x, E)$	211
APPENDIX F. ON A COMPLETENESS THEOREM BY J. R. MIKA AND R. J. BEDNARZ, CONCERNING THE ENERGY-DEPENDENT BOLTZMANN EQUATION	214
REFERENCES	222

## LIST OF TABLES

Table	Page
I. Compositions for Typical ZPR-IV Systems	133
II. Experimental Results and Comparison with a First Set of Theoretical Predictions in ZPR-IV Systems	133
III. Experimental Results and Comparison with a Second Set of Theoretical Predictions in ZPR-IV Systems	134
IV. Measurements Made on Natural Uranium	136
V. Apparent Relaxation Lengths for Different Detectors in Natural U (from Ref. 39)	138
VI. Composition and Experimental Bucklings for the Studied ZPR-IV Systems	148
VII. Experimental Values for the Lateral Bucklings and the Relaxation Length in ZPR-IV Systems	149
VIII. Group Energy Fluxes for the Asymptotic Spectra in ZPR-IV Systems	149
IX. Adjusted Values for the Parameters of the Green's Function	173

## LIST OF FIGURES

Figure	Page
1. Typical shapes for (a) $g(E)$ and (b) $h(E)$ .	21
2. The domain $\Delta$ .	23
3. Domain of integration for the Eq. (2.33).	30
4. The graph of $v = h(E)$ .	33
5. The integration path in Eq. (2.39).	36
6. Domain $D$ and curve $C$ in the $\lambda$ -complex plane.	36
7. The Bromwich contour for $v \leq 1$ .	38
8. The contour $C$ in the $z$ -complex plane.	89
9. Domain of analyticity for the Fourier-transform of $F( x , E)$ in the $K$ -complex plane.	110
10. The Bromwich contour for $F(x, E)$ (Case $x > 0$ ) in the $K$ -complex plane.	111
11. The Bromwich contour $C$ in the complex $P$ -plane.	115
12. Exponential geometries for ZPR-IV.	126
13. Fission ratios in the $x$ -direction.	130
14. Asymptotic spectrum in natural uranium: experimental curve.	136
15. Evolution of the spectrum along the $x$ -axis in the natural $U$ - exponential system.	139
16. Effect of uranium block size on fission ratio.	141
17. Experimental neutron distribution in ZPR-IV systems.	145
18. Bucklings and $U^{235}/U^{238}$ fission ratios versus enrichment and Al concentrates.	151
19. The angles $\theta$ and $\eta$ .	156

LIST OF FIGURES (Concluded)

Figure	Page
20. Asymptotic spectra for ZPR-IV.	166
21. $\rho$ as a function of energy for $x = 5$ m.f.p.	177
22. $\rho$ as a function of distance.	178
23. $\rho$ as a function of distance for system 3 ( $U^{238}/U^{235} = 6.81/1$ ).	181

## ABSTRACT

This thesis presents some aspects of the energy-dependent, static neutron transport equation, using a continuous energy formulation (rather than a multigroup scheme). Emphasis is placed on conditions of interest for the high-energy (fast) domain: both fission, inelastic, and elastic slowing-down kernels are included in the analysis.

As a first step, focusing on inelastic slowing-down problems, a synthetic inelastic scattering kernel is studied: such a synthetic operator is separable, but not degenerate. A new energy-transformation is introduced, the application of which yields a particularly simple expression for the Boltzmann equation with inelastic slowing-down and without regeneration. Exact solutions of the latter equation are found for various boundary conditions, using Case's method of singular normal modes and inversion formulae for the new energy-transformation. Asymptotic expressions are derived.

The main part of this work is centered on the properties of the transport equation with simultaneous fission regeneration and slowing-down, under the assumption of plane symmetry and simple cross-sections laws permissible in the fast domain. One draws the following conclusion: in order to achieve completeness for the normal modes, solutions of the Boltzmann equation with fission and slowing-down, one must consider fundamental space-energy separable modes reflecting the multiplicative process together with "slowing-down transients"; the "slowing-down transients" are solutions of a plain slowing-down equation with no regeneration; they characterize the spatial adjustment of the neutron distribution from the initial high-energy source to the final degraded asymptotic energy spectrum.

The final part of this work is devoted to the confrontation of these theoretical predictions with experimental observations and measurements on fast multiplying media. In many situations (typically, the fast exponential experiment), workers have tried to measure a well-defined space-energy separable asymptotic neutron distribution; however, it has been suspected that an actual equilibrium was not reached. The present work sheds some light on this question, by making a semi-quantitative evaluation of the physical importance of "slowing-down transients" in the approach to equilibrium in fast exponential experiments. The theoretical model is adjusted to experimental conditions and data in ZPR-IV systems (moderately enriched fast exponential assemblies). From the numerical results, one sees the limitations of the validity of asymptotic transport theory (including most multigroup schemes) for insufficiently large and too subcritical experimental systems related to integral experiments on fast dilute multiplying media.



## CHAPTER I

### INTRODUCTION

We deal in this thesis with some aspects of the energy-dependent neutron transport equation, using a continuous energy formulation. Of special interest to us will be the phenomena of inelastic scattering and fission. Now, it is a fact that the energy dependent Boltzmann equation has won a well deserved reputation of difficulty. One can quickly go through a complete review of former works dealing with exact solutions. The mathematical "barrage" will lie in the nonseparability of solutions: usually space, angle, and energy variables are deeply mingled in the exact solutions. To the usual transport effects found in the monokinetic equation will be added in the energy-dependent case the autonomous properties of the energy-transfer operators. Any type of exact solution, however, is welcome, since usual multigroup diffusion codes and multigroup  $S_N$  codes are reasonable for criticality calculations, but miss many spatial-transport and energy-transfer effects influencing the neutron flux shape, which are important for more refined calculations, e.g., temperature coefficients, plutonium buildup, etc.

As a review of previous work, let us first recall that there are two basic methods of solving exactly the monokinetic equation: the spatial Fourier transform (with Wiener-Hopf factorization in half-space problems)<sup>30-31</sup> and Case's method of singular modes (these eigenfunctions being complete for both full- and half-space problems).<sup>33</sup> These two methods can be simultaneously used in energy-dependent extrapolations.

For a long time, solution of the "energy dependent Boltzmann equation" was synonymous with finding exact solutions to the elastic scattering spatial slowing down problem without fission. Very early works<sup>1-5</sup> treated this problem extensively. Noticing that exponentials of the lethargy are just eigenfunctions of the elastic scattering operator, one can make an expansion in terms of these eigenfunctions (in plain words, a Laplace transformation of the lethargy variable) and obtain a set of uncoupled one-speed transport equations--the lethargy transformed variable being no more than a plain parameter. Earlier works<sup>1-5</sup> then used a further spatial Fourier transform. Double inversion usually yielded the age-diffusion approximation or solutions of the deep penetration problem. Many more recent works claiming to deal with the "energy dependent transport equation" systematically rediscovered the results of Marshak (1947).<sup>6-9</sup> Very recently,<sup>10-11</sup> using Case's method of expansion instead of a spatial Fourier transform, Pappmehl and MacInerney solved the constant cross-section, elastic slowing-down problem. MacInerney made a very valuable contribution by solving, for the first time, half-space problems in this domain. In general, elastic slowing-down problems (with constant cross-sections) are well understood now.

Much more recently tentative efforts have been made to solve the spatial Boltzmann equation with a thermalization operator.<sup>12-21,26-27</sup> A thermalization energy-transfer kernel can be considered as being isotropic<sup>21</sup>; upscattering and detailed balance laws allow it to be symmetrized (self-adjoint). However, as opposed to pulsed experiments theory<sup>32</sup> where crude spatial approximations are connected with refined energy representations, solutions of the complete static transport equation have generally used a syn-



thetic thermalization kernel. Such a synthetic kernel introduced by Corngold et al.,<sup>12</sup> is, in fact, a degenerate projection kernel: the energy distribution of neutrons after scattering is supposed to be completely independent of the energy before scattering. The kernel being very simple (degenerate) one can solve a tremendous variety of problems: half-space (Milne) problems, and practically for the first time, arbitrary variable cross-sections. Mathematically, with such a degenerate kernel, all approaches are possible: Case's method (Mika and Bednarz,<sup>13-14</sup> Stewart et al.<sup>15</sup>) and classical Fourier-Wiener-Hopf methods (Williams,<sup>16-18</sup> Arkuszewski<sup>17</sup>). The same problems with a sum of degenerate kernels are not "exactly" solvable: at best, one can reduce a set of coupled singular integral equations to a single regular Fredholm integral equation.<sup>18,26,27</sup> Also in the thermalization field, but standing somewhat apart, is the work of Ferziger and Leonard.<sup>19,20,26,27</sup> They noticed the symmetrized self-adjoint thermalization operator is, in general, compact, and thus generates a countable and usually complete set of eigenfunctions. Using this set, they make an expansion of the solution and obtain a set of uncoupled monokinetic transport equations, in the case of constant cross-sections. For variable cross-sections things are much more hermetic. Moreover, the exact shape of the eigenfunctions is rarely known.

A third category of "energy dependent transport equations" concerns the multigroup approach.<sup>13,22-25</sup> Then the greatest problem is to solve half-space questions because of the impossibility of finding the Wiener-Hopf factorization of a matrix singular integral operator. Moreover, unpleasant artificial features are introduced in a multigroup formulation: the spectrum of the energy transfer operator, usually including a continuum and a discrete

part, is dislocated into N arbitrary points. Such methods are perhaps adequate for criticality calculations, but are dangerous for the interpretation of integral experiments: in the latter case, a continuous energy formulation, even if quantitatively clumsier, gives a better physical insight. More work is being done presently on the multigroup formulation, using Case's method, at The University of Michigan.

A major limitation of most work done up to now on the energy dependent transport equation lies in the use of constant cross-sections.\* The formidable mathematical difficulty lies in that the spectral properties of the sole energy transfer operator are overshadowed by the variation of the total cross-section. Hence, all attempts to go further yielded sets of coupled Boltzmann equations. Hölte<sup>4,5</sup> solved the elastic-scattering, spatial slowing-down problem, using variable cross-sections and Fourier-Laplace transform methods, and obtained an infinite set of coupled difference equations. Hurwitz and Zweifel obtained numerical solutions of the same problem. Ferziger and Leonard, in the thermalization field<sup>26-27</sup> used an expansion with a set of rather arbitrary energy functions and obtained a set of coupled Boltzmann equations arbitrarily truncated. No decisive results were found in the half-space problems.

So, for some time again, the energy-dependent transport equation with arbitrarily varying cross-sections and realistic energy-transfer kernels, will remain within mathematical "terra incognita."

---

\*Objectively, only the degenerate synthetic kernel allows arbitrary cross-sections.

The present work will deal with conditions of interest for the high-energy (fast) domain. This requires, indeed, that the energy transfer kernels of the equation must be simultaneously the sum of these three operators: inelastic scattering, heavy elastic scattering, and fission. A continuous energy formulation will be systematically used.

It must be emphasized, above all, that each kernel requires separately a special mathematical approach. There is no general method of treating an energy-dependent Boltzmann equation with some a priori arbitrary energy transfer kernel (or a set of arbitrary ones). For, using Case's method of singular normal modes, Bednarz and Mika claimed that they have found a general procedure of solving the energy-dependent transport Eq. (13). But apart from the fact that nothing is proved in the case of half-space, even their full range completeness theorem fails: basically because some energy-transfer scattering kernels are totally unable to generate any regular discrete modes of the transport equation. Yet, one always needs such modes, because of a phenomenon of "scattering of singularities" (as we will prove in detail in Appendix F).

Thus, in our efforts to deal with specific kernels going beyond the classical ones (elastic collision slowing-down and degenerate synthetic thermalization operators), we shall first study extensively the transport equation with a separable slowing-down kernel; for, it can be used as a synthetic kernel to represent inelastic, isotropic slowing-down.<sup>28-29,31</sup> It is of the shape:

$$\begin{aligned}
 K(E \rightarrow E') &= g(E) f(E') && \text{if } E \geq E' \\
 &= 0 && \text{if } E < E' \text{ (slowing-down)}
 \end{aligned}$$

Such a kernel has, in fact, been known for a very long time in neutron physics, since it was introduced by Weisskopf through purely nuclear theoretical considerations, in his evaporation-statistical model. It was fitted for extensive computational purposes, in some cases, by Okrent et al.<sup>28,31</sup> It is now being systematically developed as a synthetic kernel for inelastic scattering on various nuclei by Cadilhac et al.<sup>29</sup> using as well multigroup data and basical nuclear considerations. The primary underlying motivation is that the multigroup inelastic matrices often disguise physical features under a huge amount of numerical data.

Mathematically the energy transfer scattering operator using such a kernel is not a degenerate one, rather it is associated with a first-order differential equation. It is neither a self-adjoint nor a normal operator. Although it is compact, it has indeed a point spectrum reduced to one point at infinity. Hence, there is no hope of making any kind of expansion in terms of a complete set of energy eigenfunctions of the scattering operator.

The second fundamental extension we have made was that of adding a fission operator to the slowing-down one. This is of course basic to a study of neutron balance in a nuclear reactor, especially in a fast reactor. Apart from multigroup cases, it seems, however, that no one has dealt extensively with simultaneous slowing-down and fission in a spatial Boltzmann equation, even though some acknowledged that adding a fission projection operator would destroy the nice spectral properties of the single slowing-down (or thermalization kernel).<sup>32</sup> And yet, from this very fact arises the famous energy-space separability well known in asymptotic diffusion reactor theory.<sup>34</sup> In transport theory too, we have under some conditions, the co-existence of energy-

space separable modes and nonseparable slowing-down transient modes. Physically, this separability comes naturally from the neutron fission regeneration.

The practical underlying motivation for all of these tentative theoretical extensions lies in the desire for a better understanding of neutron integral experiments. We have enough sufficiently sophisticated codes for critical calculations, but in neutron integral experiments, spatial-transport effects and energy-transfer continuous transients often take an overwhelming importance beyond the reach of classical "critical" computational devices. Apart from pulsed experiments, let us recall the tentative measurements of a diffusion length in uranium assemblies. There, experimentalists could measure a well-defined asymptotic, space-energy separable, distribution, only unusually far away from the source,<sup>35-42</sup> and many acknowledged honestly that they were not sure whether or not they had actually reached an asymptotic distribution.

Facing these experimental problems in the fast domain, it is understandable that the constant cross-sections approximation, found throughout our work, is permissible in the fast domain (above 0.1 MeV). In the fast domain, cross-sections vary smoothly, and in the ratio of 2:1. Physically it is obvious that in these experimental conditions, the most salient features are due to spatial and energy transfer phenomena, and not to smoothly varying probabilities of interaction.

All of these mathematical, physical, and practical considerations explain the trend of our thesis. Chapter II will deal with the transport equation with separable inelastic slowing-down kernel and no fission. We will use an

unexpected energy transformation to reduce the Boltzmann equation to a plain, pseudo-monokinetic one. This energy transformation is basically different from previous Laplace and Mellin transforms of the classical elastic scattering folklore.<sup>1-11</sup> Then we solve this associated transport equation using Case's classical method of singular normal modes, covering the whole range of full-space and half-space problems.

Chapter III will cover the transport equation with, simultaneously, a separable inelastic slowing-down kernel, heavy elastic (isotropic) scattering, and fission. The key method is decomposition into two associated transport equations, the first with complete space-energy separability, the second with slowing-down transients. Again Case's method of singular eigenfunctions allows solution of full- and half-space problems. It is of interest to note that slowing-down transients vanish in the criticality problem and the Milne problem, but are present in the full- and half-space Green's functions.

In Chapter IV, we show that most of these results hold if we consider fission simultaneously with anisotropic scattering and slowing-down. We will treat the transport equation with fission and elastic scattering slowing-down, the anisotropic components of which will be represented by synthetic Greuling-Goertzel kernels. We will no longer find a plain decomposition into two associated transport equations; but the complete solution will again be the sum of two components: one including space-energy separable regular modes, the other being a combination of nonseparable plain slowing-down transients. However, no further detailed calculations have been pursued on this case, since we are basically interested in fast media above 0.1 MeV.

Chapter V will deal with a question very important for practical purposes, yet remarkably difficult mathematically. We found previously the Green's function for (separable) inelastic slowing-down, plus heavy elastic scattering. We will have to use this Green's function to study closely the energy transients of exponential experiments in uranium assemblies. This Green's function has been obtained through an energy transformation. As usual the analytical expression for the inverse transform is intractable and one has to find an asymptotic expression. The classical asymptotic methods (residue at the first pole, saddle-point methods) turn out to be useless. In Chapter V we succeeded in finding out an asymptotic expression valid for large distances.

Chapter VI deals with qualitative and partially quantitative interpretation of the exponential experiment in uranium assemblies (tentative measurements of an asymptotic diffusion length). There has been a tremendous amount of experimental work done on this<sup>35-42</sup> with very little sound theoretical interpretation<sup>35</sup> (this one being a multigroup approach with all of the artificial features introduced by a discontinuous energy formulation). It seemed to us that such an integral experiment was best fitted to point out the physical interest of the few mathematical solutions we found. Experimentally, workers have tried to measure a diffusion length associated with an hypothetical space-energy separable asymptotic mode. This mode was found to dominate only at distances unusually far from the source. It was also firmly established that, in very subcritical systems, at distances of roughly ten mean

free paths, nonseparable modes were dominating, hence the physical introduction of slowing-down transients. Let us recall that all multigroup formulations with  $N$  groups yield  $N$  diffusion lengths (or  $N$  discrete modes), while physically there will be conservation of only one energy-space separable discrete mode with coalescence of the  $N-1$  further artificial multigroup modes into a group of continuous slowing-down transients.

So we have tried to make a partially quantitative study of the relative importance of the equilibrium asymptotic spectrum and the slowing-down transients in the exponential experiment in uranium assemblies. Of course, many other applications in the fast domain are possible.

It is hoped that all of this work can be extended to smoothly varying cross-sections. But then, one has to give up the hope of finding "exact" solutions and rather finish with Fredholm regular integral equations easily amenable to computation.<sup>18,26-27</sup>

However, the purpose of this work is not to find a universal "panacea" for the energy dependent Boltzmann equation, but to point out a few specific transport effects which appear physically in neutron energy transfer phenomena. The most interesting conclusion concerns the validity of space-energy separability which too often is the starting point of too many theories.



## CHAPTER II

### NEUTRON TRANSPORT EQUATION WITH INELASTIC SCATTERING AND WITHOUT REGENERATION

#### 2.1. INTRODUCTION

As we saw in the review of previous works, very extensive solutions have been proposed to the problem of spatial neutron slowing-down with elastic scattering.<sup>1-11</sup>

Yet, little attention has been paid to the fast domain where inelastic scattering is overwhelmingly dominant, especially for heavy nuclei. Up to now, any calculations involving inelastic scattering have used the multigroup formulation; strictly no attempts have been made to introduce a continuous energy variable formulation in solving exactly inelastic slowing-down transport problems. Yet, the necessity for a continuous energy variable has been widely recognized in the thermalization and elastic slowing-down fields. Though multigroup schemes can be appropriate for criticality calculations, a continuous energy formulation is still badly needed for the interpretation of any kind of integral experiments (pulsed, exponential, modulated).

Recent research on neutron pulsed, and wave experiments have proved the primary physical importance of the continuous spectrum of an energy transfer operator.<sup>31,32</sup> Previously, the starting point of too many theories was the existence of some complete set of discrete (regular) eigenfunctions. Corngold<sup>32</sup> was the first to prove that, under some conditions, discrete time eigenvalues (for a pulsed experiment) and discrete space eigenvalues (for an exponential experiment) could all disappear into the continuous spectrum.

It is obvious that any multigroup formulation blurs these physical effects by introducing too many artificial features: for instance, the spectrum of an energy operator which usually includes a continuum and a discrete part, is systematically dislocated into N-discrete eigenvalues in any N-group formulation.

So, a continuous energy formulation is likely to give a much better insight into the physics of an integral experiment. Thus, we are interested in the solutions of the following equation:

$$\begin{aligned} \mu \frac{\partial \psi}{\partial x}(x, \mu, E) + \sum_T(E) \psi(x, \mu, E) &= \frac{1}{2} \int_{-1}^{+1} d\mu' \int_E^{+\infty} \sum_{in}(E') K_{in}(E' \rightarrow E) \psi(x, \mu', E') dE' \\ &+ S(x, \mu, E) \end{aligned} \quad (2.1a)$$

where  $\sum_T(E)$  is the total cross-section;  $\sum_{in}(E)$  the total inelastic scattering cross-section;  $K_{in}(E' \rightarrow E)$  is the energy-transfer operator for inelastic slowing-down;  $S(x, \mu, E)$  the source terms. Inelastic scattering is of course, assumed to be isotropic in the laboratory system—which is very close to physical reality.

A closely associated equation to (2.1a) is:

$$\begin{aligned} \mu \frac{\partial \psi}{\partial x}(x, \mu, E) + \sum_T(E) \psi(x, \mu, E) &= \frac{1}{2} \int_{-1}^{+1} d\mu' \int_E^{\infty} \sum_{in}(E') K_{in}(E' \rightarrow E) \psi(x, \mu', E') dE' \\ &+ \frac{1}{2} \int_{-1}^{+1} \sum_e(E) \psi(x, \mu', E) d\mu' + S(x, \mu, E) \end{aligned} \quad (2.1b)$$

Where  $\sum_e(E)$  is the total elastic cross-section; in this latter equation, elastic scattering is supposed to be isotropic and with a negligible energy transfer, both conditions being verified in the fast domain for a heavy element.

In Section 2.2 we will introduce a synthetic kernel to represent the exact  $K_{in}(E' \rightarrow E)$ —that is, a separable slowing-down kernel inspired from Weisskopf's statistical evaporation model. Since, mathematically, this synthetic operator will be neither a projection nor a degenerate one, Section 2.3 will thoroughly investigate its spectral properties.

Though no actual discrete eigenfunctions will be found, these results will inspire an energy transformation applied to Eq. (2.1a) and (2.1b); this energy transformation will yield an associated monokinetic Boltzmann Equation in terms of the transformed energy variable (Section 2.4). Then, provided an inversion formula is found, all classical full-space and half-space transport problems are solved (Section 2.5).

## 2.2. INTRODUCTION OF A SYNTHETIC INELASTIC SCATTERING KERNEL

The exact shape of  $K_{in}(E' \rightarrow E)$  is poorly known, and as in thermalization theory, one should resort to approximate expressions. In contrast to thermalization,  $K_{in}(E \rightarrow E')$  is neither a self-adjoint, nor a normal operator, nor can it be symmetrized. The reason is of course that:

$$\begin{aligned} K_{in}(E' \rightarrow E) &\neq 0 && \text{if } E' \geq E \\ K_{in}(E' \rightarrow E) &= 0 && \text{if } E' < E \end{aligned} \quad (2.2)$$

that is, there is no upscattering whatsoever. Rigorously, it is not even a compact operator in any Banach  $L_p[0, \infty]$  energy-space, because of the individual quantum excited levels of the compound nucleus; for such an isolated level:

$$K_{in}(E' \rightarrow E) = \delta(E' - (E + \epsilon)) \quad (2.3)$$

where  $\epsilon$  is the energy of the excited level. The Dirac distribution prevents compactness.

So, the simplest approximation is to write:

$$\begin{aligned} K_{in}(E' \rightarrow E) &= f(E') g(E); & E' &\geq E \\ &= 0 & ; & E' < E \end{aligned} \quad (2.4)$$

where  $f(E)$  and  $g(E)$  are a priori arbitrary functions. The synthetic kernel (2.4) was first introduced by Okrent et al.<sup>28,31</sup> in connection with Weisskopf's statistical evaporation model; recently, it was proposed as a synthetic kernel per se, by Cadilhac et al. that is, a kernel adaptable to experimental data or more involved nuclear theory.<sup>29</sup>

Kernel (2.4) has, in fact, only one arbitrary function, namely  $g(E)$ ; this stems from the requirement of the conservation of the total inelastic cross-section:

$$\int_0^{E'} K_{in}(E' \rightarrow E) dE = 1 \quad (2.5a)$$

so

$$f(E') \int_0^{E'} g(E') dE' = 1 \quad (2.5b)$$

and defining

$$h(E) = \frac{1}{f(E)} \quad (2.6)$$

we get:

$$h(E) = \int_0^E g(E') dE' \quad (2.7a)$$

equivalently

$$g(E) = \frac{dh}{dE}(E) \quad (2.7b)$$

Okrent determined  $g(E)$  from Weisskopf's statistical evaporation model.<sup>28,31</sup>

In this model the states of the compound nucleus which are obtained by the absorption of the incident neutron are treated as a statistical assembly and the compound nucleus is assimilated to a Fermi gas. This yields for the microscopic inelastic transfer cross-section  $\sigma(E' \rightarrow E)$ :

$$\sigma(E' \rightarrow E) \approx \sigma_{in}(E') \frac{E}{T^2} e^{-E/T} \quad (2.8a)$$

where  $\sigma_{in}(E')$  is the total inelastic cross-section and  $T$  is the nuclear temperature, measure of the excitation of the product nucleus after the emission of the inelastically scattered neutron.  $T$  is dependent upon the excitation energy  $E' - E$  of the residual nucleus. But in most cases,  $T \ll E'$  and the major part of the spectrum of inelastically scattered neutrons is in the range  $E \ll E'$ . This enables us to make the approximation:

$$T \approx \text{constant} \quad (2.8b)$$

and yields immediately an expression for the synthetic kernel (2.4), using (2.5) - (2.7):

$$\begin{aligned} K_{in}(E' \rightarrow E) &= \frac{E e^{-E/T}}{\int_0^{E'} E e^{-E/T} dE} \quad \text{for } E' \geq E \\ &= 0 \quad \text{for } E' < E \end{aligned} \quad (2.9a)$$

that is:

$$g(E) = E e^{-E/T} \quad (2.9b)$$

$$h(E) = \int_0^E E' e^{-E'/T} dE' \quad (2.9c)$$

Okrent improved this kernel for computational purposes<sup>28,31</sup>:

$$\begin{aligned} K_{in}(E' \rightarrow E) &= \frac{E c(E) e^{-E/T}}{\int_0^{E'} E c(E) e^{-E/T} dE} \quad \text{for } E' \geq E \\ &= 0 \quad \text{for } E' < E \end{aligned} \quad (2.10a)$$

with

$$\begin{aligned} c(E) &= 1 \quad ; \quad E > 0.5 \text{ MeV} \\ &= \frac{15}{E} \quad ; \quad E \leq 0.5 \text{ MeV} \end{aligned} \quad (2.10b)$$

$$T = 1 \text{ MeV} \quad (2.10c)$$

Form (2.10) has been used by M. M. R. Williams in establishing an existence theorem concerning the time-dependent transport equation.<sup>49</sup>

Cadilhac's approach<sup>29</sup> is more general; it consists in keeping  $g(E)$  in Eq. (2.4) an a priori arbitrary (no special mathematical shape), and fitting it so that the approximate operator has the same action as the exact one on a particular reference spectrum  $\Phi_o(E)$ :

$$\int_E^\infty \sum_{in}(E') K_{in}(E' \rightarrow E) \Phi_o(E') dE' = \rho(E) = g(E) \int_E^\infty \frac{\sum_{in}(E') \Phi_o(E') dE'}{h(E')} \quad (2.11a)$$

Then  $h(E)$  and  $g(E)$  can be numerically obtained from the solution of:

$$\rho(E) = \frac{dh}{dE}(E) \int_E^\infty \frac{\sum_{in}(E') \Phi_o(E') dE'}{h(E')} \quad (2.11b)$$

$\rho(E)$  can be computed exactly, either through experimental data, or detailed nuclear theory (work now in progress).

A primary interest of this approach is that static and kinetic parameters of the fast medium are very little sensitive to the choice of a particular reference spectrum  $\Phi_o(E)$ .

This approach will enable us to keep an arbitrary shape for kernel (2.4), and solve Eq. (2.1b) modified as:

$$\begin{aligned} \mu \frac{\partial \psi}{\partial x}(x, \mu, E) + \sum_T(E) \psi(x, \mu, E) &= \frac{g(E)}{2} \int_{-1}^{+1} d\mu' \int_E^\infty \frac{\sum_{in}(E') \psi(x, \mu', E') dE'}{h(E')} \\ &+ \frac{1}{2} \int_{-1}^{+1} d\mu' \sum_e(E) \psi(x, \mu', E) d\mu' + S(x, \mu, E) \end{aligned} \quad (2.12a)$$

It must be stressed that in Eq. (2.12a), the synthetic "separable" inelastic slowing-down kernel is completely different from the degenerate (projection) synthetic kernels used to represent a thermalization operator<sup>12-18</sup>; in the latter case,  $\sum_{th}(E' \rightarrow E)$ , the thermalization energy-transfer cross-section, is approximated by:

$$\sum_{th}(E' \rightarrow E) = \sum_{i,j} a_{ij} \sum^i(E) \sum^j(E') M(E) \quad (2.13a)$$

where  $M(E)$  is a Maxwellian distribution; and the transport thermalization equation

$$\begin{aligned} \mu \frac{\partial \psi}{\partial x}(x, \mu, E) + \Sigma_T(E) \psi(x, \mu, E) \\ = \frac{1}{2} \int_{-1}^{+1} d\mu' \int_0^{\infty} \Sigma_{th}(E' \rightarrow E) \psi(x, \mu', E') dE' + S(x, \mu, E) \end{aligned} \quad (2.13b)$$

becomes:

$$\begin{aligned} \mu \frac{\partial \psi}{\partial x}(x, \mu, E) + \Sigma_T(E) \psi(x, \mu, E) = \frac{M(E)}{2} \int_{-1}^{+1} d\mu' \left\{ \sum_{i,j} \Sigma^i(E) \int_0^{\infty} \Sigma^j(E') \psi(x, \mu, E') dE' \right\} \\ + S(x, \mu, E) \end{aligned} \quad (2.13c)$$

Equation (2.13c) is very different from Eq. (2.12a): in the latter, kernels are not degenerate.

A further step is to assimilate cross-sections to constants in Eq. (2.12a). This is valid for fast media and heavy (fissionable) nuclei, where most cross-sections are slowly varying above the inelastic scattering threshold energy ( $\approx 30$  keV). Then:

$$\begin{aligned} \mu \frac{\partial \psi}{\partial x}(x, \mu, E) + \psi(x, \mu, E) = \frac{c_i}{2} g(E) \int_{-1}^{+1} d\mu' \int_E^{\infty} \frac{\psi(x, \mu', E') dE'}{h(E')} \\ + \frac{c_e}{2} \int_{-1}^{+1} d\mu' \psi(x, \mu', E) + S(x, \mu, E) \end{aligned} \quad (2.12b)$$

where  $c_i$  and  $c_e$  are the number of secondaries associated respectively with the inelastic and elastic scattering.

### 2.3. SPECTRAL STUDY OF THE SYNTHETIC INELASTIC SLOWING-DOWN OPERATOR

In order to solve equations of the kind:

$$\mu \frac{\partial \psi}{\partial x}(x, \mu, E) + \psi(x, \mu, E) = \frac{1}{2} \int_{-1}^{+1} d\mu' \mathcal{O}_E \psi(x, \mu, E') + S(x, \mu, E) \quad (2.14a)$$



where  $\mathcal{O}_E$  is an isotropic energy-transfer kernel (thermalization or slowing-down), a general method consists in studying the spectrum and eigenfunctions of  $\mathcal{O}_E$ : in many cases, one finds a set of eigenfunctions such that:

$$\mathcal{O}_E \phi_K(E) = c(k) \phi_K(E) \quad (2.15)$$

$c(k)$  being the eigenvalue associated with  $\phi_K(E)$ . The set  $\{\phi_K(E)\}$  may be associated with a continuous as well as a discrete spectrum.

Then the next step is to prove the eventual completeness of  $\{\phi_K(E)\}$ , i.e., that functions of physical interest can be expanded as:

$$\psi(x, \mu, E) = \int_D A(x, \mu, k) \phi_K(E) dk \quad (2.16a)$$

$$S(x, \mu, E) = \int_D \mathcal{S}(x, \mu, k) \phi_K(E) dk \quad (2.16b)$$

$D$  being the domain of integration (or discrete summation) for the continuous (or discrete) parameter  $K$ . Then inserting (2.16a) and (2.16b) into Eq. (2.14a) and using (2.15) yields an associated equation for  $A(x, \mu, k)$ :

$$\mu \frac{\partial}{\partial x} A(x, \mu, k) + A(x, \mu, k) = \frac{c(k)}{2} \int_{-1}^{+1} d\mu' A(x, \mu', k) + \mathcal{S}(x, \mu, k) \quad (2.14b)$$

The crux of the method lies in that, Eq. (2.13b) is, in fact, a plain mono-kinetic Boltzmann equation:  $K$  is simply a parameter, and the solutions of (2.14b) are well known.<sup>33</sup> So finally

$$\psi(x, \mu, E) = \int_D A(x, \mu, k) \phi_K(E) dk \quad (2.16a)$$

This method of solving equations of the kind (2.14a) is, of course, very powerful but, the delicate points are the existence and the completeness of  $\{\phi_K(E)\}$  defined by (2.15).

Two classical examples of successful applications of this general method are:

(I) Isotropic elastic slowing down, where, in terms of the lethargy  $u$ -variable,  $\mathcal{O}_u$  is a convolution operator:

$$\mathcal{O}_u \boxtimes \psi(x, \mu, u) = \int_{-\infty}^{+u} g(u-u') \psi(x, \mu, u') du' \quad (2.17)$$

The eigenfunctions  $\phi_K(u)$  form a continuum:

$$\phi_K(u) = e^{iku} \quad (2.18a)$$

such that

$$\mathcal{O}_u \boxtimes \phi_K(u) = \bar{g}(k) e^{iku} \quad (2.18b)$$

where the eigenvalue  $\bar{g}(k)$  is the Fourier transform of  $g(u)$ :

$$g(k) = \int_0^{+\infty} g(u) e^{-iku} du \quad (2.18c)$$

$\{\phi_K(u)\}$  is complete, since

$$\text{Fourier-Laplace inversion formulae} \begin{cases} \psi(x, \mu, u) = \frac{1}{2\pi} \int_{-\infty}^{+\infty} A(x, \mu, k) e^{iku} dk \\ A(x, \mu, k) = \int_{-\infty}^{+\infty} \psi(x, \mu, u) e^{-iku} du \end{cases} \quad (2.18d)$$

This explains the success of the Laplace-Fourier transformation of the lethargy variable widely applied to elastic slowing-down problems. <sup>1-11</sup>

(II) Isotropic thermalization, where the kernel can be symmetrized; then if the kernel can be proved to be compact, a classical property is the existence and completeness of a countable set of discrete (regular) eigenfunctions, the completeness holding for functions belonging to the range of the thermalization operator. This has been used extensively in recent works on thermalization, see the monograph by M.M.R. Williams,<sup>31</sup> and the work of Ferziger<sup>20,26,27</sup> (Static Boltzmann Equation).

So it is quite useful to study the spectral properties of  $\mathcal{O}_E$  defined by:

$$\mathcal{O}_E \psi(x, \mu, E) = g(E) \int_E^{E_0} \frac{\psi(x, \mu, E')}{h(E')} dE' \quad \text{for } E \geq E_T \quad (2.19)$$

where  $g(E)$ ,  $h(E)$  are defined by (2.5)-(2.7).

In general  $g(E)$  is everywhere positive, and so is  $h(E) = \int_0^E g(E') dE'$ .

Typical shapes can be found in Ref. 29 (Fig. 1).

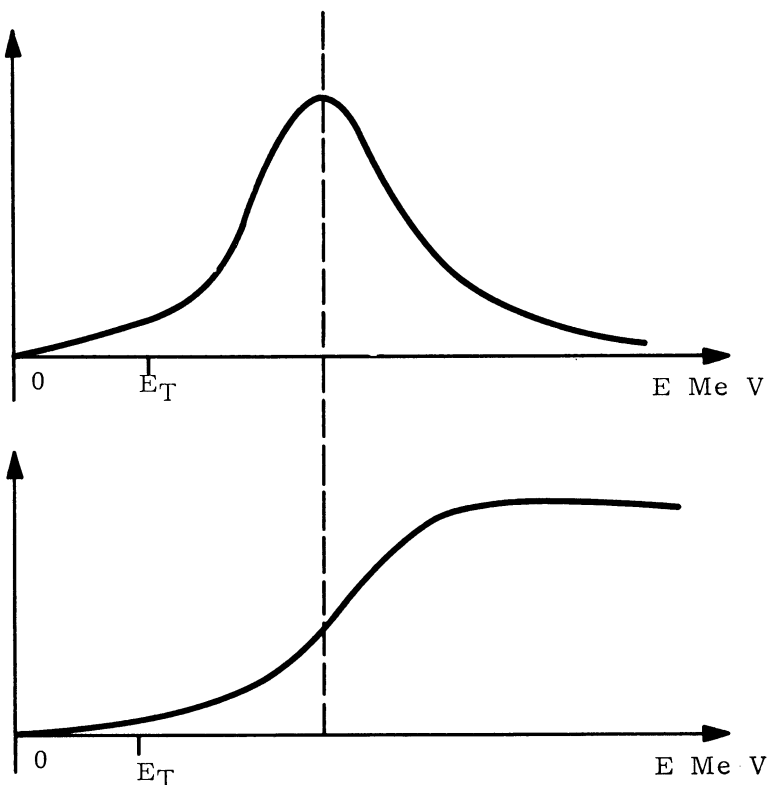


Fig. 1. Typical shapes for (a)  $g(E)$  and (b)  $h(E)$ .

From now on, we restrict ourselves to  $g(E)$  positive everywhere in  $]0, +\infty[$ .

$E_0$  is an upper-energy bound,  $E_T$  is the inelastic threshold energy ( $E_T \approx 30$  keV).

It is important to notice that

$$g(E_T) \neq 0$$

$$h(E_T) \neq 0$$

and

$$h(\infty) = \int_0^{\infty} g(E') dE' < \infty$$

We use the functional energy-space  $C[E_T, E_0]$ , i.e., the Banach space of functions continuous on  $[E_T, E_0]$ . In this space, the norm is defined by:

$$\|\phi\| = \sup \{ |\phi(E)|, E \in [E_T, E_0] \} \quad (2.20)$$

Theorem 2.3.1. As an operator acting in this space,  $\mathcal{O}_E$  is linear and continuous.

Proof: If

$$\Phi(E) = \mathcal{O}_E \phi(E) = g(E) \int_E^{E_0} \frac{\phi(E') dE'}{h(E')}$$

then, obviously

$$\Phi(E) \in C[E_T, E_0]$$

and

$$\|\Phi\| \leq \sup \left\{ |g(E)| \int_E^{E_0} \frac{|\phi(E')|}{|h(E')|} dE' \right\}$$

$$\|\Phi\| \leq \frac{\sup |g(E)|}{\inf |g(E)|} \log \left| \frac{h(E_0)}{h(E_T)} \right| \|\phi\|$$

$$\|\Phi\| \leq M \|\phi\| \quad (\text{since } \inf |g(E)| \neq 0 \text{ for } E \in [E_T, E_0])$$

where  $M$  is some constant, Q.E.D.

Theorem 2.3.2. In  $C[E_T, E_O]$ ,  $\mathcal{O}_E$  is a compact operator.

Proof: Defining  $K_{in}(E' \rightarrow E)$  through Eq. (2.4), we have

$$\iint_{\Delta} dE dE' |K_{in}(E' \rightarrow E)|^2 < \infty$$

in the domain  $\Delta$  defined in Fig. 2:

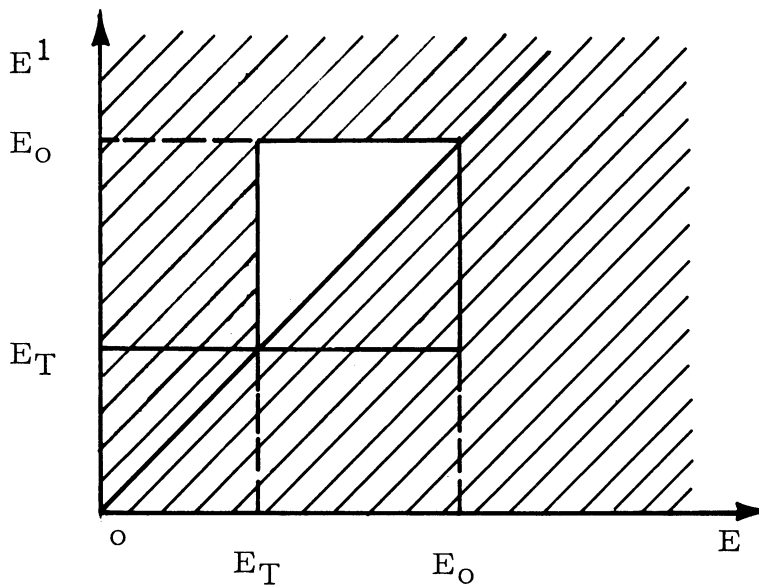


Fig. 2. The domain  $\Delta$ .

From Taylor (p. 276),<sup>43</sup> this is enough to assure the compactness of  $\mathcal{O}_E$  in  $C[E_T, E_O]$ . These theorems lead to:

Theorem 2.3.3. The point-spectrum of  $\mathcal{O}_E$  contains, at most, a countable set of points, and these have no accumulation point, except possibly at  $\infty$ .

Proof: Taylor (p. 281).<sup>43</sup>\* The spectrum being defined as the comple-

\*"Suppose  $T \in [X]$  and  $T$  compact. Then  $P_O(T)$  contains at most a countable set of points, and these have no accumulation point, except possibly at  $\lambda = \infty$ ."

ment of the set  $\{\lambda\}$  such that:  $(I - \lambda \mathcal{O}_E)^{-1}$  exists as an operator and is con-  
tinuous.

Theorem 2.3.3 does not imply that the point spectrum is not empty. Let us look specifically for eigenfunctions of  $\mathcal{O}_E$ ; if  $\lambda$  belongs to the point spectrum:

$$(I - \lambda \mathcal{O}_E) \boxtimes \phi_\lambda(E) = 0 \quad (2.21a)$$

The  $\phi_\lambda(E)$  being the associated eigenfunction—Eq. (2.21a) can be rewritten as:

$$\phi_\lambda(E) - \lambda g(E) \int_E^{E_0} \frac{\phi_\lambda(E') dE'}{h(E')} = 0, \quad \text{for } E \geq E_T \quad (2.21b)$$

Put

$$\psi(E) = \frac{\phi_\lambda(E)}{g(E)} \quad (2.22)$$

And Eq. (2.21b) becomes

$$\psi(E) - \lambda \int_E^{E_0} \frac{g(E')}{h(E')} \psi(E') dE' = 0 \quad (2.21c)$$

We differentiate (2.21c) and obtain:

$$\frac{d\psi}{dE} = -\lambda \frac{g(E)}{h(E)} \psi(E) \quad (2.23a)$$

Keeping in mind Eq. (2.7b), the solution of Eq. (2.23a) is straightforward

$$\psi(E) = K[h(E)]^{-\lambda} \quad (2.23b)$$

where  $K$  is arbitrary, and, from (2.22)

$$\phi_{\lambda}(E) = K g(E) [h(E)]^{-\lambda} \quad (2.23c)$$

But Eq. (2.23a) is not equivalent to the initial Eq. (2.21b), and we must verify that  $\phi_{\lambda}(E) = g(E) h(E)^{-\lambda}$  is indeed a solution of the initial equation.

$$\begin{aligned} \phi_{\lambda}(E) - \lambda g(E) \int_E^{E_0} \frac{\phi_{\lambda}(E') dE'}{h(E')} &= g(E) h(E)^{-\lambda} - \lambda g(E) \int_E^{E_0} g(E') h(E')^{-\lambda-1} dE' \\ &= g(E) h(E)^{-\lambda} + g(E) \left[ h(E)^{-\lambda} \right]_E^{E_0} \\ &= g(E) h(E_0)^{-\lambda} \\ &\neq 0 \end{aligned} \quad (2.24)$$

Since  $h(E_0) \neq 0$  even for  $E_0 \rightarrow \infty$ , Eq. (2.24) expresses that  $g(E) h(E)^{-\lambda}$  is not a solution of Eq. (2.21). This means that the point spectrum is empty—indeed, the result is stronger.

Theorem 2.3.4. The whole spectrum (continuous, point, residual) of  $\mathcal{O}_E$  is empty, except for the point at  $\infty$ .

Proof: Let us show that the operator  $(I - \lambda \mathcal{O}_E)^{-1}$  exists for  $\forall \lambda, \lambda \neq \infty$ .

Given  $S(E)$  arbitrary,  $S(E) \in C[E_T, E_0]$ , the existence of  $(I - \lambda \mathcal{O}_E)^{-1}$  is equivalent to the existence of a solution  $\phi(E) \in C[E_T, E_0]$  to the equation:

$$(I - \lambda \mathcal{O}_E) \boxtimes \phi(E) = S(E) \quad (2.25a)$$

i.e.,

$$\phi(E) - \lambda g(E) \int_E^{E_0} \frac{\phi(E')}{h(E')} dE' = S(E) \quad (2.25b)$$

From result (2.24), we find easily that the solution of the more specialized equation

$$\phi(E) - \lambda g(E) \int_E^{E_0} \frac{\phi(E')}{h(E')} dE' = \delta(E - E_0) \quad (2.25c)$$

is

$$\phi(E) = \delta(E - E_0) + \mathcal{Y}(E_0 - E) \frac{\lambda g(E) h(E)^{-\lambda}}{h(E_0)^{1-\lambda}} \quad (2.26a)$$

$\mathcal{Y}(E - E_0)$  being the Heaviside distribution. From Eqs. (2.25c) and (2.26a), we find the final solution of Eq. (2.25):

$$\phi(E) = S(E) + \lambda g(E) h(E)^{-\lambda} \int_E^{E_0} \frac{S(E')}{h(E')^{1-\lambda}} dE' \quad (2.26b)$$

This means that the operator  $(I - \lambda \mathcal{O}_E)^{-1}$  exists. Then, since  $\mathcal{O}_E$  is compact (Theorem 2.3.2),  $(I - \lambda \mathcal{O}_E)^{-1}$  is continuous (as proved in Taylor\*, p. 281). So,  $\lambda \neq \infty$  belongs to the resolvent set of  $\mathcal{O}_E$ . Since the spectrum of any linear continuous operator is not empty (Taylor\*\*, p. 261), it means that, the spectrum of  $\mathcal{O}_E$  is reduced to  $\lambda = \infty$ , Q.E.D.

Theorem 2.3.4 is also valid if we extend  $E_0$  to  $\infty$ ; but then we must use another functional Banach-space, namely  $L'[E_T, \infty]$  where the norm is defined by:

$$\|\phi\| = \int_{E_T}^{\infty} |\phi(E')| dE' \quad (2.27)$$

---

\* "Suppose  $T \in [X]$ ,  $T$  compact, and  $\lambda \neq 0$ . Then  $(\lambda - T)^{-1}$  is continuous if it exists."

\*\* "If  $T \in [X]$  and  $X$  is a complex Banach space,  $\sigma(T)$  is not empty."



detailed proofs will be found in Appendix A.

In conclusion, we find a rather surprising fact—that is, the spectrum of our synthetic, inelastic kernel is reduced to one single point at  $\infty$ —in plain words, the kernel is too regular though not degenerate! However, it can be easily seen that the nonexistence of discrete eigenfunctions for the synthetic kernel has a precise origin: namely, that  $h(E)$  is bounded for  $E \rightarrow \infty$  (or equivalently, that  $g(E)$  is integrable). For, if  $h(E)$  were not bounded, then  $g(E) \cdot h(E)^{-\lambda}$  would be an actual eigenfunction (see Eq. (2.24)). But physical evidence seems to point out that  $h(E)$  is bounded indeed. This, of course, limits somewhat the validity of the general method we outlined at the beginning of this Section 2.3.

However, let us keep in mind that we have found pseudo-eigenfunctions\* of  $\Theta_E$  namely:

$$\phi_\lambda(E) = g(E) h(E)^{-\lambda}$$

This will be the starting point of a new energy transformation different from the classical Fourier-Laplace-Mellin Transforms, in order to reduce Eq. (2.12b) to a monokinetic one.

#### 2.4. INTRODUCTION AND PROPERTIES OF A NEW ENERGY TRANSFORMATION

The equation of interest is

$$\begin{aligned} \mu \frac{\partial}{\partial x} \psi(x, \mu, E) + \psi(x, \mu, E) &= \frac{c}{2} g(E) \int_{-1}^{+1} d\mu' \int_E^\infty dE' \frac{\psi(x, \mu', E')}{h(E')} \\ &+ \frac{1}{2} \delta(x - x_0) S(E) \end{aligned} \quad (2.28)$$

---

\*In fact, it can be quite easily seen that the operator adjoint to  $\Theta_E$  has the set of eigenfunctions  $\{h(E)^{\lambda-1}\}$ ; this adjoint is a Volterra operator with an unbounded kernel.

(Heavy elastic scattering has been omitted for brevity, since it does not involve an energy change.)

Keeping in mind the existence of pseudo-eigenfunctions  $g(E) \cdot h(E)^{\lambda-1}$  [see (2.23c) and (2.24)], divide both sides of Eq. (2.28) by  $g(E)$ :

$$\begin{aligned} \mu \frac{\partial}{\partial x} \frac{\psi(x, \mu, E)}{g(E)} + \frac{\psi(x, \mu, E)}{g(E)} &= \frac{c}{2} \int_{-1}^{+1} d\mu' \int_E^{\infty} \frac{g(E')}{h(E')} \cdot \frac{\psi(x, \mu', E')}{g(E')} dE' \\ &+ \frac{1}{2} \delta(x - x_0) \frac{S(E)}{g(E)} \end{aligned} \quad (2.29a)$$

Let us introduce the modified functions:

$$\begin{aligned} \Psi(x, \mu, E) &= \frac{\psi(x, \mu, E)}{g(E)} \\ \mathcal{S}(E) &= \frac{S(E)}{g(E)} \end{aligned} \quad (2.30)$$

Then Eq. (2.29a) becomes:

$$\begin{aligned} \mu \frac{\partial}{\partial x} \Psi(x, \mu, E) + \Psi(x, \mu, E) &= \frac{c}{2} \int_{-1}^{+1} d\mu' \int_E^{\infty} \frac{g(E')}{h(E')} \Psi(x, \mu', E') dE' + \frac{\delta(x - x_0)}{2} \mathcal{S}(E) \end{aligned} \quad (2.29b)$$

At this stage, recall that, from Eqs. (2.5) - (2.7):

$$g(E) = 0 \quad \text{for } E = 0$$

$$g(E) \rightarrow 0 \quad \text{for } E \rightarrow +\infty$$

$$h(E) = \int_0^E g(E') dE'$$

$$h(E) = 0 \quad \text{for } E = 0$$

$$h(E) \rightarrow M \quad \text{for } E \rightarrow +\infty$$

Let us introduce the following fundamental energy transformation:

$$\begin{aligned} \bar{\Psi}(x, \mu, \lambda) &= \int_0^{\infty} \Psi(x, \mu, E) g(E) h(E)^{\lambda-1} dE \\ \bar{\mathcal{J}}(\lambda) &= \int_0^{\infty} \mathcal{J}(E) g(E) h(E)^{\lambda-1} dE \end{aligned} \quad (2.31a)$$

or equivalently, from (2.30):

$$\begin{aligned} \bar{\Psi}(x, \mu, \lambda) &= \int_0^{\infty} \Psi(x, \mu, E) h(E)^{\lambda-1} dE \\ \bar{\mathcal{J}}(\lambda) &= \int_0^{\infty} \mathcal{S}(E) h(E)^{\lambda-1} dE \end{aligned} \quad (2.31b)$$

or in a condensed notation:

$$\begin{aligned} \bar{\Psi}(x, \mu, \lambda) &= \mathfrak{M} \Psi(x, \mu, E) \\ \bar{\mathcal{J}}(x, \mu, \lambda) &= \mathfrak{M} \mathcal{J}(E) \end{aligned} \quad (2.31c)$$

from (2.31b), the transformation  $\mathfrak{M}$  always exists provided

$$\begin{aligned} \int_0^{\infty} |\Psi(x, \mu, E)| dE &< \infty \\ \int_0^{\infty} |\mathcal{S}(E)| dE &< \infty \end{aligned} \quad (2.32)$$

which is always verified in practice.

Apply transformation  $\mathfrak{M}$  to Eq. (2.29b), multiplying both sides of this equation by  $g(E) \cdot h(E)^{\lambda-1}$  and integrating over the whole range of energy we obtain

$$\begin{aligned} \mu \frac{\partial \bar{\Psi}}{\partial x}(x, \mu, \lambda) + \bar{\Psi}(x, \mu, \lambda) &= \frac{c_i}{2} \int_{-1}^{+1} d\mu' \int_0^{\infty} dE g(E) h(E)^{\lambda-1} \int_E^{\infty} \frac{g(E')}{h(E')} \Psi(x, \mu, E') dE' \\ &+ \frac{\delta(x - x_0)}{2} \bar{\mathcal{J}}(\lambda) \end{aligned} \quad (2.33)$$

In Eq. (2.33a), let us examine the factor:

$$\begin{aligned} \int_0^{\infty} g(E) h(E)^{\lambda-1} dE \int_E^{\infty} \frac{g(E')}{h(E')} \Psi(x, \mu', E') dE' &= \int_0^{\infty} dE' \frac{g(E')}{h(E')} \Psi(x, \mu', E') \\ &\int_0^{E'} g(E) h(E)^{\lambda-1} dE \end{aligned} \quad (2.34)$$

(by inverting the order of integration over  $E$  and  $E'$  (Fig. 3) .)

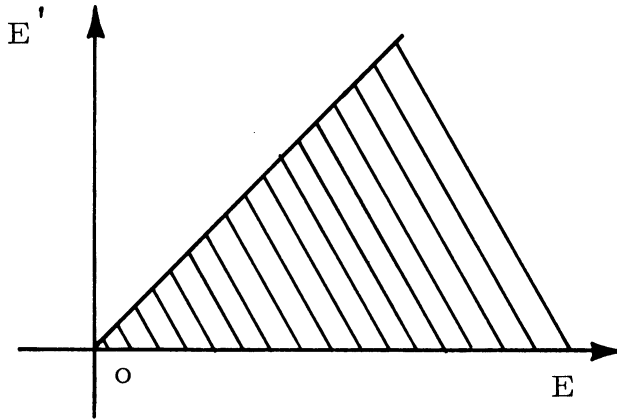


Fig. 3. Domain of integration for the Eq. (2.33).

But,

$$\int_0^{E'} g(E) h(E)^{\lambda-1} dE = \left[ \frac{1}{\lambda} h(E)^{\lambda} \right]_0^{E'} = \frac{1}{\lambda} h(E')^{\lambda}$$

(provided  $\lambda > 0$ ). And (2.34) becomes:

$$\begin{aligned}
 &= \int_0^{\infty} \frac{g(E')}{h(E')} \Psi(x, \mu', E') \frac{1}{\lambda} h(E')^{\lambda} dE' \\
 &= \frac{1}{\lambda} \int_0^{\infty} g(E') h(E')^{\lambda-1} \Psi(x, \mu', E') dE' \\
 &= \frac{1}{\lambda} \bar{\Psi}(x, \mu', \lambda) \tag{2.34}
 \end{aligned}$$

Inserting this result into Eq. (2.33) yields:

$$\mu \frac{\partial}{\partial x} \bar{\Psi}(x, \mu, \lambda) + \bar{\Psi}(x, \mu, \lambda) = \frac{c_i}{2\lambda} \int_{-1}^{+1} d\mu' \bar{\Psi}(x, \mu', \lambda) + \frac{\delta(x - x_0)}{2} \bar{J}(\lambda) \tag{2.35}$$

So, the transformation  $\mathfrak{M}$  applied to the initial transport Eq. (2.29) yields a "monokinetic" transport equation in terms of the transformed distribution:

$$\bar{\Psi}(x, \mu, \lambda) = \mathfrak{M} \boxtimes \Psi(x, \mu, E) = \mathfrak{M} \boxtimes \left( \frac{\Psi(x, \mu, E)}{g(E)} \right),$$

where  $\lambda$  stands as a plain parameter, and the average number of secondaries becomes  $c_i/\lambda$ . Notice objectively, that we obtain a "monokinetic" transformed equation only because we integrated the initial neutron distribution from the energy  $E = 0$  to  $E = \infty$  (see Eq. (2.34)); this implies that the inelastic cross-section is considered constant starting at  $E = 0$ . Physically, it means that we are setting the threshold energy  $E_T$  to zero and neglecting neutrons below the inelastic threshold.

The "monokinetic" equation (2.35) is easily solvable by the classical method of Case,<sup>33</sup> and typical problems will be dealt with in Section 2.5.

However, an important problem is to find an expression for the inverse transform  $\mathcal{M}^{-1}$ . From (2.30) and (2.31), recall that:

$$\begin{aligned}\Psi(x, \mu, E) &= \frac{\psi(x, \mu, E)}{g(E)} \\ \bar{\Psi}(x, \mu, \lambda) &= \mathcal{M} \Psi(x, \mu, E) \\ &= \int_0^\infty g(E) h(E)^{\lambda-1} \Psi(x, \mu, E) dE\end{aligned}$$

First, let us normalize  $h(E)$  according to the source term  $S(E)$ :

$$\begin{aligned}h(E_0) &= 1 \quad \text{if} \quad S(E) = 0 \quad \text{for} \quad E > E_0 \\ h(\infty) &= 1 \quad \text{if} \quad S(E) \text{ covers the whole energy-range.}\end{aligned} \quad (2.36)$$

Normalization (2.36) simply takes into account the fact that the transport equation (2.28) is a down-scattering one, and no neutrons are found above the maximum energy of the source  $S(E)$ .

Then, let us define the following change of variable:

$$v = h(E) \quad (2.37a)$$

Equation (2.37) defines a one-to-one mapping of

$$E \in [0, E_0] \quad \text{onto} \quad v \in [0, 1] \quad ,$$

i.e., to one  $E$  corresponds a unique  $v$ , and to one  $v \in [0, 1]$ , corresponds a unique  $E$ , (Fig. 4), since the Jacobian of the transformation (2.37) is always  $\neq 0$ :

$$\begin{aligned} dh/dE &= g(E) \\ &\neq 0 \quad \text{for } E \in ]0, E_0] \end{aligned} \quad (2.37b)$$

Since we consider  $g(E) \neq 0$  for  $E \in ]0, +\infty[$ .

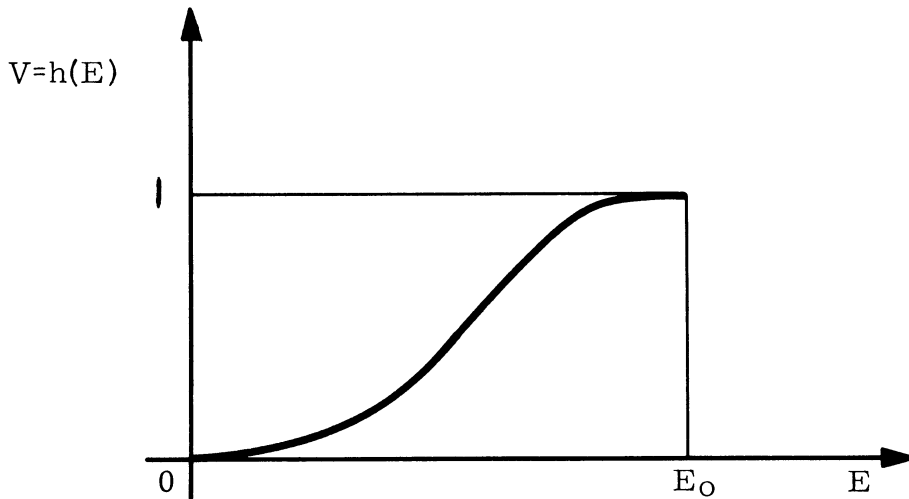


Fig. 4. The graph of  $v = h(E)$ .

Then in terms of the new variable  $v$ , transformation  $\mathfrak{M}$  can be rewritten as

$$\begin{aligned} \bar{\Psi}(x, \mu, \lambda) &= \int_0^{\infty} g(E) h(E)^{\lambda-1} \Psi(x, \mu, E) dE \\ &= \int_0^{E_0} g(E) h(E)^{\lambda-1} \Psi(x, \mu, E) dE \\ &= \int_0^1 \Psi(x, \mu, v) v^{\lambda-1} dv \end{aligned} \quad (2.38a)$$

(where we used  $dv = g(E) dE$ ) and (2.38a) is nothing but a classical Mellin transform in terms of the new variable  $v$ .

Then the inverse transformation is well-known<sup>44</sup>; if

$$\bar{\Psi}(x, \mu, \lambda) = \int_0^1 \Psi(x, \mu, v) v^{+\lambda-1} dv \quad (2.38b)$$

then

$$\Psi(x, \mu, v) = \frac{1}{2\pi i} \int_{c-i\infty}^{c+i\infty} \bar{\Psi}(x, \mu, \lambda) v^{-\lambda} d\lambda \quad (2.39)$$

The symmetry of the formulas (2.38) and (2.39) stems from the fact that a Mellin transform is closely related to Fourier and Laplace transforms<sup>44</sup>:

$$\begin{aligned} \mathfrak{M}\{f(v); \lambda\} &= \int_0^{\infty} f(v) v^{\lambda-1} dv \\ &= \mathfrak{F}\{f(e^v); i\lambda\} \\ &= \mathcal{L}\{f(e^v); -\lambda\} + \mathcal{L}\{f(e^{-v}); +\lambda\} \end{aligned} \quad (2.40)$$

In (2.39), the integration path in the complex  $\lambda$ -plane must be to the right of all  $\lambda$ -singularities of  $\bar{\Psi}(x, \mu, \lambda)$ ; this is realized if

$$\operatorname{Re}(\lambda) \geq 1$$

i.e.,

$$c \geq 1 \quad (2.41a)$$

(This is easily seen from (2.31), (2.32), and (2.38).)

Checking (2.38), the fact that:

$$\Psi(x, \mu, v) \equiv 0 \quad \text{for } v > 1 \quad (\text{from (2.36)}),$$

yields the following strong result:

Theorem 2.4.1.  $\bar{\Psi}(x, \mu, \lambda)$  is uniformly bounded for  $\operatorname{Re} \lambda \geq 1$



Proof:

$$\bar{\Psi}(x, \mu, \lambda) = \int_0^1 \Psi(x, \mu, v) v^{\operatorname{Re}\lambda-1} v^{\operatorname{Im}\lambda} dv$$

$$|\bar{\Psi}(x, \mu, \lambda)| \leq \int_0^1 |\Psi(x, \mu, v)| \cdot |v^{\operatorname{Re}\lambda-1}| dv$$

but

$$\left. \begin{array}{l} 0 \leq v \leq 1 \\ \operatorname{Re}\lambda - 1 \geq 0 \end{array} \right\} \implies |v^{\operatorname{Re}\lambda-1}| \leq 1$$

so

$$|\bar{\Psi}(x, \mu, \lambda)| \leq \int_0^1 |\Psi(x, \mu, v)| dv$$

$$\leq M$$

Q.E.D.

In the inversion formula (2.39), the integration path can be shifted along a Bromwich contour; two possibilities occur, according to  $v > 1$  or  $v \leq 1$ :

Theorem 2.4.2. The inversion formula (2.39) yields an identically null function if  $v > 1$ .

Proof: The integration path defined in Fig. 5 can be extended by a curve  $c$  so as to surround a domain  $D$  where  $\bar{\Psi}(x, \mu, \lambda)$  has no singularities in  $\lambda$  (Fig. 6). Then

$$\oint_D \bar{\Psi}(x, \mu, \lambda) v^{-\lambda} d\lambda \equiv 0$$

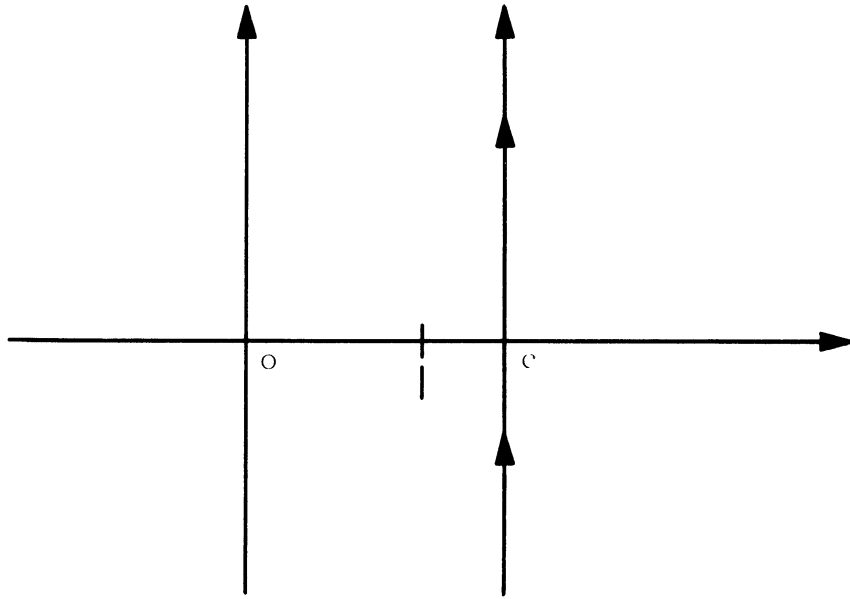


Fig. 5. The integration path in Eq. (2.39).

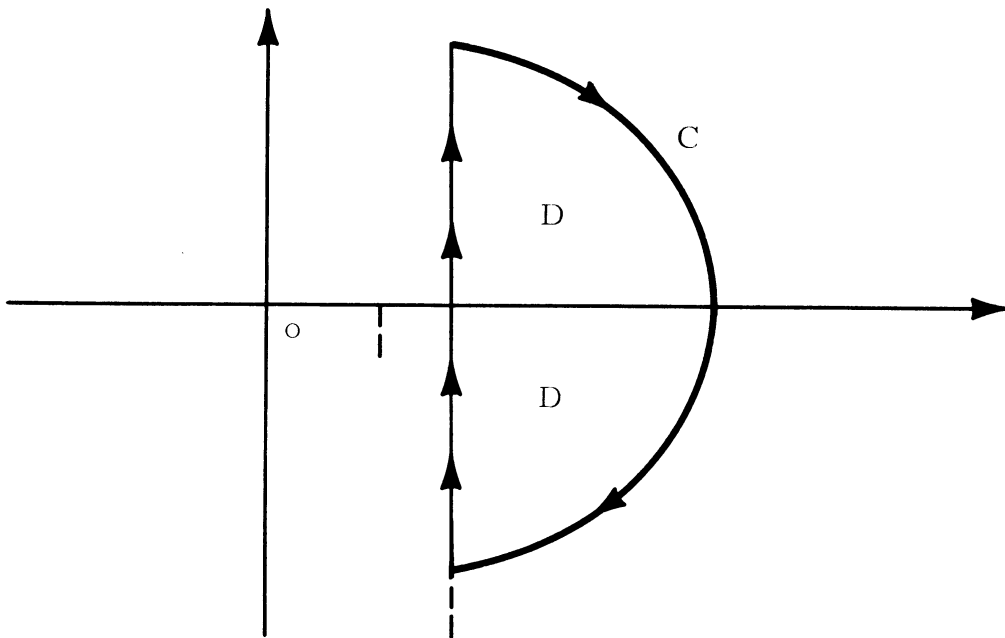


Fig. 6. Domain D and curve C in the  $\lambda$ -complex plane.

But, along C:

$$\left| \int_C \bar{\Psi}(x, \mu, \lambda) v^{-\lambda} d\lambda \right| \leq \int_C \left| \bar{\Psi}(x, \mu, \lambda) \right| \cdot \left| v^{-\lambda} \right| d\lambda$$

Using Theorem 2.4.1:  $|\bar{\Psi}(x, \mu, \lambda)| \leq M$  in the domain D, we get:

$$\left| \int_C \bar{\Psi}(x, \mu, \lambda) d\lambda \right| \leq M \int_C \left| v^{-\lambda} \right| d\lambda$$

However, on C;

$$\left. \begin{array}{l} |v| > 1 \\ \operatorname{Re} \lambda > 1 \end{array} \right\} \Rightarrow |v^{-\lambda}| \rightarrow 0 \quad \text{if } |\lambda| \rightarrow \infty$$

Hence

$$\left| \int_C \bar{\Psi}(x, \mu, \lambda) v^{-\lambda} d\lambda \right| \rightarrow 0 \quad \text{if the curve C is extended to infinity.}$$

So

$$\int_{c-i\infty}^{c+i\infty} \bar{\Psi}(x, \mu, \lambda) v^{-\lambda} d\lambda = 2i\pi \Psi(x, \mu, v)$$

$$= 0$$

Q.E.D.

Theorem 2.4.2 implies that transformation  $\mathfrak{M}$  is coherent with the fact

that:

$$\Psi(x, \mu, v) \equiv 0 \quad \text{for } v > 1 \quad (\text{from (2.36)})$$

If  $v \leq 1$ , the integration path of the inversion formula (2.39) can be shifted along a Bromwich contour defined by Fig. 7, the first singularity on the real axis being  $\lambda = 0$ , as it can be easily deduced from an inspection of

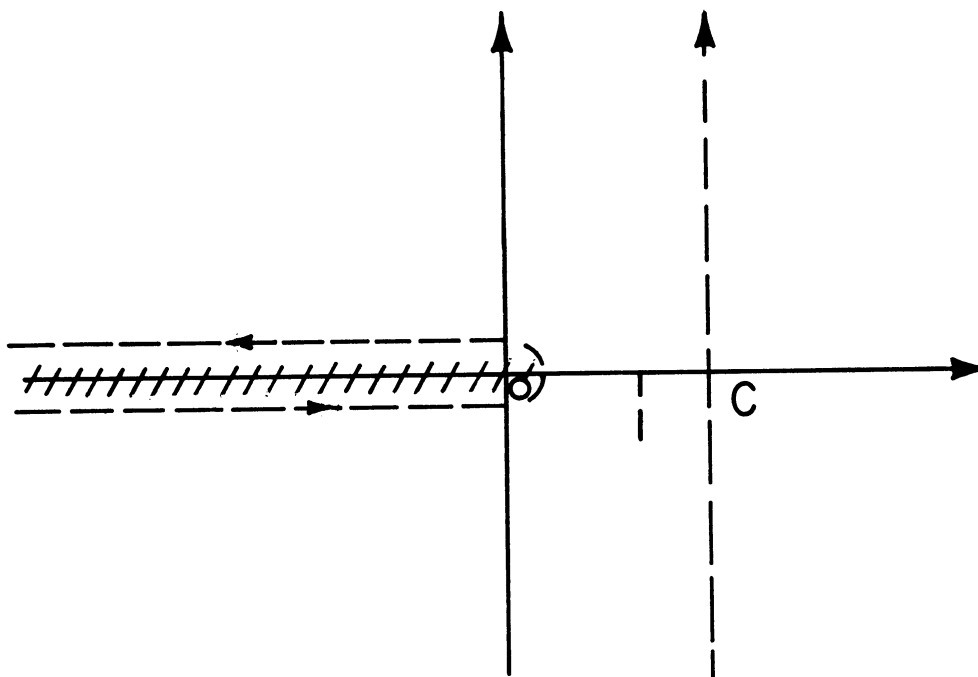


Fig. 7. The Bromwich contour for  $v \leq 1$ .

Eq. (2.35). This fact can also be verified by careful inspection of the Green's function, solution of Eq. (2.28), Eq. (2.35) being the transformed of Eq. (2.28).\*

To summarize, if the transformation  $\mathfrak{M}$  is defined by:

$$\bar{\Psi}(x, \mu, \lambda) = \int_0^{\infty} \psi(x, \mu, E) h(E)^{+\lambda-1} dE \quad (2.42)$$

(where  $h(E) = v$ ) then

$$\psi(x, \mu, E) = \frac{g(E)}{2i\pi} \int_{c-i\infty}^{c+i\infty} \bar{\Psi}(x, \mu, \lambda) h(E)^{-\lambda} d\lambda \quad (2.43)$$

\*See Section 2.5.4, "Green's function and other applications."

## 2.5. SOLUTION OF FULL-SPACE AND HALF-SPACE PROBLEMS

The introduction of the energy transformation  $\mathfrak{M}$  (Eq. (2.31)) reduced the initial transport Eq. (2.28) to:

$$\mu \frac{\partial \bar{\psi}}{\partial x}(x, \mu, \lambda) + \psi(x, \mu, \lambda) = \frac{c_1}{2\lambda} \int_{-1}^{+1} \bar{\psi}(x, \mu', \lambda) d\mu' + \frac{\delta(x - x_0)}{2} \mathcal{S}(\lambda) \quad (2.35)$$

This monokinetic equation can be solved by the classical Case technique, keeping in mind that the actual neutron distribution is given by the inversion formula (2.43).

## 2.5.1. Eigenfunctions and Eigenvalues

Consider the ansatz:

$$\bar{\psi}(x, \mu, \lambda) = \phi(v, \mu, \lambda) e^{-x/v} \quad (2.44)$$

Substitution into Eq. (2.35) yields:

$$(v - \mu) \phi(v, \mu, \lambda) = \frac{c_1}{2\lambda} v \quad (2.45)$$

With the normalization

$$\int_{-1}^{+1} \phi(v, \mu, \lambda) d\mu = 1 \quad (2.46)$$

for  $v \notin [-1, +1]$ , Eq. (2.45) has the solution:

$$\phi(v, \mu, \lambda) = \frac{c_1}{2\lambda} \frac{v}{v - \mu} \quad (2.45b)$$

The normalization specified by Eq. (2.46) will be verified for a set  $\{v_i\}$

of discrete eigenvalues such that:

$$\Lambda(v_i, \lambda) = 0 \quad (2.47)$$

where:

$$\Lambda(z, \lambda) = 1 + \frac{c_i}{\lambda} \frac{z}{2} \int_{-1}^{+1} \frac{d\mu}{\mu - z} \quad (2.48)$$

The solution of Eq. (2.45) for  $v \in [-1, +1]$  is given by:

$$\phi(v, \mu, \lambda) = \frac{c_i}{2\lambda} v P \frac{1}{v - \mu} + \xi(v, \lambda) \delta(v - \mu) \quad (2.49)$$

Again the requirement of normalization (Eq. (2.46)) yields the expression of  $\xi(v, \lambda)$ :

$$\xi(v, \lambda) = 1 + \frac{c_i}{\lambda} \frac{v}{2} P \int_{-1}^{+1} \frac{d\mu}{\mu - v} \quad (2.50a)$$

or, checking (Eq. (2.48)):

$$\xi(v, \lambda) = \frac{1}{2} \left( \Lambda^+(v, \lambda) + \Lambda^-(v, \lambda) \right) \quad (2.50b)$$

### 2.5.2. The Set $\{v_i(\lambda)\}$

The discrete eigenvalues are given by the roots of Eq. (2.48). They appear in pairs; if we call  $J(\lambda)$  the number of pairs, depending upon the value of the complex number  $\lambda$ ,  $J(\lambda)$  is given by the argument theorem:

$$2\pi \left( 2J(\lambda) \right) = \Delta_c \arg \Lambda(v, \lambda) \quad (2.51a)$$

where  $\Delta_c \arg \Lambda(v, \lambda)$  is the change in the argument of  $\Lambda(z, \lambda)$  as  $z$  encircles the cut  $[-1, +1]$ . It is readily seen that:

$$J(\lambda) = \frac{1}{2\pi} \arctan \left| \frac{\Lambda^+(+1, \lambda)}{\Lambda^-(+1, \lambda)} \right| \quad (2.51b)$$

Now, the values of interest for  $\lambda$  are on the real axis, since the inversion formula (2.39) will, in general, imply a Bromwich contour along the cut real axis (see Theorem 2.4.1 and following). Then:

$$\begin{aligned} J(\lambda) &= \frac{1}{\pi} \arctan |\Lambda^+(+1, \lambda)| \\ &= \lim_{\nu \rightarrow +1} \arctan \frac{\frac{\pi c_i \nu}{2\lambda}}{1 - \frac{c_i}{2\lambda} \nu \operatorname{argth} \nu} \end{aligned} \quad (2.51c)$$

And:

$$\begin{aligned} J(\lambda) &= 0 \quad \text{if } \lambda < 0 \\ J(\lambda) &= 1 \quad \text{if } \lambda > 0 \end{aligned} \quad (2.52)$$

So, for values of  $\lambda$  of interest we have, at most, one pair of eigenvalues  $\pm v_0$ .

### 2.5.3. Completeness Theorems

The full range completeness theorem can be stated as:

$$\begin{aligned} \phi(\mu, \lambda) &= \sum A_0(\pm v_0, \lambda) \phi(\pm v_0, \mu, \lambda) \\ &+ \int_{-1}^{+1} A(\nu, \lambda) \phi(\nu, \mu, \lambda) d\nu \end{aligned} \quad (2.53a)$$

where  $\phi(\mu, \lambda)$  is arbitrary and satisfies a Hölder condition in  $\mu$ . The completeness proof is entirely similar to the procedure of the monokinetic

case,<sup>33</sup> involving the function  $\Lambda(z, \lambda)$  analytic in the cut  $z$ -plane.<sup>33</sup>

The half-range completeness theorem is also true:

$$\begin{aligned} \phi(\mu, \lambda) &= a_0(+v_0, \lambda) \phi(+v_0, \mu, \lambda) \\ &+ \int_0^{+1} A(v, \lambda) \phi(v, \mu, \lambda) dv \end{aligned} \quad (2.53b)$$

There, one must use the function  $X(z, \lambda)$  analytic in the  $z$ -plane, with the exception of the cut  $[0, +1]$  and defined by:

$$X(z, \lambda) = \frac{1}{1-z} \exp \left[ \frac{1}{2\pi i} \int_0^1 \log \frac{\Lambda^+(\mu, \lambda)}{\Lambda^-(\mu, \lambda)} \frac{d\mu}{\mu - z} \right] \quad (2.54)$$

#### 2.5.4. Green's Function and Other Applications

The expansion coefficients defined in Eqs. (2.53a) and (2.53b) are obtained through boundary conditions and orthogonality relations strictly similar to the one speed case.<sup>33</sup>

In the full-space Green's function, the source term  $\frac{\delta(x)}{2} \cdot S(E)$  (from Eq. (2.28)) becomes  $\frac{\delta(x)}{2} \cdot \delta(E - E_0)$ . Then

$$\begin{aligned} \overline{\mathcal{G}}(\lambda) &= \int_0^\infty h(E)^{\lambda-1} \delta(E - E_0) dE \\ &= h(E_0) = 1 \end{aligned} \quad (2.55)$$

(from the normalization defined in (2.36)). And the Green's function

$$G(x, E_0, E) = \int_{-1}^{+1} \Psi(x, \mu, E) d\mu$$

is easily obtained:



$$\begin{aligned}
G(x, E_0, E) &= \frac{g(E)}{2\pi i} \int_{c-i\infty}^{c+i\infty} B(\lambda) e^{-\frac{|x|}{v_0(\lambda)}} v^{-\lambda} d\lambda \\
&+ \frac{g(E)}{2\pi i} \int_{c-i\infty}^{c+i\infty} d\lambda v^{-\lambda} \int_0^{+1} A(v, \lambda) e^{-\frac{|x|}{v}} dv
\end{aligned} \tag{2.56a}$$

( $v = h(E)$ ) with

$$B(\lambda) = \frac{1}{2} \frac{\mathcal{J}(\lambda)}{N_0(\lambda)} = \frac{1}{2N_0(\lambda)} \tag{2.56b}$$

$$A(v, \lambda) = \frac{1}{2} \frac{\mathcal{J}(\lambda)}{N(v, \lambda)} = \frac{1}{2N(v, \lambda)} \tag{2.56c}$$

$v_0(\lambda)$  being the root of

$$1 = \frac{c}{\lambda} v_0(\lambda) \operatorname{argth} \frac{1}{v_0(\lambda)} \tag{2.56d}$$

$N_0(\lambda)$  is the associated discrete mode normalization constant and  $N(v, \lambda)$  is a similar quantity for  $v \in [-1, +1]$ :

$$N(v, \lambda) = v \left\{ \left( 1 - \frac{c}{\lambda} v \operatorname{argth} v \right)^2 + \pi^2 \left( \frac{c}{\lambda} \right)^2 \frac{v^2}{4} \right\} \tag{2.56e}$$

A typical half-space problem is the Albedo problem; its solution

$\psi_a(x, \mu, E)$  satisfies:

$$\psi_a(x, \mu, E) \rightarrow 0 \text{ as } x \rightarrow +\infty$$

$$\psi_a(0, \mu, E) = \delta(\mu - \mu_0) \delta(E - E_0) \text{ for all } \mu \geq 0$$

then, defining:

$$\gamma(\mu, \lambda) = \frac{c}{\lambda} \frac{\mu}{2} \frac{X^-(\mu, \lambda)}{\Lambda^-(\mu, \lambda)} \tag{2.57a}$$

$$M_{0+}(\lambda) = \int_0^1 \gamma(\mu, \lambda) \phi(+v_0, \mu, \lambda) d\mu \quad (2.57b)$$

We obtain, following the one-speed case pattern<sup>33</sup>:

$$\begin{aligned} \psi_a(x, \mu, E) &= \frac{g(E)}{2\pi i} \int_{c-i\infty}^{c+i\infty} a_{0+}(\lambda) \phi(+v_0, \mu, \lambda) e^{-x/v_0(\lambda)} v^{-\lambda} d\lambda \\ &+ \frac{g(E)}{2\pi i} \int_{c-i\infty}^{c+i\infty} v^{-\lambda} d\lambda \int_0^1 A(v, \lambda) \phi(v, \mu, \lambda) e^{-x/v} dv \end{aligned} \quad (2.58a)$$

with

$$a_{0+}(\lambda) = \frac{\gamma(\mu_0, \lambda)}{M_{0+}(\lambda)} \quad (2.58b)$$

Since we are considering a plain slowing-down situation, there is no Milne problem.

Introducing heavy elastic scattering in Eqs. (2.28) and (2.35), as defined in (2.12b), does not involve any special difficulty: one must replace everywhere  $\frac{c}{\lambda}$  by  $\left(\frac{c}{\lambda} + c_e\right)$ . Again, for values of  $\lambda$  of interest we have at most, one pair of discrete eigenvalues:

$$\begin{aligned} J(\lambda) &= 0 \quad \text{if } \lambda < 0 \\ J(\lambda) &= 1 \quad \text{if } \lambda > 0 \end{aligned} \quad (2.59)$$

The next problem is to find asymptotic expressions simplifying the rather complex formulae for the Green's function. This will be studied in Chapter V.

## CHAPTER III

### NEUTRON TRANSPORT EQUATION WITH FISSION AND ISOTROPIC SLOWING-DOWN: A METHOD OF SOLUTION

#### 3.1. INTRODUCTION

The addition of a fission kernel to the transport equation is naturally of prime importance when it comes to studying fast systems. In thermal systems, one is used to considering fission neutrons as high energy sources, the degradation of which feeds the bulk of thermalized neutrons. Fast systems offer a sharp contrast: their asymptotic energy distribution overlaps the fission spectrum; the rate of fission reactions is comparable to the rate of slowing down reactions throughout the whole energy range.

Physically, the classical slowing-down problem of thermal reactor theory, is changed to a situation with simultaneous neutron degradation and regeneration; this may allow self-sustaining modes.

Mathematically, this implies that the sum of fission and slowing-down operators is likely to have a discrete, regular eigenfunction, which is not true for the plain slowing-down kernel. Discrete modes also appear in the thermalization case (upscattering); however, the present case is basically different, since we have the sum of two energy-transfer operators instead of a single one. There indeed lies the whole difficulty: mathematics do not yield any plain relationship between the respective spectra of two distinct operators and the spectrum of their sum. We may have investigated the spectral properties of the slowing-down kernel; we know that a fission operator

is a compact projector; yet we are not allowed to make any general extrapolations as to the properties of their sum.

Nevertheless, little work has been done up to now to study simultaneous fission and slowing-down in the Boltzmann transport equation: apart from multigroup schemes, the only method has been that of "successive collisions"<sup>35</sup> where the fission term is considered as an extraneous source; but it is limited to infinite-space solutions, and its only natural extensions are asymptotic transport and diffusion theories. The following sections propose a different approach based on the spectral properties of the global energy-transfer operator.

### 3.2. ISOTROPIC ELASTIC SCATTERING WITH FISSION: SPECTRAL STUDY OF THE CORRESPONDING ENERGY TRANSFER OPERATOR

We consider the equation:

$$\begin{aligned} \mu \frac{\partial \psi}{\partial x}(x, \mu, u) + \psi(x, \mu, u) = & \frac{c_F}{2} \int_{-1}^{+1} d\mu' \chi(u) \int_{-\infty}^{+\infty} \psi(x, \mu', u') du' \\ & + \frac{c_S}{2} \int_{-1}^{+1} d\mu' \int_{-\infty}^u g(u-u') \psi(x, \mu', u') du' \\ & + \frac{1}{2} \delta(x-x_0) S(u) \end{aligned} \quad (3.1)$$

Here  $c_F$  represents the average number of fission secondaries per collision, while  $c_S$  is a similar quantity for elastic scattering. Also  $\chi(u)$  is the fission spectrum and  $g(u)$  the elastic scattering kernel,  $u$  being the lethargy-variable;  $S$  represents the extraneous source.

Define an operator  $T$  by:

$$T \phi(u) = c_F \chi(u) \int_{-\infty}^{+\infty} \phi(u') du' + c_S \int_{-\infty}^u g(u-u') \phi(u') du' \quad (3.2)$$

We are considering functions in the Banach space  $L^1[-\infty, +\infty]$ , such that:

$$\phi(u) \in L^1[-\infty, +\infty]$$

$$\text{iff} \quad \|\phi\| = \int_{-\infty}^{+\infty} |\phi(u)| du \quad \text{is} < \infty \quad (3.3)$$

Such functions always possess a Fourier-transform:

$$\bar{\phi}(k) = \int_{-\infty}^{+\infty} \phi(u) e^{-iku} du \quad (3.4)$$

So we can, in fact, consider a broader class: namely "tempered distributions," which, according to L. Schwartz,<sup>52</sup> possess a Fourier-transform. Now, let us look for eigenfunctions of  $T$ :

$$T \phi(u) = \lambda \phi(u) \quad (3.5a)$$

Fourier-transforming Eq. (3.5a), we get:

$$\lambda \bar{\phi}(k) = c_F \bar{\chi}(k) \int_{-\infty}^{+\infty} \phi(u) du + c_S \bar{g}(k) \bar{\phi}(k) \quad (3.5b)$$

where

$$\bar{\chi}(k) = \int_{-\infty}^{+\infty} \chi(u) e^{-iku} du \quad (3.6a)$$

$$\bar{g}(k) = \int_{+0}^{+\infty} g(u) e^{-iku} du \quad (3.6b)$$

with the normalizations:

$$\bar{\chi}(0) = \bar{g}(0) = 1 \quad (3.6c)$$

Let us note that:

$$\int_{-\infty}^{+\infty} \phi(u) du = \bar{\phi}(0) \quad (3.7)$$

Using Eq. (7), Eq. (5b) becomes:

$$\lambda \bar{\phi}(k) = c_F \bar{\chi}(k) \bar{\phi}(0) + c_S \bar{g}(k) \bar{\phi}(k) \quad (3.5b)$$

This is our eigenfunction equation. Two cases occur:

(I) Eigenfunctions  $\phi(u)$  such that  $\bar{\phi}(0) \neq 0$ , or

$$\int_{-\infty}^{+\infty} \phi(u) du \neq 0$$

Then, the solution of (3.5b) is:

$$\bar{\phi}(k) = \frac{c_F \bar{\chi}(k) \bar{\phi}(0)}{\lambda - c_S \bar{g}(k)} \quad (3.8a)$$

But Eq. (3.8a) must be true for all values of  $k$ ; thus for  $k = 0$ , it must yield an identity; using Eq. (6c):

$$\bar{\phi}(0) = \frac{c_F}{\lambda - c_S} \bar{\phi}(0) \quad (3.8b)$$

Hence

$$\lambda \equiv c_F + c_S \quad (3.9)$$

So we have an unique eigenvalue  $\lambda = c_F + c_S$ , to which corresponds an unique eigenfunction  $\chi$ :

$$\bar{\chi}(k) = \frac{c_F \bar{\chi}(k)}{c_F + c_S (1 - \bar{g}(k))} \quad (3.10)$$

where we normalized  $\bar{\chi}(0) = \int_{-\infty}^{+\infty} \chi(u) du = 1$ .

(II) Eigenfunctions  $\phi(u)$  such that  $\bar{\phi}(0) = 0$  or

$$\int_{-\infty}^{+\infty} \phi(u) du = 0$$

Then Eq. (5b) reduces to:

$$\lambda \bar{\phi}(k) = c_S \bar{g}(k) \bar{\phi}(k) \quad (3.5c)$$

This is the plain slowing-down eigenvalue problem. The solutions form a continuum of eigenfunctions such that:

$$\bar{\phi}_{\lambda}(k) = \delta(k - k_0) \quad \text{with } k_0 \neq 0$$

$$\lambda = c_s \bar{g}(k_0)$$

$$\phi_\lambda(u) = \frac{1}{2\pi} e^{ik_0 u} = \int_{-\infty}^{+\infty} \frac{1}{2\pi} \delta(k-k_0) e^{iku} dk \quad (3.11)$$

Indeed, we verify that:

$$\int_{-\infty}^{+\infty} \phi_\lambda(u) du = \frac{1}{2\pi} \int_{-\infty}^{+\infty} e^{ik_0 u} du$$

$$= \delta(k-k_0) \quad \text{for } k = 0$$

$$= 0 \quad \text{in the distribution sense} \quad (3.12a)$$

In summary, the eigenfunctions of  $T$  split into two groups:

On the one hand, the discrete regular eigenfunction  $\mathcal{X}(u)$ , with the associated eigenvalue  $\lambda = c_F + c_S$ . This eigenfunction is characteristic of the neutron regeneration.

On the other hand, eigenfunctions of the plain slowing-down operator,  $\phi_\lambda(u) = \frac{1}{2\pi} e^{iK_0 u}$ , with  $\lambda = c_S \bar{g}(k_0)$ —provided  $K_0 \neq 0$ . These eigenfunctions form a continuum, and have a null "measure" (in the space of distributions).

Let us now prove a completeness theorem:

Theorem 3.2.1. The eigenfunctions defined by Eq. (10) and (11) form a complete set for functions belonging to  $L_1[-\infty, +\infty]$ .

Proof: Let  $\phi(u) \in L_1[-\infty, +\infty]$ . The completeness theorem which we wish to prove can be stated as:



$$\phi(u) = \mathcal{Y} \mathcal{H}(u) + \frac{1}{2\pi} \int_{-\infty}^{+\infty} A(k_0) e^{ik_0 u} dk_0$$

where  $\mathcal{Y}$  and  $A(k_0)$  are the unknown expansion coefficients associated respectively with the discrete eigenfunction  $\mathcal{H}(u)$  and the continuum eigenfunctions  $e^{ik_0 u}$ . We must have  $A(0) \equiv 0$ .

Remembering that  $\int_{-\infty}^{+\infty} \mathcal{H}(u) du = 1$ , we have obviously:

$$\mathcal{Y} = \int_{-\infty}^{+\infty} \phi(u) du$$

Now, we have to find  $A(k_0)$ . Defining  $\Gamma(u) = \phi(u) - \mathcal{Y}\mathcal{H}(u)$ , we verify that:

$$\int_{-\infty}^{+\infty} \Gamma(u) du \equiv 0$$

Now, we must prove that  $\Gamma(u)$  can be written as follows:

$$\Gamma(u) = \frac{1}{2\pi} \int_{-\infty}^{+\infty} A(k_0) e^{ik_0 u} dk_0$$

This is immediate, since  $\Gamma(u)$  is Fourier-transformable, and inverse Fourier-transformation yields:

$$A(k_0) = \int_{-\infty}^{+\infty} \Gamma(u) e^{-ik_0 u} du$$

So our expansion coefficients are known. We have only to verify that  $A(0) \equiv 0$ , which is true since:

$$A(0) \equiv \int_{-\infty}^{+\infty} \Gamma(u) du \equiv 0$$

Q.E.D.

The completeness of the eigenfunctions of our energy-transfer operator will be used to decompose the transport equation (3.1) into two associated equations corresponding to the two groups of eigenfunctions.

### 3.3. ISOTROPIC INELASTIC SCATTERING WITH FISSION: SPECTRAL STUDY OF THE CORRESPONDING ENERGY TRANSFER OPERATOR

The results of Section 3.2 hold if we consider the synthetic inelastic slowing-down kernel studied in Chapter II. We consider the equation:

$$\begin{aligned} \mu \frac{\partial \Psi}{\partial x}(x, \mu, E) + \Psi(x, \mu, E) &= \frac{c_F}{2} \int_{-1}^{+1} d\mu' \chi(E) \int_0^{+\infty} \Psi(x, \mu', E') dE' \\ &+ \frac{c_S}{2} g(E) \int_E^{+\infty} \frac{dE'}{h(E')} \int_{-1}^{+1} \Psi(x, \mu', E') d\mu' \\ &+ \frac{1}{2} \delta(x-x_0) S(E) \end{aligned} \quad (3.13)$$

Notations are similar to those of Eq. (3.11), except that the energy-variable  $E$  is used in connection with the synthetic inelastic scattering kernel defined in Section 2.2.

Define the operator  $T$  by:

$$T\phi(E) = c_F \chi(E) \int_0^{+\infty} \phi(E) dE + c_S g(E) \int_E^{+\infty} \frac{\phi(E')}{h(E')} dE' \quad (3.14)$$

We again consider functions  $\phi(E) \in L^1[0, +\infty]$ . Such functions always possess the  $\mathcal{M}$ -transform defined in Section 2.4:

$$\bar{\phi}(\lambda) = \int_0^{+\infty} \phi(E) h(E)^{\lambda-1} dE \quad (2.38)$$

$$\phi(E) = \frac{g(E)}{2\pi i} \int_{c-i\infty}^{c+i\infty} \bar{\phi}(\lambda) h(E)^{-\lambda} d\lambda \quad (2.39)$$

Now, looking for eigenfunctions of  $T$ :

$$T \phi(E) = v \phi(E) \quad (3.15a)$$

We  $\mathcal{M}$ -transform Eq. (3.15a), use Eq. (2.35) and get:

$$v \bar{\phi}(\lambda) = c_F \bar{\chi}(\lambda) \int_0^{+\infty} \phi(E) dE + \frac{c_S}{\lambda} \bar{\phi}(\lambda) \quad (3.15b)$$

where

$$\bar{\chi}(\lambda) = \int_0^{+\infty} \chi(E) h(E)^{\lambda-1} dE \quad (3.16a)$$

$$\bar{\chi}(1) = 1 \quad (3.16b)$$

Let us note that

$$\int_0^{+\infty} \phi(E) dE = \bar{\phi}(1) \quad (3.17)$$

Using Eq. (3.17), Eq. (3.15b) becomes:

$$v \bar{\phi}(\lambda) = c_F \bar{\chi}(\lambda) \bar{\phi}(1) + \frac{c_S}{\lambda} \bar{\phi}(\lambda) \quad (3.15b)$$

Solutions of (3.15b) belong to two categories:

(I) Eigenfunctions  $\phi(E)$  such that  $\bar{\phi}(1) \neq 0$ , or

$$\int_0^{+\infty} \phi(E) dE \neq 0$$

Then, the solution of (3.15b) is:

$$\overline{\Phi}(\lambda) = \frac{c_F \overline{\chi}(\lambda) \overline{\Phi}(1)}{\nu - \frac{c_S}{\lambda}} \quad (3.18a)$$

But Eq. (3.18a) must be verified for all values of  $\lambda$ ; hence, for  $\lambda = 1$ , it must yield an identity (using Eq. (3.16b)):

$$\overline{\Phi}(1) = \frac{c_F}{\nu - c_S} \overline{\Phi}(1) \quad (3.18b)$$

Hence

$$\begin{aligned} \nu - c_S &= c_F \\ \nu &= c_F + c_S \end{aligned} \quad (3.19)$$

So we have a unique eigenvalue  $\nu = c_F + c_S$ , to which corresponds a unique eigenfunction):

$$\overline{H}(\lambda) = \frac{c_F \overline{\chi}(\lambda)}{c_F + c_S \left(1 - \frac{1}{\lambda}\right)} \quad (3.20a)$$

In fact, we have already implicitly solved the direct Eq. (3.15a) in Section 2.3; using the solution (2.26b) we obtain the direct expression for  $H(E)$ :

$$\begin{aligned} H(E) &= \frac{c_F}{c_F + c_S} \chi(E) \\ &+ \frac{c_S}{c_F + c_S} g(E) h(E) \frac{-c_S}{c_F + c_S} \int_E^{+\infty} \frac{c_F}{c_F + c_S} \frac{\chi(E') dE'}{h(E') \frac{c_F}{c_F + c_S}} \end{aligned} \quad (3.20b)$$

(II) Eigenfunctions  $\phi(E)$  such that  $\bar{\phi}(1) = 0$  or  $\int_0^\infty \phi(E) dE = 0$ . Then Eq. (3.15b) reduces to:

$$v \bar{\phi}(\lambda) = \frac{c_s}{\lambda} \bar{\phi}(\lambda) \quad (3.15c)$$

This is the plain slowing-down eigenvalue problem. As we know from Section 2.3, solutions form a continuum of "pseudo-eigenfunctions" such that:

$$\bar{\phi}_v(\lambda) = \delta(\lambda - \lambda_0) \quad \text{with } \lambda_0 \neq 1$$

$$v = \frac{c_s}{\lambda_0} \quad (3.21)$$

$$\phi_v(E) = \frac{g(E)}{2i\pi} \int_{c-i\infty}^{c+i\infty} \delta(\lambda - \lambda_0) h(E)^{-\lambda} d\lambda = \frac{g(E) h(E)^{-\lambda_0}}{2\pi}$$

We know from Section 2.3 (Eq. (2.24)) that the  $\{\phi_v(E)\}$  are only "pseudo-eigenfunctions" of the synthetic inelastic scattering kernel.

This does not prevent a completeness theorem from being valid:

Theorem 3.3.1. The discrete eigenfunction  $\chi(E)$  defined by Eq. (3.20b) and the "pseudo-eigenfunctions" defined by Eq. (3.21) form a complete set for functions  $\in L'[0, +\infty]$ .

Proof: Let  $\phi(E) \in L'[0, +\infty]$ . The completeness theorem can be stated as:

$$\phi(E) = \mathcal{Y} \cdot \chi(E) + \frac{g(E)}{2\pi i} \int_{c-i\infty}^{c+i\infty} A(\lambda_0) h(E)^{-\lambda_0} d\lambda_0$$

with  $A(1) \equiv 0$ ;  $\mathcal{Y}$  and  $A(\lambda_0)$  being the unknown expansion coefficients associated respectively with the discrete eigenfunction  $\chi(E)$  and the continuum

eigenfunctions  $h(E)^{-\lambda_0}$ . Then we have obviously  $\mathcal{Y} = \int_0^\infty \phi(E) dE$ . Defining

$\Gamma(E) = \phi(E) - \mathcal{Y} \cdot \mathcal{H}(E)$ , we have:

$$\int_0^\infty \Gamma(E) dE \equiv 0$$

(Since  $\int_0^\infty \mathcal{H}(E) dE \equiv 1$ ). Then, we must prove that we can write

$$\Gamma(E) = \frac{g(E)}{2i\pi} \int_{c-i\infty}^{c+i\infty} A(\lambda_0) h(E)^{-\lambda_0} d\lambda_0$$

But, applying an inverse  $\mathcal{M}$ -transformation (see Eqs. (2.38) and (2.39)), we get, since  $\Gamma(E)$  is  $\mathcal{M}$ -transformable:

$$A(\lambda_0) = \int_0^\infty \Gamma(E) h(E)^{\lambda_0-1} dE$$

Our expansion coefficients are therefore known. We have only to verify that

$A(1) \equiv 0$ , which is true since:

$$A(1) = \int_0^\infty \Gamma(E) dE \equiv 0$$

Q.E.D.

Hence, it seems that, quite generally, the eigenfunctions of the fission-slowing-down energy transfer operator form a complete set, and that they can be classified into two groups: (i) one discrete regular eigenfunction corresponding to fission regeneration; (ii) a continuous set of slowing-down (pseudo) eigenfunctions of null measure.

#### 3.4. SOLUTION OF THE COMPLETE TRANSPORT EQUATION: DECOMPOSITION INTO TWO ASSOCIATED EQUATIONS

Let us now consider Eqs. (3.1) and (3.13):

$$\begin{aligned} \mu \frac{\partial \Psi}{\partial x}(x, \mu, u) + \Psi(x, \mu, u) &= \frac{C_F}{2} \int_{-1}^{+1} d\mu' \chi(u) \int_{-\infty}^{+\infty} \Psi(x, \mu', u') du' \\ &+ \frac{C_S}{2} \int_{-1}^{+1} d\mu' \int_{-\infty}^u g(u-u') \Psi(x, \mu', u') du' + \frac{1}{2} \delta(x-x_0) S(u) \end{aligned} \quad (3.1)$$

$$\begin{aligned} \mu \frac{\partial \Psi}{\partial x}(x, \mu, E) + \Psi(x, \mu, E) &= \frac{C_F}{2} \int_{-1}^{+1} d\mu' \chi(E) \int_0^{+\infty} \Psi(x, \mu', E') dE' \\ &+ \frac{C_S}{2} \int_{-1}^{+1} d\mu' g(E) \int_E^{+\infty} \frac{\Psi(x, \mu', E')}{h(E')} dE' + \frac{1}{2} \delta(x-x_0) S(E) \end{aligned} \quad (3.13)$$

If the source term [Eq. (3.1) and (3.13)] were of the form:

$$\frac{1}{2} \delta(x-x_0) S(u) = \mathcal{H}(u) \frac{\delta(x-x_0)}{2}$$

or

$$\frac{1}{2} \delta(x-x_0) S(E) = \mathcal{H}(E) \frac{\delta(x-x_0)}{2} \quad (3.22)$$

That is, if the initial source distribution were proportional to the discrete regular mode of the energy-transfer kernel, then Eqs. (3.1) and (3.13) would reduce to a one-speed equation; the solution is then separable into a function of space and angle times  $\mathcal{H}(E)$  (or  $\mathcal{H}(u)$ ). More precisely:

$$\Psi(x, \mu, E) = \Phi_E(x, \mu) \cdot \mathcal{H}(E) \quad (3.23a)$$

Where  $\Phi_E(x, \mu)$  obeys:

$$\mu \frac{\partial}{\partial x} \Phi_E(x, \mu) + \Phi_E(x, \mu) = \frac{C_F + C_S}{2} \int_{-1}^{+1} d\mu' \Phi_E(x, \mu') + \frac{\delta(x-x_0)}{2} \quad (3.23b)$$

However, in general, the source-term is not proportional to  $\mathcal{H}(E)$ . The idea is then to decompose the actual source through an expansion using the complete set of energy-eigenfunctions, defined in Sections 3.2 and 3.3; for inelastic scattering:

$$S(E) = \mathcal{Y} \cdot \mathcal{H}(E) + \Gamma(E) \quad (3.24a)$$

where

$$\mathcal{Y} = \int_0^{+\infty} S(E) dE \quad (3.24b)$$

clearly

$$\int_0^{\infty} \Gamma(E) dE = 0 \quad (3.24c)$$

Then, from the completeness theorem 3.3.1:

$$\Gamma(E) = \frac{g(E)}{2i\pi} \int_{c-i\infty}^{c+i\infty} \bar{\Gamma}(\lambda) h(E)^{-\lambda} d\lambda \quad (3.24d)$$

with

$$\bar{\Gamma}(\lambda) = \int_0^{\infty} \Gamma(E) h(E)^{\lambda-1} dE \quad (3.24e)$$

$$\bar{\Gamma}(1) = 0 \quad (3.24f)$$



A similar decomposition holds for the source-term of Eq. (3.1), using a lethargy variable and a lethargy integration range  $[-\infty, +\infty]$ ; then completeness Theorem 3.2.1 yields:

$$\Gamma(u) = \frac{1}{2\pi} \int_{-\infty}^{+\infty} \bar{\Gamma}(k) e^{iku} dk \quad (3.24d)$$

$$\bar{\Gamma}(k) = \int_{-\infty}^{+\infty} \Gamma(u) e^{-iku} du \quad (3.24e)$$

$$\bar{\Gamma}(0) \equiv 0 \quad (3.24f)$$

Since there is a close parallel between elastic (Eq. (3.1)) and inelastic scattering (Eq. (3.13)), we will, from now on, focus our attention on the latter case.

The transport equation (3.13) is linear; so its solution can be expressed as the one speed solution due to the component  $\mathcal{Y} \cdot \mathcal{H}(E)$  plus the solution due to a source  $\Gamma(E)$  of zero measure. Call the former solution  $\mathcal{H}(E) \phi_E(x, \mu)$ , and the latter  $\phi_{tr}(x, \mu, E)$ :

$$\Psi(x, \mu, E) = \mathcal{H}(E) \phi_E(x, \mu) + \phi_{tr}(x, \mu, E) \quad (3.25)$$

$\phi_E(x, \mu)$  obeys:

$$\mu \frac{\partial}{\partial x} \phi_E(x, \mu) + \phi_E(x, \mu) = \frac{c_E + c_S}{2} \int_{-1}^{+1} \phi_E(x, \mu') d\mu' + \frac{\mathcal{J} \cdot \delta(x-x_0)}{2} \quad (3.26)$$

As to  $\Phi_{\text{tr}}(x, \mu, E)$ , let us show that it obeys:

$$\begin{aligned} \mu \frac{\partial}{\partial x} \Phi_{\text{tr}}(x, \mu, E) + \Phi_{\text{tr}}(x, \mu, E) &= \frac{c_s}{2} \int_{-1}^{+1} d\mu' g(E) \int_E^{\infty} \frac{\Phi_{\text{tr}}(x, \mu', E')}{h(E')} dE' \\ &+ \Gamma(E) \frac{\delta(x-x_0)}{2} \end{aligned} \quad (3.27a)$$

Equation (3.27a) is a plain slowing-down equation, without any fission-term. Equivalently, its solution has null measure, due to the fact that the source term  $\Gamma(E)$  has itself null measure. To verify this point, let us  $\mathcal{M}$ -transform equation (3.27a):

$$\begin{aligned} \mu \frac{\partial}{\partial x} \bar{\Phi}_{\text{tr}}(x, \mu, \lambda) + \bar{\Phi}_{\text{tr}}(x, \mu, \lambda) &= \frac{c_s}{2\lambda} \int_{-1}^{+1} \bar{\Phi}_{\text{tr}}(x, \mu', \lambda) d\mu' \\ &+ \bar{\Gamma}(\lambda) \frac{\delta(x-x_0)}{2} \end{aligned} \quad (3.27b)$$

Call  $\bar{G}(x_0 \rightarrow x, \mu, \lambda)$  the corresponding Green's function, solution of:

$$\mu \frac{\partial \bar{G}}{\partial x} + \bar{G}(x_0 \rightarrow x, \mu, \lambda) = \frac{c_s}{2\lambda} \int_{-1}^{+1} \bar{G}(x_0 \rightarrow x, \mu', \lambda) d\mu' + \frac{1}{2} \delta(x-x_0) \quad (3.27c)$$

Then, we obtain:

$$\bar{\Phi}_{\text{tr}}(x, \mu, \lambda) = \bar{\Gamma}(\lambda) \cdot \bar{G}(x_0 \rightarrow x, \mu, \lambda)$$

$$\Phi_{\text{tr}}(x, \mu, E) = \frac{g(E)}{2i\pi} \int_{c-i\infty}^{c+i\infty} \bar{\Gamma}(\lambda) \bar{G}(x_0 \rightarrow x, \mu, \lambda) h(E)^{-\lambda} d\lambda \quad (3.27d)$$

Keeping in mind that  $\Gamma(E)$  has zero-measure, we see from Eq. (3.27d) that this is also true for  $\phi_{\text{tr}}(x, \mu, E)$  [see the definition of  $\Gamma(E)$  in the set of Eq. (3.24)].

So, we have successfully decomposed the initial transport equation (3.13) into two associated equations (3.26) and (3.27a). Since Eq. (3.26) is a monokinetic one, its solutions are well known for a wide range of boundary conditions.<sup>33</sup> As to Eq. (3.27a), this is a plain slowing-down problem without regeneration: Section 2.5 obtained analytical expressions for the full- and half-space Green's functions corresponding to inelastic slowing-down without regeneration.

As we have already noticed, very close results hold for the transport equation (3.1), which also splits into two parts: a monokinetic equation, and a plain elastic slowing-down problem without regeneration. The latter one has been extensively solved by Jacobs and MacInerney<sup>19</sup> who treated both half- and full-space problems, using the Fourier-Laplace transformation of the lethargy variable.

The decomposition we introduced is not a mere mathematical trick; we have gained more than reducing a complex problem to the well-known solution of two closely related equations. In fact, the underlying physical implication lies in the complete partition of the space-energy separable components from the nonseparable transients of the global solution.

On the one hand, the space-energy separable components are all proportional to the characteristic energy mode  $\chi(E)$ ; they are representative of

self-sustaining modes in the fast multiplying medium; they are likely to be the asymptotic dominant modes in any integral experiments.

On the other hand, one could have, a priori, considered space-energy separable solutions and injected them into the original transport equation. The limits of such an asymptotic transport theory are hinted by the second part of our decomposition: we must also take into account nonseparable slowing-down transients, solution of a plain slowing-down equation.

This states a clear goal for further investigation. One must study the relative importance of asymptotic separable modes and slowing-down transients in integral experiments. It must be emphasized that such transients are not mere classical spatial transport transients; they also reflect the adjustment of the neutron field from the initial source-energy distribution to the final asymptotic spectral mode. As we will show it later on, part of these slowing-down transients are decaying into space more slowly than  $e^{-\sum_t \min|x|}$ , where  $\sum_t \min$  is the minimal total cross-section. So there will be spatial competition between these slowing-down transients and asymptotic modes; it is quite likely that this is very sensitive to the degree of criticality of the fast multiplying system.

### 3.5. ANALYTICAL EXPRESSIONS OF SOLUTIONS FOR VARIOUS BOUNDARY CONDITIONS

Using results of the preceding section, we are now able to give explicit solutions to the equation:

$$\begin{aligned}
\mu \frac{\partial}{\partial x} \Psi(x, \mu, E) + \Psi(x, \mu, E) &= \frac{c_F}{2} \chi(E) \int_{-1}^{+1} d\mu' \int_0^\infty \Psi(x, \mu', E') dE' \\
&+ \frac{c_i}{2} \int_{-1}^{+1} d\mu' g(E) \int_E^\infty \frac{\Psi(x, \mu', E')}{h(E')} dE' + \frac{c_e}{2} \int_{-1}^{+1} \Psi(x, \mu', E) d\mu' \\
&+ \frac{\delta(x-x_0)}{2} S(E)
\end{aligned} \tag{3.28}$$

Equation (3.28) is also similar to Eq. (3.13) except that we are adding a "heavy" elastic scattering term to the inelastic one;  $c_i$  is the average number of secondaries after an inelastic collision,  $c_e$ , the corresponding one after an elastic collision.

Since "heavy" elastic scattering does not involve any energy change (or physically, a negligible one compared to inelastic slowing-down), there are no modifications to the results of the preceding sections. In particular, the discrete energy-eigenfunction  $\mathcal{H}(E)$  (see Section 3.3) is not influenced by heavy elastic scattering; from Eq. (3.20b):

$$\mathcal{H}(E) = \frac{c_F}{c_F + c_i} \chi(E) + \frac{c_i}{c_F + c_i} g(E) h(E) \frac{-c_i}{c_F + c_i} \int_E^\infty \frac{c_F}{c_F + c_i} \frac{\chi(E')}{h(E') \frac{c_F}{c_F + c_i}} dE' \tag{3.29}$$

However, the associated eigenvalue is  $\nu = c_F + c_i + c_e$ . Following Eq. (3.25), we decompose  $\Psi(x, \mu, E)$ :

$$\Psi(x, \mu, E) = \mathcal{H}(E) \Phi_E(x, \mu) + \Phi_{tr}(x, \mu, E) \tag{3.25}$$

Following the set of Eq. (3.24) we decompose  $S(E)$ :

$$S(E) = \mathcal{J} \cdot \mathcal{H}(E) + \Gamma(E) \quad (3.24a)$$

$$\mathcal{J} = \int_0^{\infty} S(E') dE' \quad (3.24b)$$

Then  $\phi_E(x, \mu)$  and  $\phi_{tr}(x, \mu, E)$  obey slightly modified Eq. (3.26) and (3.27a):

$$\mu \frac{\partial}{\partial x} \phi_E(x, \mu) + \phi_E(x, \mu) = \frac{c_F + c_e + c_i}{2} \int_{-1}^{+1} d\mu' \phi_E(x, \mu') + \frac{1}{2} \mathcal{J} \cdot \delta(x - x_0) \quad (3.30)$$

$$\begin{aligned} \mu \frac{\partial}{\partial x} \phi_{tr}(x, \mu, E) + \phi_{tr}(x, \mu, E) = & \frac{c_i}{2} \int_{-1}^{+1} d\mu' g(E) \int_E^{\infty} \frac{\phi_{tr}(x, \mu', E')}{h(E')} dE' \\ & + \frac{c_e}{2} \int_{-1}^{+1} \phi_{tr}(x, \mu', E) d\mu' + \frac{1}{2} \Gamma(E) \delta(x - x_0) \end{aligned} \quad (3.31)$$

The monokinetic Eq. (3.30) has been solved for a wide range of boundary conditions.<sup>33</sup> Solutions of Eq. (3.31) for full- and half-space problems have been described in Section 2.5. So, we can immediately write down the analytical expression of solutions of Eq. (3.28) for a wide range of cases.

### 3.5.1. Full-Space Green's Function

The source term in Eq. (3.28) is  $\delta(x)/2 \cdot S(E)$ . Call  $G(|x|, E)$  the Green's function:

$$G(|x|, E) = \int_{-1}^{+1} \psi(|x|, \mu, E) d\mu \quad (3.32)$$

Using results of Section 2.5 (where we normalized  $h(E)$  so that  $h(\infty) \equiv +1$ ), we have:

$$\begin{aligned} G(|x|, E) = & \mathcal{J} \chi(E) \left\{ \frac{1}{2} \frac{e^{-\frac{|x|}{v_0}}}{N_0} + \frac{1}{2} \int_0^1 \frac{e^{-\frac{|x|}{v}}}{N(v)} dv \right\} \\ & + \frac{g(E)}{2i\pi} \int_{c-i\infty}^{c+i\infty} \frac{1}{2} \cdot \frac{\bar{\Gamma}(\lambda)}{N_0(\lambda)} \cdot e^{-\frac{|x|}{v_0(\lambda)}} \cdot h(E)^{-\lambda} d\lambda \\ & + \frac{g(E)}{2i\pi} \int_{c-i\infty}^{c+i\infty} h(E)^{-\lambda} d\lambda \int_0^{+1} \frac{1}{2} \frac{\bar{\Gamma}(\lambda)}{N(v, \lambda)} e^{-\frac{|x|}{v}} dv \end{aligned} \quad (3.33a)$$

with  $v_0$  being the root of:

$$1 = (c_f + c_e + c_i) v_0 \operatorname{argth} \frac{1}{v_0} \quad (3.33b)$$

$v_0(\lambda)$  being the root of:

$$1 = \left( \frac{c_i}{\lambda} + c_e \right) v_0(\lambda) \operatorname{argth} \frac{1}{v_0(\lambda)} \quad (3.33c)$$

$$N_0 = \left( \frac{c_f + c_e + c_i}{2} \right) v_0^3 \left( \frac{c_f + c_e + c_i}{v_0^2 - 1} - \frac{1}{v_0^2} \right) \quad (3.33d)$$

$$N_0(\lambda) = \frac{1}{2} \left( \frac{c_i}{\lambda} + c_e \right) \cdot \nu_0^3(\lambda) \left( \left( \frac{c_i}{\lambda} + c_e \right) \cdot \frac{1}{\nu_0^2(\lambda) - 1} - \frac{1}{\nu_0^2(\lambda)} \right) \quad (3.33e)$$

$$N(\nu) = \nu \left\{ \left( 1 - (c_e + c_F + c_i) \nu \operatorname{arctanh} \nu \right)^2 + \frac{\pi^2}{4} (c_e + c_F + c_i)^2 \nu^2 \right\} \quad (3.33f)$$

$$N(\nu, \lambda) = \nu \left\{ \left( 1 - \left( \frac{c_i}{\lambda} + c_e \right) \nu \operatorname{arctanh} \nu \right)^2 + \frac{\pi^2}{4} \left( c_e + \frac{c_i}{\lambda} \right)^2 \nu^2 \right\} \quad (3.33g)$$

$$\bar{\Gamma}(\lambda) = \int_0^\infty \Gamma(E) h(E) \lambda^{-1} dE \quad (3.33h)$$

### 3.5.2. Albedo Problem

Its solution  $\psi_A(x, \mu, E)$  satisfies:

$$\psi_A(x, \mu, E) \rightarrow 0 \quad \text{as } x \rightarrow +\infty$$

$$\psi_A(0, \mu, E) = \delta(\mu - \mu_0) \cdot S(E) \quad \text{for all } \mu \geq 0$$

Then, defining the discrete regular modes of Case's method<sup>33</sup>:

$$\phi_0(\nu_0, \mu) = \frac{c_F + c_e + c_i}{2} \frac{\nu_0}{\nu_0 - \mu} \quad (3.34a)$$



$$\phi_0(\nu_0(\lambda), \mu) = \frac{1}{2} \left( c_e + \frac{c_i}{\lambda} \right) \frac{\nu_0(\lambda)}{\nu_0(\lambda) - \mu} \quad (3.34b)$$

where  $\nu_0$  and  $\nu_0(\lambda)$  are the roots of Eqs. (3.33b) and (3.33c); we introduce:

$$\gamma(\mu) = \frac{c_e + \frac{c_i}{\lambda}}{2} \mu \frac{X^-(\mu)}{\Lambda^-(\mu)} \quad (3.35a)$$

$$\gamma(\mu, \lambda) = \left( c_e + \frac{c_i}{\lambda} \right) \frac{\mu}{2} \frac{X^-(\mu, \lambda)}{\Lambda^-(\mu, \lambda)} \quad (3.35b)$$

where  $X(z)$  and  $\Lambda(z)$  are well-known functions in Case's theory,<sup>33</sup> providing we use the average number of secondaries  $c_F + c_e + c_i$ .  $\Lambda(z, \lambda)$  has been defined in Eq. (2.48) and  $X(z, \lambda)$  in Eq. (2.54), providing we replace  $\left(\frac{c_i}{\lambda}\right)$  by  $\left(\frac{c_i}{\lambda} + c_e\right)$ . Furthermore, define:

$$M_{0+} = \int_0^1 \gamma(\mu) \phi_0(\nu_0, \mu) d\mu \quad (3.36a)$$

$$M_{0+}(\lambda) = \int_0^1 \gamma(\mu, \lambda) \phi_0(\nu_0(\lambda), \mu) d\mu \quad (3.36b)$$

$$a_{0+} = \frac{\gamma(\mu_0)}{M_{0+}} \quad (3.37a)$$

$$a_{o+}(\lambda) = \frac{\gamma(\mu_o, \lambda)}{M_{o+}(\lambda)} \quad (3.37b)$$

We finally obtain:

$$\begin{aligned} \psi_A(x, \mu, E) = & \mathcal{J} \cdot \mathcal{H}(E) \cdot \left\{ a_{o+} \cdot \phi_o(\nu_o, \mu) \cdot e^{-\frac{x}{\nu_o}} + \int_0^1 A(\nu) \phi(\nu, \mu) e^{-\frac{x}{\nu}} d\nu \right\} \\ & + \frac{g(E)}{2i\pi} \int_{c-i\infty}^{c+i\infty} a_{o+}(\lambda) \bar{\Gamma}(\lambda) \phi_o(\nu_o(\lambda), \mu) e^{-\frac{x}{\nu_o(\lambda)}} h(E)^{-\lambda} d\lambda \\ & + \frac{g(E)}{2i\pi} \int_{c-i\infty}^{c+i\infty} d\lambda h(E)^{-\lambda} \int_0^1 \bar{\Gamma}(\lambda) A(\nu, \lambda) \phi(\nu, \mu, \lambda) e^{-\frac{x}{\nu}} d\nu \end{aligned} \quad (3.38)$$

where  $\phi(\nu, \mu)$  are Case's singular modes<sup>33</sup> for the monokinetic transport equation and  $\phi(\nu, \mu, \lambda)$  are similar singular modes defined in Eq. (2.49);  $A(\nu)$  and  $A(\nu, \lambda)$  are the respective expansion coefficients corresponding to these continuums of singular modes.

### 3.5.3. Milne Problem

Given a half-space with no incident neutrons, we want to find  $\psi(x, \mu, E)$ , the distribution of neutrons within the medium. Then, the asymptotic expression of  $\psi(x, \mu, E)$  for  $x \rightarrow +\infty$ , must be an infinitely increasing self-sustaining mode of the transport equation (3.28); but there is only one such mode, (from Section 3.3), namely:

$$\Phi_0(\nu_0, \mu) e^{+\frac{x}{\nu_0}} \chi(E) = \frac{c_F + c_i + c_e}{2} \frac{\nu_0}{\nu_0 + \mu} e^{+\frac{x}{\nu_0}} \chi(E) \quad (3.39)$$

where  $\nu_0$  is the root of Eq. (3.33b).

So keeping in mind this asymptotic condition, and considering the decomposition introduced in Section 3.4, we realize that we have to keep the space-energy separable Eq. (3.30) only, and that there are no slowing-down transients. Throughout the whole space, we have:

$$\Psi(x, \mu, E) = \Phi_E(x, \mu) \chi(E) \quad (3.40)$$

Hence, the solution is that of a one-speed problem, times  $\chi(E)$ . In particular, the extrapolation distance given by the one-speed extrapolation distance (providing one uses  $c_F + c_e + c_i$  as the multiplication coefficient). Of course, one might object to the fact that, physically, the Milne problem corresponds to an infinite-strength source at infinity, but that the spectrum of this source need not be  $\chi(E)$ . However, the corresponding slowing-down transients would be damped at infinity, and the spectrum of the source would be shifted to  $\chi(E)$  at infinity; so there is no contradiction with the asymptotic condition (3.39).

#### 3.5.4. Slab Criticality Problem

A classical theorem<sup>33</sup> states that the solution to the criticality problem is unique, providing it exists. But an obvious solution is given by the monokinetic Eq. (3.30): the neutron distribution is space-energy separable

throughout the whole space, proportional to the fundamental energy-mode  $\psi(E)$ , and the criticality conditions are those given by a one-speed equation with the multiplication coefficient  $c_F + c_i + c_e$ .<sup>33</sup> Since such a solution is unique, the criticality problem involves only self-sustaining energy-modes, which is quite reasonable physically.

In conclusion, though the Milne and criticality problems involve only space-energy separable modes, we have in most cases competition between these asymptotic modes and slowing-down transients.

For, checking again the infinite-medium Green's function (Eq. (3.33a)) and the solution of the Albedo problem (Eq. (3.38)), we see that both consist of three components.

The first one corresponds to space-energy separable modes, asymptotically dominant; the third one is negligible, being simultaneously an energy-transient (slowing-down transients) and a transport transient (decaying faster than  $e^{-|x|}$ ). The second one is a slowing-down transient, but not a transport transient: it is a combination of Case's regular modes. This is indeed the component on which we must focus our attention. Clearly, a necessary step is to simplify the  $\mathcal{M}$ -transform inversion-formula involved in this component.

## CHAPTER IV

### NEUTRON TRANSPORT EQUATION WITH FISSION AND ANISOTROPIC SCATTERING

#### 4.1. ISOTROPY VERSUS ANISOTROPY

This chapter stands somewhat apart, since most of the further applications will be dealing with fast-systems where isotropic scattering is dominant (inelastic slowing-down).

Yet one must question to what extent the fundamental results obtained are bound to the isotropic character of collisions: the coexistence of space-energy separable modes with slowing-down transients of null measure could be a mere consequence of the (relative) simplicity of isotropic scattering, or it could have a much more general existence and meaning. It is, indeed, the purpose of this chapter to show that similar results hold for fission and general anisotropic elastic scattering slowing-down. We will show that the solution still includes asymptotic space-energy separable components, and slowing-down transients, solution of a plain slowing-down equation. However, the technique of solution is much more complicated since we have not been able to obtain a decomposition analogous to the one outlined in Section 3.4. The reason is that energy-transfer between different angular harmonics takes place. Nevertheless, we keep as a guideline the idea of using slowing-down transient modes, whose total measure is zero.

#### 4.2. A METHOD OF SOLUTION USING SINGULAR NORMAL MODES

We will treat the case of a light elastic scatterer, using a sequence of

Greuling-Goertzel kernels to approximate the different angular harmonics.

The general equation is:

$$\begin{aligned}
 \mu \frac{\partial \Psi}{\partial x}(x, \mu, u) + \Psi(x, \mu, u) = & \frac{c_s}{2} \int_{-\infty}^u G_0(u-u') du' \int_{-1}^{+1} \Psi(x, \mu', u') d\mu' \\
 & + \frac{c_F}{2} \chi(u) \int_{-\infty}^{+\infty} du' \int_{-1}^{+1} \Psi(x, \mu', u') d\mu' \\
 & + \frac{c_s}{2} \left\{ \sum_{n=1}^{\infty} (2n+1) P_n(\mu) \int_{-\infty}^u G_n(u-u') \right. \\
 & \left. (x) \int_{-1}^{+1} P_n(\mu') \Psi(x, \mu', u') d\mu' \right\} \\
 & + S(x, \mu, u) \tag{4.1}
 \end{aligned}$$

The  $P_n(\mu)$  are Legendre polynomials and  $G_n(u)$  the Greuling-Goertzel kernels representing energy-transfer in the  $n$ th angular harmonic.<sup>34</sup> One could as well use the exact energy-transfer kernels of elastic scattering, since they are convolution kernels, too. However, if one uses Laplace or Fourier transforms of the lethargy variable, the inversion is made much easier with Greuling-Goertzel kernels.

If one now integrates Eq. (4.1) over the whole lethargy range, one obtains the one-speed anisotropic problem solved extensively by Mika.<sup>50</sup> By suppressing the fission kernel in Eq. (4.1), one finds the elastic slowing-down problem solved by Jacobs and MacInerney.<sup>11</sup> Though none of these works

can be straightforwardly extended to solve Eq. (4.1), we will refer to them for many techniques of calculation.

For the sake of brevity, we will deal with linear anisotropy. Extension to general anisotropy is readily made. The equations are:

$$\begin{aligned}
\mu \frac{\partial \Psi}{\partial x}(x, \mu, u) + \Psi(x, \mu, u) &= \frac{C_S}{2} \int_{-\infty}^u G_0(u-u') du' \int_{-1}^{+1} \Psi(x, \mu', u') d\mu' \\
&+ \frac{C_F}{2} \chi(u) \int_{-\infty}^{+\infty} du' \int_{-1}^{+1} \Psi(x, \mu', u') d\mu' \\
&+ \frac{3}{2} C_S \mu \int_{-\infty}^u G_1(u-u') du' \int_{-1}^{+1} \Psi(x, \mu', u') \mu' d\mu' + S(x, \mu, u)
\end{aligned} \tag{4.2a}$$

We transform Eq. (4.2a) by using a Fourier transform of the lethargy:

$$\begin{aligned}
\bar{\Psi}(x, \mu, k) &= \int_{-\infty}^{+\infty} \Psi(x, \mu, u') e^{-iku'} du' \\
\mu \frac{\partial \bar{\Psi}}{\partial x}(x, \mu, k) + \bar{\Psi}(x, \mu, k) &= \frac{C_S}{2} \bar{G}_0(k) \int_{-1}^{+1} \bar{\Psi}(x, \mu', k) d\mu' \\
&+ \frac{C_F}{2} \bar{\chi}(k) \int_{-1}^{+1} \bar{\Psi}(x, \mu', 0) d\mu' \\
&+ \frac{3}{2} C_S \mu \bar{G}_1(k) \int_{-1}^{+1} \bar{\Psi}(x, \mu', k) \mu' d\mu' + \bar{S}(x, \mu, k)
\end{aligned} \tag{4.2b}$$

By setting  $k = 0$

$$\bar{\Psi}(x, \mu, 0) = \int_{-\infty}^{+\infty} \Psi(x, \mu, u') du'$$

we find Mika's one-speed equation:

$$\begin{aligned} \mu \frac{\partial \bar{\Psi}}{\partial x}(x, \mu, 0) + \bar{\Psi}(x, \mu, 0) &= \frac{c_F + c_S}{2} \int_{-1}^{+1} \bar{\Psi}(x, \mu', 0) d\mu' \\ &+ \frac{3}{2} \mu c_S B_1 \int_{-1}^{+1} \mu' \bar{\Psi}(x, \mu', 0) d\mu' + \bar{S}(x, \mu, 0) \end{aligned} \quad (4.2c)$$

(where  $B_1 = \bar{G}_1(0)$ ).

Let us look for normal modes solutions of the homogeneous Eq. (4.2b),

that is, solutions of the shape:

$$\Phi(t, \mu, k) e^{-x/t} \quad (4.3a)$$

put

$$\Phi_0(t, k) = \int_{-1}^{+1} \Phi(t, \mu, k) d\mu \quad (4.3b)$$

$$\Phi_1(t, k) = \int_{-1}^{+1} \mu \Phi(t, \mu, k) d\mu \quad (4.3c)$$

Then, following a classical approach<sup>33,50</sup>:



$$\begin{aligned} \Phi(t, \mu, k) = & \frac{t}{2} P \frac{1}{t-\mu} \left\{ c_s \bar{G}_0(k) \Phi_0(t, k) \right. \\ & \left. + c_F \bar{\chi}(k) \Phi_0(t, 0) + 3\mu c_s \bar{G}_1(k) \Phi_1(t, k) \right\} \\ & + \delta(t-\mu) \lambda(t, k) \end{aligned} \quad (4.4)$$

with

$$\begin{aligned} \lambda(t, k) = & \Phi_0(t, k) - t c_s \Phi_0(t, k) \bar{G}_0(k) Q_0(t) \\ & - t c_F \Phi_0(t, 0) \bar{\chi}(k) Q_0(t) - 3t c_s \Phi_1(t, k) \bar{G}_1(k) Q_1(t) \end{aligned} \quad (4.5a)$$

$Q_0(z)$ ,  $Q_1(z)$  are Legendre functions of the second kind

$$Q_0(z) = \frac{1}{2} \int_{-1}^{+1} \frac{d\mu}{z-\mu}, \quad Q_1(z) = \frac{1}{2} \int_{-1}^{+1} \frac{\mu d\mu}{z-\mu} \quad (4.5b)$$

If  $\Phi_0(t, k)$  is arbitrary, then  $\Phi_1(t, k)$  is readily obtained (see Ref. 11 and 50):

$$\Phi_1(t, k) = t \left\{ \Phi_0(t, k) \cdot (1 - c_s \bar{G}_0(k)) - c_F \bar{\chi}(k) \cdot \Phi_0(t, 0) \right\} \quad (4.6)$$

Let us look now for discrete regular modes. In general, there are only two such modes, corresponding to eigenvalues  $\pm L_0$ , such that (see Eqs. (4.4) and (4.5a)):

$$\lambda(L_0, k) = 0 \quad (4.7a)$$

One sees at once that  $\pm L_0$  are also the discrete eigenvalues of the one-speed equation (4.2c). For critical review of these eigenvalues, we refer to Mika.<sup>50</sup>

The discrete modes will be:

$$\Phi(\pm L_0, \mu, k) e^{(\mp x/L_0)} \quad (4.7b)$$

with

$$\begin{aligned} \Phi(L_0, \mu, k) = \frac{1}{2} \frac{L_0}{L_0 - \mu} \left\{ c_s \bar{G}_0(k) \Phi_0(L_0, k) + c_F \bar{\chi}(k) \right. \\ \left. + 3c_s \bar{G}_1(k) \mu \Phi_1(L_0, k) \right\} \quad (4.7c) \end{aligned}$$

Here, we normalized

$$\Phi_0(L_0, 0) = 1 \quad (4.7d)$$

And  $\Phi_0(L_0, k)$  is solution of Eq. (4.7a), that is:

$$\begin{aligned} \frac{1}{L_0} \Phi_0(L_0, k) = c_s \bar{G}_0(k) Q_0(L_0) \Phi_0(L_0, k) \\ + 3c_s \bar{G}_1(k) Q_1(L_0) \Phi_1(L_0, k) + c_F \bar{\chi}(k) Q_0(L_0) \quad (4.8) \end{aligned}$$

Using Eq. (4.6), which yields  $\Phi_1(L_0, k)$  in terms of  $\Phi_0(L_0, k)$ , Eq. (4.8) is very easily soluble. Then one can easily find the inverse Fourier transform of  $\Phi_0(L_0, k)$ , provided one has been using Greuling-Goertzel kernels.

Anticipating future developments, we can stress that the discrete regular modes  $\Phi(\pm L_0, \mu, u) e^{\pm x/L_0}$  will be the only space-energy separable components of the complete solution. In an exponential experiment, one tries usually to measure these asymptotic separable modes, and an isotropic detector will be therefore sensitive to the "equilibrium" spectrum  $\Phi_0(\pm L_0, u)$ .

#### 4.3. INCOMPLETENESS AND COMPLETENESS OF THE NORMAL MODES

Now let us turn to the completeness of our set of normal modes, as defined by Eq. (4.4) and Eq. (4.7). As we shall see, these modes are not complete by themselves, and we shall have to add "slowing-down transients" of measure zero, for both full- and half-range completeness. First, the full-range hypothetical completeness theorem can be stated as:

$$\Psi(\mu, k) = \sum A_{0\pm} \bar{\Phi}(\pm L_0, \mu, k) + \int_{-1}^{+1} \bar{\Phi}(t, \mu, k) dt \quad (4.9)$$

where  $\Psi(\mu, k)$  is an arbitrary function of  $\mu$  and of the lethargy-transformed variable  $K$ .

Checking Eq. (4.3b) and Eq. (4.4), where we define  $\Phi(t, \mu, k)$ , one sees immediately that we are taking  $\Phi_0(t, k)$  as the unknown expansion coefficient of our continuum of singular modes, similar to the coefficient used by Mika and Jacobs-MacInerney in their respective completeness proofs.<sup>11,50</sup> Hence, for many intermediate steps in the following proof, the reader is referred to Mika's work.<sup>50</sup>

So, applying Mika's procedure, we define, omitting many calculations:

$$\begin{aligned}
\Psi''(\mu, k) &= \Psi(\mu, k) - \sum A_{0\pm} \Phi(\pm L_0, \mu, k) \\
&\quad - \frac{1}{2} \left\{ c_s \bar{G}_0(k) \int_{-1}^{+1} \Phi_0(t, k) dt + c_F \bar{\chi}(k) \int_{-1}^{+1} \Phi_0(t, 0) dt \right\} \\
&\quad - \frac{3}{2} c_s \bar{G}_1(k) \mu \left\{ (1 - c_s \bar{G}_0(k)) \int_{-1}^{+1} t \Phi_0(t, k) dt - c_F \bar{\chi}(k) \int_{-1}^{+1} t \Phi_0(t, 0) dt \right\} \\
&\quad - \frac{3}{2} \mu^2 c_s \bar{G}_1(k) \left\{ (1 - c_s \bar{G}_0(k)) \int_{-1}^{+1} \Phi_0(t, k) dt - c_F \bar{\chi}(k) \int_{-1}^{+1} \Phi_0(t, 0) dt \right\}
\end{aligned}$$

Then define:

$$F(z, k) = \frac{1}{2i\pi} \int_{-1}^{+1} \Psi''(\mu, k) \frac{d\mu}{\mu - z} \quad (4.11)$$

also

$$\Omega_s(z, k) = 1 - z \left\{ c_s \bar{G}_0(k) Q_0(z) + 3 c_s \bar{G}_1(k) (1 - c_s \bar{G}_0(k)) Q_1(z) \right\} \quad (4.12)$$

$$\Omega_F(z, k) = -z \left\{ c_F \bar{\chi}(k) Q_0(z) - 3 c_s \bar{G}_1(k) c_F \bar{\chi}(k) Q_1(z) \right\} \quad (4.13)$$

$$N(z, k) = \frac{1}{2\pi i} \int_{-1}^{+1} \frac{\Phi_0(t, k)}{t - z} dt \quad (4.14)$$

(let us recall that  $\Phi_0(t, k)$  is the unknown expansion coefficient). The functions  $N(z, k)$  and  $F(z, k)$  are analytic in the  $z$ -complex plane cut from

$[-1,+1]$ .  $\Omega_S(z,k)$  and  $\Omega_F(z,k)$  are analytic in the  $z$ -complex plane cut from  $[-1,+1]$ , with the exception of possible poles.

Moreover,

$$\Omega_S(z,0) + \Omega_F(z,0) \equiv \Lambda(z) \quad (4.15)$$

$\Lambda(z)$  is the function used by Case and Mika<sup>33,50</sup> in the monokinetic case.

This function is associated with the well-known solution of Eq. (4.2c).

Then, one can prove the following fact: Eq. (4.9) is strictly equivalent to:

$$\begin{aligned} F^+(\mu,k) - F^-(\mu,k) = & \left\{ \Omega_S^+(\mu,k) N^+(\mu,k) - \Omega_S^-(\mu,k) N^-(\mu,k) \right\} \\ & + \left\{ \Omega_F^+(\mu,k) N^+(\mu,0) - \Omega_F^-(\mu,k) N^-(\mu,0) \right\} \end{aligned} \quad (4.16)$$

(where  $\pm$  means the value taken by an analytic function of  $z$  above and below the cut  $[-1,+1]$ ). Thus:

$$F(z,k) = \Omega_S(z,k) N(z,k) + \Omega_F(z,k) N(z,0) \quad (4.17)$$

Setting  $k = 0$  in Eq. (4.17) and using Eq. (4.15), one finds at once  $N(z,0)$ :

$$N(z,0) = \frac{F(z,0)}{\Lambda(z)} \quad (4.18)$$

And we get:

$$N(z, k) = \frac{1}{\Omega_s(z, k)} \left\{ F(z, k) - \frac{\Omega_F(z, k) F(z, 0)}{\Lambda(z)} \right\} \quad (4.19)$$

Thus, the problem of finding  $N(z, k)$  (that is the unknown expansion coefficient, see Eq. (4.14)), seems to be solved. However  $N(z, k)$  must not have any singularities in  $z$  outside the cut  $[-1, +1]$ . Checking Eq. (4.19), we see that the delicate points are the zeros of  $\Lambda(z)$  and  $\Omega_s(z, k)$ . First:

$\Lambda(\pm L_0) = 0$ ; hence we must have

$$F(\pm L_0, 0) = 0 \quad (4.20)$$

Condition (4.20) is fulfilled through the discrete modes (4.7) introduced in Eqs. (4.9) and (4.10). One verifies easily that the discrete expansion coefficients  $A_{0\pm}$  (Eqs. (4.9), (4.10), (4.11)) are exactly the same as those given by the well-known solutions of the monokinetic equation (4.2c).<sup>33,50</sup>

A more difficult problem lies in the zeros of  $\Omega_s(z, k)$ . For a fixed  $k$ ,  $\Omega_s(z, k)$  has zeros  $z = J(k)$  such that:

$$\Omega_s[J(k), k] = 0 \quad (4.21)$$

$z = J(k)$  is of course a function of  $k$  (possibly multivalued). However, we have exhausted our supply of discrete regular modes solution of Eq. (4.2c), in order to cope with the further singularities introduced by  $\Omega_s(z, k)$ . We

should therefore conclude that the set of normal modes defined by Eqs. (4.3), (4.4), (4.5), (4.7), is incomplete.

But we can notice that  $\Omega_s(z, k)$  is a function associated with the plain slowing-down problem (Eq. (4.2b) without fission) as solved extensively by Jacobs and MacInerney.<sup>11</sup> One can think of using the discrete regular normal modes of the plain slowing-down problem:

$$\Psi(J(k), \mu, k) e^{-x/J(k)} \quad (4.22)$$

with  $J(k)$  given by (4.21), as introduced by these former authors. Instead of expanding

$$\Psi(\mu, k) - \sum A_{o\pm} \Phi(\pm L_o, \mu, k)$$

as in Eq. (4.9), one can try to expand:

$$\Psi(\mu, k) - \sum A_{o\pm} \Phi(\pm L_o, \mu, k) - B(k) \Psi(J(k), \mu, k) \quad (4.23a)$$

or, equivalently, instead of  $F(z, k)$ , use:

$$F(z, k) - \frac{B(k)}{2\pi i} \int_{-1}^{+1} \frac{\Psi(J(k), \mu, k)}{\mu - z} d\mu \quad (4.23b)$$

In order that the expressions (4.23a) and (4.23b) correspond to a solution of the complete transport equation with a fission kernel, one must have:

for

$$B(k) = 0 \quad \text{FOR } k=0 \quad (4.24)$$

That is, one is introducing discrete normal modes of the plain slowing-down equation, whose integral over the whole lethargy range (measure) is zero ("slowing down transients"). One verifies indeed that this scheme works fully. For, if

$$\Omega_s [J(k), k] = 0 \quad (4.21)$$

we get immediately  $B(k)$  from Eq. (4.19):

$$B(k) = \left\{ F(J(k), k) - \frac{\Omega_F(J(k), k) F(J(k), 0)}{\Lambda(J(k))} \right\} \\ (x) \left\{ \frac{1}{2\pi i} \int_{-1}^{+1} \frac{\Psi(J(k), \mu, k) d\mu}{\mu - J(k)} \right\}^{-1} \quad (4.25)$$

The crucial point is the verification of (4.24). Indeed,  $B(0)$  is proportional to:

$$F(J(0), 0) - \Omega_F [J(0), 0] \frac{F(J(0), 0)}{\Lambda(J(0))} \\ = F(J(0), 0) \left\{ \frac{\Lambda(J(0)) - \Omega_F [J(0), 0]}{\Lambda(J(0))} \right\} \\ = F(J(0), 0) \frac{\Omega_s [J(0), 0]}{\Lambda(J(0))} \quad (4.26)$$



(if we remember Eq. (4.15)). But, in Eq. (4.26),  $\Omega_s(J(0),0) = 0$ , because of Eq. (4.21). While  $\Lambda(J(0)) \neq 0$ . Hence

$$B(0) = 0 \quad (4.24)$$

To summarize, we have proved that the full-range completeness theorem must be stated as:

$$\begin{aligned} \Psi(\mu, k) = & \sum A_{o\pm} \Phi(\pm L_o, \mu, k) + B(k) \Psi(J(k), \mu, k) \\ & + \int_{-1}^{+1} \Phi(t, \mu, k) dt \end{aligned} \quad (4.27)$$

where  $\Phi(\pm L_o, \mu, k)$  are the discrete regular modes of Eq. (4.2b), as defined in Eq. (4.7), and  $\Psi(J(k), \mu, k)$  are the discrete regular modes of the plain slowing-down problem, as introduced by Jacobs and MacInerney. The superposition of the latter modes has indeed a null measure, hence the name of "slowing down transients."

The very same completeness theorem holds for the half-range domain, as it will be shown in the Appendix, although calculations are more involved.

$$\Psi(\mu, k) = a_o \Phi(+L_o, \mu, k) + B(k) \Psi(J(k), \mu, k) + \int_0^1 \Phi(t, \mu, k) dt \quad (4.28)$$

And the solution of Milne's problem will be:

$$\begin{aligned}
\psi(x, \mu, u) = & \Phi(-L_0, \mu, u) e^{+x/L_0} \\
& + a_0 \Phi(+L_0, \mu, u) e^{-x/L_0} + \frac{1}{2\pi} \int_{-\infty}^{+\infty} B(k) \Psi[J(k), \mu, k] e^{-x/J(k)} e^{iku} dk \\
& + \frac{1}{2\pi} \int_{-\infty}^{+\infty} e^{iku} dk \int_0^1 \Phi(t, \mu, k) dt
\end{aligned} \tag{4.29}$$

$a_0$  and  $L_0$  will be identical to the equivalent parameters found in solving the one-speed equation (4.2c). The great difference lies in the presence of slowing-down transients.

#### 4.4. CONCLUSION

The present work has shown that the solution of the energy-dependent Boltzmann equation with anisotropic elastic slowing-down and fission, is far from being straightforward. Neither prior works dealing with a monokinetic equation (Mika), nor works solving the plain slowing-down problem<sup>11</sup> could foretell the following basic features due to fission regeneration, that is: the coexistence, in the solution of any transport problem (half-space, full-space) of space-energy separable regular discrete modes, with nonseparable (but regular) "slowing-down transient" modes.

It has to be stressed that the "slowing-down transients", though decaying spatially faster than the separable modes, still decay more slowly than the classical continuum transport transients. Hence, these effects will be

important in the interpretation of integral experiments in the fast-energy range; for instance, in an exponential experiment, one usually wishes to measure a well-defined, space-energy separable asymptotic (equilibrium) mode. However, experimentalists often acknowledged that they were not sure whether or not they had reached such an equilibrium distribution.<sup>36-42</sup> As far as we can know, the present work gives the first theoretical explanation of this experimental difficulty: there is competition between space-energy separable modes and slowing-down transients, the latter decaying sometimes rather slowly into space. In the next chapters, we will do a detailed study and calculation on this transport-interpretation of exponential experiments.

#### 4.5. APPENDIX B. HALF-RANGE COMPLETENESS THEOREM IN THE ANISOTROPIC CASE

In this concise appendix complete familiarity will be assumed with the completeness theorem of Jacobs and MacInerney,<sup>11</sup> though by no means will it be a straightforward extension.

We wish to prove half-range completeness. The starting point will be Eq. (4.16):

$$\begin{aligned} \psi''(\mu, k) = & \left\{ \Omega_S^+(\mu, k) N^+(\mu, k) - \Omega_S^-(\mu, k) N^-(\mu, k) \right\} \\ & + \left\{ \Omega_F^+(\mu, k) N^+(\mu, 0) - \Omega_F^-(\mu, k) N^-(\mu, 0) \right\} \end{aligned} \quad (4.16)$$

With, this time:

$$N(z, k) = \frac{1}{2\pi i} \int_0^1 \frac{\Phi_0(t, k)}{t-z} dt \quad (4.30)$$

If we set  $k = 0$  in Eq. (4.16), we find the solution of the associated one-speed equation (4.2c); hence  $N(z, 0)$  is perfectly well known from previous half-space one-speed solutions.<sup>33,50</sup> So, we are permitted to consider  $N(z, 0)$ ,  $N^+(\mu, 0)$ ,  $N^-(\mu, 0)$  as perfectly well known functions. Hence, set

$$\Psi'''(\mu, k) = \Psi''(\mu, k) - \left\{ \Omega_F^+(\mu, k) N^+(\mu, 0) - \Omega_F^-(\mu, k) N^-(\mu, 0) \right\} \quad (4.31a)$$

and Eq. (4.16) becomes:

$$\Psi'''(\mu, k) = \Omega_S^+(\mu, k) N^+(\mu, k) - \Omega_S^-(\mu, k) N^-(\mu, k) \quad (4.31b)$$

Define

$$X_S(z, k) = \frac{1}{1-z} \exp \left\{ \frac{1}{2i\pi} \int_0^1 \log \left\{ \frac{\Omega_S^+(\mu, k)}{\Omega_S^-(\mu, k)} \right\} \frac{d\mu}{\mu-z} \right\} \quad (4.32)$$

we have

$$\frac{X_S^+(\mu, k)}{X_S^-(\mu, k)} = \frac{\Omega_S^+(\mu, k)}{\Omega_S^-(\mu, k)} \quad (4.33)$$

Then Eq. (4.31b) can be rewritten as:

$$\frac{X_s^-(\mu, k)}{\Omega_s^-(\mu, k)} \Psi'''(\mu, k) = X_s^+(\mu, k) N^+(\mu, k) - X_s^-(\mu, k) N^-(\mu, k) \quad (4.34)$$

Define

$$S(z, k) = \frac{1}{2i\pi} \int_0^1 \frac{X_s^-(\mu, k)}{\Omega_s^-(\mu, k)} \frac{\Psi'''(\mu, k)}{\mu - z} d\mu \quad (4.35)$$

$S(z, k)$ ,  $X_s(z, k)$ ,  $N(z, k)$  are all functions analytic in  $z$  outside the cut  $[0, +1]$ . Thus from Eq. (4.34):

$$N(z, k) = \frac{S(z, k)}{X_s(z, k)} \quad (4.36)$$

$N(z, k)$  must behave as  $1/z$  at infinity. This requires classically<sup>33</sup> that, instead of expanding  $\Psi'''(\mu, k)$ , we expand:

$$\Psi'''(\mu, k) - B(k) \Psi(J(k), \mu, k) \quad (4.37)$$

$\Psi(J(k), \mu, k)$  being defined in (4.22). Classically,  $B(k)$  will be given by:

$$B(k) \int_0^1 \frac{X_s^-(\mu, k)}{\Omega_s^-(\mu, k)} \Psi(J(k), \mu, k) d\mu = \int_0^1 \frac{X_s^-(\mu, k)}{\Omega_s^-(\mu, k)} \Psi'''(\mu, k) d\mu \quad (4.38)$$

Again we must have condition (4.24):  $B(0) \equiv 0$  (slowing-down transients).

Equation (4.24) is equivalent to:

$$\int_0^1 \frac{X_s^-(\mu, 0)}{\Omega_s^-(\mu, 0)} \psi'''(\mu, 0) d\mu = 0 \quad (4.39a)$$

Using Eq. (4.34), Eq. (4.39a) becomes:

$$\int_0^1 \left\{ X_s^+(\mu, 0) N^+(\mu, 0) - X_s^-(\mu, 0) N^-(\mu, 0) \right\} d\mu = 0 \quad (4.39b)$$

This is indeed the crucial step; for  $X_s(z, 0)$  and  $N(z, 0)$  are perfectly well-known functions, analytic in the  $z$ -plane cut from  $0, +1$  and both behaving as  $1/z$  at infinity. So:

$$\begin{aligned} & \int_0^1 \left\{ X_s^+(\mu, 0) N^+(\mu, 0) - X_s^-(\mu, 0) N^-(\mu, 0) \right\} d\mu \\ &= \oint_c X_s(z, 0) N(z, 0) dz \end{aligned} \quad (4.39c)$$

where  $c$  is a contour in the complex  $z$ -plane (see Fig. 8). Then from Cauchy's theorem (no singularities within  $c$ ):

$$\oint_c X_s(z, 0) N(z, 0) dz \equiv 0 \quad (4.39d)$$

and, indeed

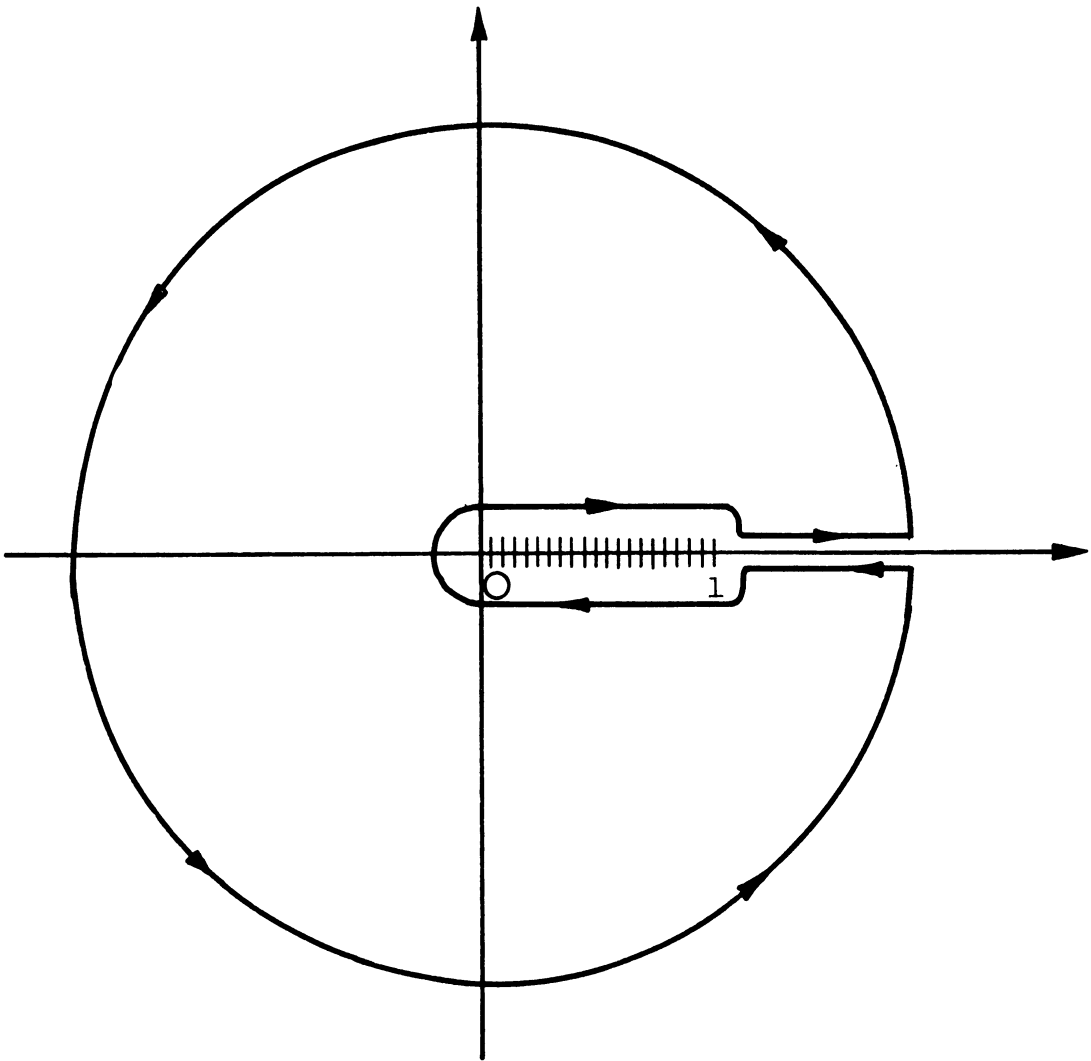


Fig. 8. The contour  $C$  in the  $z$ -complex plane.

for

$$B(k) \equiv 0 \quad \text{For} \quad k \equiv 0 \quad (4.24)$$

So, we proved the following half-range completeness theorem, similar to the full-range one:

$$\begin{aligned} \Psi(\mu, k) = a_0 \Phi(L_0, \mu, k) + B(k) \Psi(J(k), \mu, k) \\ + \int_0^1 \Phi(t, \mu, k) dt \end{aligned} \quad (4.28)$$

The coefficient  $a_0$  is readily given by the solution of the associated one-speed equation (4.2c).<sup>33,50</sup>



## CHAPTER V

### ASYMPTOTIC BEHAVIOR OF THE SLOWING-DOWN TRANSIENTS

#### 5.1. INTRODUCTION

The preceding chapters emphasized the importance and generality of the coexistence of space-energy separable modes, asymptotically dominant, with slowing-down transients. A goal for further investigation is to make a numerical evaluation of the extent to which these slowing-down transient modes delay the approach to equilibrium in integral experiments on fast multiplying media. Of prime importance would be those slowing-down transients which decay more slowly than  $e^{-\Sigma_T \min|x|}$ , where  $\Sigma_T \min$  is the minimum of the total cross-section; such terms are energy-spectral transients, but not transport spatial transients; they have been already considered explicitly at the end of Section 3.5 (Eqs. (3.33a) and (3.38)); however, their analytical expressions are not immediately amenable to numerical evaluation, since they involve a contour-integral in a complex plane (see Sections 2.5 and 3.5). The purpose of this chapter is to develop improved asymptotic formulae for the solutions of the plain slowing-down problem we introduced in Section 2.5 and used in problems on multiplying media (Section 3.5).

#### 5.2. INTRODUCTION OF AN ENERGY-GREEN'S FUNCTION

Consider the slowing-down Eq. (2.12b)

$$\begin{aligned} \mu \frac{\partial \Psi}{\partial x}(x, \mu, E) + \Psi(x, \mu, E) &= \frac{c_i}{2} \int_{-1}^{+1} d\mu' g(E) \int_E^{\infty} \frac{\Psi(x, \mu', E')}{h(E')} dE' \\ &+ \frac{c_e}{2} \int_{-1}^{+1} \Psi(x, \mu', E) d\mu' + \frac{1}{2} \delta(x-x_0) S(E) \end{aligned} \quad (2.12b)$$

Applying an  $\mathcal{M}$ -transformation to Eq. (2.12b), we obtained:

$$\begin{aligned} \mu \frac{\partial \bar{\Psi}}{\partial x}(x, \mu, \lambda) + \bar{\Psi}(x, \mu, \lambda) &= \frac{1}{2} \left( c_e + \frac{c_i}{\lambda} \right) \int_{-1}^{+1} \bar{\Psi}(x, \mu', \lambda) d\mu' \\ &+ \frac{1}{2} \delta(x-x_0) \bar{S}(\lambda) \end{aligned} \quad (2.35)$$

At this point, let us recall from Section 2.4 that:

$$\begin{aligned} \bar{\Psi}(x, \mu, \lambda) &= \mathcal{M} \circ \Psi(x, \mu, E) \\ &= \int_0^{\infty} \Psi(x, \mu, E) h(E)^{\lambda-1} dE \\ &= \int_0^1 \Psi(x, \mu, v) v^{\lambda-1} dv \end{aligned}$$

where

$$\begin{aligned} \Psi(x, \mu, E) &= \frac{1}{g(E)} \psi(x, \mu, E) \\ v &= h(E) \end{aligned}$$

with the normalization  $h(\infty) = 1$ . Let us also recall the inversion formula (2.43):

$$\Psi(x, \mu, E) = \frac{1}{2\pi i} g(E) \int_{c-i\infty}^{c+i\infty} \bar{\Psi}(x, \mu, \lambda) v^{-\lambda} d\lambda \quad (2.43)$$

Considering the transformed equation (2.35), we note that it is homogeneous in the  $\lambda$ -variable; this leads us to introduce an energy-Green's function  $G(x, \mu, E)$  such that:

$$G(x, \mu, \lambda) = \mathcal{M} \otimes G(x, \mu, E) \quad (5.1a)$$

where  $\bar{G}(x, \mu, \lambda)$  obeys the transformed equation:

$$\begin{aligned} \mu \frac{\partial \bar{G}}{\partial x}(x, \mu, \lambda) + \bar{G}(x, \mu, \lambda) &= \frac{1}{2} \left( ce + \frac{ci}{\lambda} \right) \int_{-1}^{+1} \bar{G}(x, \mu', \lambda) d\mu' \\ &+ \frac{1}{2} \delta(x - x_0) \end{aligned} \quad (5.1b)$$

The energy-Green's function  $G(x, \mu, E)$  corresponds to a Dirac distribution source at infinite energy. Then, we have the obvious relation between  $G(x, \mu, \lambda)$  and the general solution of Eq. (2.35) corresponding to an arbitrary source spectrum:

$$\bar{\Psi}(x, \mu, \lambda) = \bar{S}(\lambda) \bar{G}(x, \mu, \lambda) \quad (5.2)$$

The next problem is to invert the relation (5.2), that is, to find a "convolution" theorem for the  $\mathcal{M}$ -transformation:

Theorem 5.2.1. If  $\bar{F}(\lambda)$  and  $\bar{G}(\lambda)$  are the  $\mathcal{M}$ -transforms of  $F(E)$  and  $G(E)$ , then the inverse-transform of the product  $\bar{F}(\lambda) \cdot \bar{G}(\lambda)$  is:

$$\mathcal{M}^{-1} [ \bar{F}(\lambda) \cdot \bar{G}(\lambda) ] = g(E) \int_v^1 F' \left( \frac{v}{w} \right) G' \left( \frac{v}{w} \right) \frac{dw}{w}$$

where

$$F'(E) = F(E)/g(E) \quad G'(E) = G(E)/g(E)$$

$$v = h(E) \quad w = h(E')$$

Proof: Defining  $F'(E) = F(E)/g(E)$ ,  $G'(E) = G(E)/g(E)$ , we can rewrite the transformation  $\mathcal{M}$  as:

$$\bar{F}(\lambda) = \int_0^1 F'(v) v^{\lambda-1} dv$$

$$\bar{G}(\lambda) = \int_0^1 G'(v) v^{\lambda-1} dv$$

where we used the transformation defined in (2.37):

$$v = h(E) \tag{2.37}$$

As we know from (2.38), this is nothing but a classical Mellin-transform.

Then, a classical "convolution theorem" for the Mellin transform\*<sup>44</sup> states that:

---

\*Bateman tables, Vol. I, p. 245, relation 35.

$$\frac{1}{2\pi i} \int_{c-i\infty}^{c+i\infty} \overline{F(\lambda)} \overline{G(\lambda)} v^{-\lambda} d\lambda = \int_0^1 F\left(\frac{v}{w}\right) G\left(\frac{v}{w}\right) \frac{dw}{w}$$

In fact, this can be proved very easily:

$$\begin{aligned} \frac{1}{2\pi i} \int_{c-i\infty}^{c+i\infty} \overline{F(\lambda)} \overline{G(\lambda)} v^{-\lambda} d\lambda &= \frac{1}{2\pi i} \int_{c-i\infty}^{c+i\infty} \overline{F(\lambda)} v^{-\lambda} d\lambda \int_0^1 G'(w) w^{\lambda-1} dw \\ &= \int_0^1 G'(w) \frac{dw}{w} \frac{1}{2\pi i} \int_{c-i\infty}^{c+i\infty} \overline{F(\lambda)} \left(\frac{v}{w}\right)^{-\lambda} d\lambda \\ &= \int_0^1 F'\left(\frac{v}{w}\right) G'(w) \frac{dw}{w} \end{aligned}$$

We notice that:

$$F'(v) = G'(v) = 0 \quad \text{for } v > 1$$

So:

$$\int_0^1 F'\left(\frac{v}{w}\right) G'(w) \frac{dw}{w} = \int_v^1 F'\left(\frac{v}{w}\right) G'(w) \frac{dw}{w}$$

And finally, taking into account the factor  $g(E)$ :

$$\mathcal{M}^{-1} \otimes [\overline{F(\lambda)} \overline{G(\lambda)}] = g(E) \int_v^1 F'\left(\frac{v}{w}\right) G'(w) \frac{dw}{w}$$

Q.E.D.

We can clarify further this result by making another change of variable and introducing a new "lethargy" variable related to the inelastic slowing-down:

$$v = h(E)$$

$$u = -\log v$$

or

$$u = -\log \{h(E)\} \quad (5.3)$$

The change of variable  $E \Leftrightarrow u$  is a one-to-one mapping of  $E \in [0, +\infty]$  onto  $u \in [+\infty, 0]$ . The Jacobian of the transformation is:

$$du = -\frac{dv}{v} = -\frac{g(E)}{h(E)} dE \quad (5.4)$$

Then our "convolution theorem" can be rewritten as:

$$\begin{aligned} \mathcal{M}^{-1} \otimes [F(\lambda) G(\lambda)] &= g(E) \int_v^1 F'(\frac{v}{w}) G'(w) \frac{dw}{w} \\ &= g(E) \int_0^{-\log \{h(E)\}} \left\{ \frac{F}{g}(u-u') \right\} \cdot \left\{ \frac{G}{g}(u') \right\} \cdot du' \end{aligned} \quad (5.5a)$$

where

$$u = -\text{Log } h(E) = -\text{Log } V \quad (5.5b)$$

$$u' = -\text{Log } W \quad (5.5c)$$

This similarity with the classical convolution theorem for Fourier-Laplace transforms, stems from the close relationship between Mellin and Laplace transforms (see (2.40)).

Finally, returning to Eq. (2.12b), (5.1), and (5.2), we obtain the relation between the energy-Green's function  $G(x, \mu, E)$ , the source  $S(E)$  and the distribution  $\psi(x, \mu, E)$ :

$$\psi(x, \mu, E) = G(E) \int_0^{-\text{Log } \{h(E)\}} \frac{S}{g}(u-u') \cdot \frac{G}{g}(x, \mu, u') du' \quad (5.6a)$$

where

$$u = -\text{Log } h(E) \quad (5.6b)$$

This convolution relation enables us to focus our attention on the solution of Eq. (5.1).

### 5.3. FAILURE OF CLASSICAL METHODS OF ASYMPTOTIC EVALUATION

The very nature of the mathematical asymptotic expression desired for

$G(|x|, E)^*$  is closely bound to the requirement of the experimental situations we wish to interpret. In most integral experiments, the source will have a fission-energy spectrum, and we will have to consider solutions of:

$$\begin{aligned} \mu \frac{\partial \Psi}{\partial x} (x, \mu, E) + \Psi(x, \mu, E) &= \frac{c_i}{2} \int_{-1}^{+1} d\mu' g(E) \int_E^{+\infty} \frac{\Psi(x, \mu', E')}{h(E')} dE' \\ &+ \frac{c_e}{2} \int_{-1}^{+1} \Psi(x, \mu', E) d\mu' + \frac{c_f}{2} \int_{-1}^{+1} d\mu' \chi(E) \int_0^{\infty} \Psi(x, \mu', E') dE' \\ &+ \frac{1}{2} \delta(x-x_0) \chi(E) \end{aligned} \quad (5.7)$$

From Eq. (3.33), we know the full-space solution of this problem; call it

$$\Delta(|x|, E) \quad (5.8)$$

As we know from Section 3.4, part of  $\Delta(|x|, E)$  is solution of a plain slowing-down equation, the source-term of which is (see Eq. (3.24)):

$$\frac{1}{2} \delta(x-x_0) \Gamma(E) = \frac{1}{2} \delta(x-x_0) \{ \chi(E) - \mathcal{H}(E) \} \quad (5.9)$$

This source term is quite unusual, to the extent that it has a broad energy-spread:  $\chi(E)$  has a maximum around 0.8 MeV, and  $\mathcal{H}(E)$  peaks typically around 0.1 MeV. This situation is very different from the slowing-down problem in thermal-reactors, where one is chiefly interested in thermalized neutrons:

---

\* $G(|x|, E)$  is the angle-integrated distribution  $G(x, \mu, E)$ .



since the energy of the latter is very far from the fission-source energy, one can usually consider source neutrons and slowed-down neutrons as two sharply distinct groups.<sup>34</sup>

On the contrary, in a fast multiplying medium, the average energy-spectrum of the neutron field is deeply imbedded into the energy-range of the "slowing-down transients" source ( $\chi(E) - \lambda(E)$ ).

Another experimental requirement stems from the generalized use of threshold detectors (such as  $U^{238}$  and  $N_p^{237}$ ) in fast multiplying media: such detectors are commonly used as indicators of spectral equilibrium; for instance, the ratio of  $U^{238}/U^{235}$  fission chambers measurements is a classical spectral index for fast neutron fluxes.<sup>36-42</sup> This means that our mathematical formulae must give us practical information about very high-energy neutrons as well as medium- and low-energy neutrons; otherwise, these mathematics will be mere "pièces de Musée". In plain words, one needs an asymptotic expression valid for absolutely all energies.

This unusually stringent requirement makes useless the classical asymptotic methods used in classical spatial elastic slowing-down problems.<sup>1-11,30,31</sup> In such problems, interest was chiefly concentrated on the spatial distribution of very low energy-neutrons (improved "age-diffusion" theories) or the distribution of very far-away neutrons ("deep/penetration problem"). Then, the most efficient tool was the "saddle-point" method for evaluation of contour integrals.<sup>1-5,11,30,31</sup> Referring to these previous works, we can quickly show how this classical approach fails in our case. Consider the inelastic slowing-down Green's function, solution of Eq. (5.1):

$$\begin{aligned}
G(|x|, E) &= \frac{g(E)}{2\pi i} \int_{c-i\infty}^{c+i\infty} \frac{1}{N_0(\lambda)} \frac{e^{-|x|/\nu_0(\lambda)}}{2} h(E)^{-\lambda} d\lambda \\
&+ \frac{g(E)}{2\pi i} \int_{c-i\infty}^{c+i\infty} h(E)^{-\lambda} d\lambda \int_0^1 \frac{1}{N(\tau, \lambda)} \frac{e^{-|x|/\nu}}{2} d\tau
\end{aligned}
\tag{2.56}$$

Classically, one keeps only terms decaying more slowly than  $e^{-|x|}$ ; namely:

$$G_{AS}(|x|, E) = \frac{g(E)}{2i\pi} \int_{c-i\infty}^{c+i\infty} h(E)^{-\lambda} \frac{1}{N_0(\lambda)} \frac{e^{-|x|/\nu_0(\lambda)}}{2} d\lambda
\tag{5.10}$$

where  $N_0(\lambda)$  is defined in Eq. (3.33e), and  $\nu_0(\lambda)$  is the root of:

$$1 = \left( c_e + \frac{c_i}{\lambda} \right) \cdot \nu_0(\lambda) \operatorname{argth} \left\{ \frac{1}{\nu_0(\lambda)} \right\}
\tag{3.33c}$$

Introducing the "lethargy" variable  $u$  (see Eq. (5.3)):

$$G_{AS}(|x|, E) = \frac{g(E)}{2\pi i} \int_{c-i\infty}^{c+i\infty} \frac{1}{2N_0(\lambda)} e^{\{-|x|/\nu_0(\lambda) + \lambda u\}} d\lambda
\tag{5.11}$$

The next classical step is to apply a saddle-point formula. Defining  $1/v_0(\lambda) = K_0(\lambda)$ , the position of the saddle-point  $\lambda_0$  is given for fixed  $u$  and  $|x|$ , by the equation:

$$\left. \frac{dK_0}{d\lambda} \right|_{\lambda=\lambda_0} = \frac{u}{|x|} \quad (5.12)$$

And  $G_{AS}(|x|, E)$  becomes classically: <sup>1-5,30,31</sup>

$$G_{AS}(|x|, E) = \frac{g(E)}{2N_0(\lambda_0)} \frac{e^{\left\{ \lambda_0 \left\{ \frac{u}{|x|} \right\} \cdot u - K_0(\lambda_0) \cdot |x| \right\}}}{\sqrt{\left\{ -2\pi |x| \left( \left. \frac{d^2 K_0}{d\lambda^2} \right|_{\lambda=\lambda_0} \right) \right\}}} \quad (5.13)$$

However, such a formula is still a dead-end, since it involves the solution of a set of two complex implicit equations (3.33c) and (5.12). These implicit equations can themselves be solved asymptotically in two limiting-cases:

(I)  $u \gg 1$ ; this yields an "age-diffusion" approximation

(II)  $\frac{u}{|x|} \ll 1$ ; this is the "deep-penetration" problem

However, applying Wick's\* method of error-calculation, we find that the corresponding approximate expressions for  $G_{AS}(|x|, E)$  are valid only if:

(I)  $\sqrt{u} \gg 1$  for the "age-diffusion" approximation

(II)  $(uz)^{1/4} \gg 1$  for the "deep-penetration" problem

---

\*See Ref. 3.

In our experimental situations, it will turn out that "lethargies" of interest are all  $\leq 2$ , and the spatial dimensions of experimental systems are all  $\leq 20$  m.f.p. This is in sharp contrast to conditions (I) and (II); the classical saddle-point method does not lead to any practical results for spatial slowing-down problems in fast media. All these considerations justify the highly unconventional mathematical method of asymptotical evaluation introduced in the next section.

#### 5.4. EXACT $\mathcal{M}$ -INVERSION OF THE ENERGY-GREEN'S FUNCTION

Consider again Eq. (5.1):

$$\begin{aligned} \mu \frac{\partial \bar{G}}{\partial x}(x, \mu, \lambda) + \bar{G}(x, \mu, \lambda) &= \frac{c_e}{2} \int_{-1}^{+1} \bar{G}(x, \mu', \lambda) d\mu' \\ &+ \frac{c_i}{2\lambda} \int_{-1}^{+1} \bar{G}(x, \mu', \lambda) d\mu' + \frac{1}{2} \delta(x) \end{aligned} \quad (5.1)$$

where  $\bar{G}(x, \mu, \lambda)$  is the full-space Green's function. Define:

$$\bar{G}(x, \lambda) = \int_{-1}^{+1} \bar{G}(x, \mu, \lambda) d\mu \quad (5.14)$$

In Eq. (5.1), the scattering term involves two components, the first one without energy-transfer, the second with energy-transfer. The idea is to

consider the inelastic scattering-term as an extraneous source:

$$\begin{aligned} \mu \frac{\partial \bar{G}}{\partial x}(x, \mu, \lambda) + \bar{G}(x, \mu, \lambda) - \frac{c_e}{2} \int_{-1}^{+1} \bar{G}(x, \mu', \lambda) d\mu' \\ + \frac{1}{2} \left\{ \delta(x) + \frac{c_i}{\lambda} \bar{G}(x, \lambda) \right\} \end{aligned} \quad (5.15)$$

Then call  $G_e(|x|)$  the Green's function corresponding to the monokinetic transport equation with plain elastic-scattering:

$$\mu \frac{\partial}{\partial x} G_e(|x|, \mu) + G_e(|x|, \mu) = \frac{c_e}{2} \int_{-1}^{+1} G_e(|x|, \mu') d\mu' + \frac{\delta(x)}{2} \quad (5.16a)$$

where

$$G_e(|x|) = \int_{-1}^{+1} G_e(|x|, \mu) d\mu \quad (5.16b)$$

The exact expression of  $G_e(|x|)$  is well known<sup>30</sup>:

$$G_e(|x|) = \frac{1}{2} \frac{dK_e^2}{dc_e} \frac{e^{-K_e|x|}}{K_e} + \frac{1}{2} \int_0^1 \frac{e^{-|x|/\nu}}{\nu g(c_e, \nu)} d\nu \quad (5.17a)$$

where  $K_e$  is the root of:

$$1 = \frac{c_e}{K_e} \operatorname{argth} K_e$$

(5.17b)

And

$$g(c_e, \nu) = \left(1 - c_e \nu \operatorname{argth} \nu\right)^2 + \frac{\pi^2 c_e^2 \nu^2}{4} \quad (5.17c)$$

Then, using a spatial-convolution theorem, the solution of Eq. (5.15) can be rewritten as:

$$\bar{G}(|x|, \lambda) = G_e(|x|) + \int_{-\infty}^{+\infty} G_e(|x-y|) \frac{c_i}{\lambda} \bar{G}(|y|, \lambda) dy \quad (5.18)$$

Now, apply a Fourier spatial transformation to Eq. (5.18):

$$\bar{G}(x^2, \lambda) = \int_{-\infty}^{+\infty} \bar{G}(|x|, \lambda) e^{-ixx} dx \quad (5.19a)$$

$$G_e(x^2) = \int_{-\infty}^{+\infty} G_e(|x|) e^{-ixx} dx \quad (5.19b)$$

We get:

$$\overline{G}(x^2, \lambda) = G_e(x^2) + G_e(x^2) \cdot \frac{c_i}{\lambda} \cdot \overline{G}(x^2, \lambda) \quad (5.19c)$$

From (5.19c), we obtain the desired expression for  $G(\kappa^2, \lambda)$ :

$$\overline{G}(x^2, \lambda) = \frac{G_e(x^2)}{1 - \frac{c_i}{\lambda} G_e(x^2)} \quad (5.20)$$

We could have obtained Eq. (5.20) by immediately Fourier-transforming Eq. (5.15) and (5.16a):

$$\begin{aligned} (ix\mu + 1) \overline{G}(x^2, \mu, \lambda) &= \frac{c_e}{2} \int_{-1}^{+1} \overline{G}(x^2, \mu', \lambda) d\mu' \\ &\quad + \frac{1}{2} \left\{ 1 + \frac{c_i}{\lambda} \overline{G}(x^2, \lambda) \right\} \end{aligned} \quad (5.21a)$$

$$(ix\mu + 1) G_e(x^2, \mu) = \frac{c_e}{2} \int_{-1}^{+1} G_e(x^2, \mu') d\mu' + \frac{1}{2} \quad (5.21b)$$

Since Eqs. (5.21a) and (5.21b) are homogeneous in both  $\kappa$  and  $\lambda$ , this yields:

$$\overline{G}(x^2, \lambda) = G_e(x^2) \left( 1 + \frac{c_i}{\lambda} \overline{G}(x^2, \lambda) \right) \quad (5.21c)$$

From this, we deduce again the fundamental relation (5.20). Let us recall from Eq. (5.17),<sup>30</sup> that:

$$G_e(x^2) = \frac{dK_e^2}{dc_e} \frac{1}{K_e^2 + x^2} + \int_0^1 \frac{d\nu}{(1+x^2\nu^2)g(c_e, \nu^2)} \quad (5.22)$$

Then, let us try to isolate  $G_e(x^2)$  in the relation (5.20):

$$\begin{aligned} \overline{G}(x^2, \lambda) &= \left\{ \frac{G_e(x^2)}{1 - \frac{c_i}{\lambda} G_e(x^2)} - G_e(x^2) \right\} + G_e(x^2) \\ &= G_e(x^2) + \frac{c_i \{G_e(x^2)\}^2}{\lambda - c_i G_e(x^2)} \end{aligned} \quad (5.23)$$

At this stage, inverse  $\mathcal{M}$ -transformation of Eq. (5.23) is immediate:

$$G(x^2, E) = G_e(x^2) \delta(u) + c_i g(E) \{G_e(x^2)\}^2 h(E)^{-c_i G_e(x^2)} \quad (5.24)$$

where  $\delta(u)$  is the Dirac distribution,  $u$  the "lethargy" defined in (5.3),

and where we used the elementary pair of  $\mathcal{M}$ -transforms:



$$\begin{aligned} \mathcal{M} \circ \{g(E) h(E)^{-\rho}\} &= \int_0^1 g(E) h(E)^{\lambda-\rho-1} dE \\ &= \frac{1}{\lambda-\rho} \end{aligned} \tag{5.25}$$

(set  $\rho = c_i G_e(\kappa^2)$  and remember that  $h(\infty) \equiv 1$ ).

Relation (5.24) is quite interesting; we have succeeded in performing the exact-inverse  $\mathcal{M}$ -transformation for the energy-Green's function of the infinite medium.\* We obtain an expression which is exact for all energies: this is quite unusual in the field of spatial slowing-down problems; for similar elastic slowing-down spatial problems, one is always stuck with an energy-inversion contour integral, which all authors without exception (even Ref. 11) approximate by an implicit saddle-point formula (see Chapter X, in Ref. 31).

The first term in Eq. (5.24) corresponds to the elastic-scattering of the source: the very success of our method lies in its isolation.

## 5.5. SPATIAL ASYMPTOTIC COMPONENT OF THE ENERGY-GREEN'S FUNCTION

Having relation (5.24) valid for all energies without exception, we may now focus our attention on the purely spatial behavior of the energy-Green's function and look for an expression valid for large distances and all energies.

Let us apply an inverse, spatial Fourier-transformation to Eq. (5.24):

---

\*A similar procedure could be extended to half-space problems, using a Wiener-Hopf-Fourier method.

$$G(|x|, E) = G_e(|x|) \delta(u) + c_i g(E) \frac{1}{2\pi} \int_{-\infty}^{+\infty} \{G_e(x^2)\}^2 e^{\{u c_i G_e(x^2) + i x x\}} dx \quad (5.26)$$

(remember that  $u = -\text{Log}\{h(E)\}$ ).

In Eq. (5.26), the first term  $G_e(|x|) \delta(u)$  is perfectly well known (see Eq. (5.17)). We notice that we even know in detail the spatial-transport transients in  $G_e(|x|)$ ; this will turn out to be useful for an improved expression of the Green's function close to the source (see Chapter VI).

Let us now turn our attention to the second term of Eq. (5.26) which includes all the spatial inelastic slowing-down effects:

$$F(|x|, E) = c_i g(E) \frac{1}{2\pi} \int_{-\infty}^{+\infty} \{G_e(x^2)\}^2 e^{\{u c_i G_e(x^2) + i x x\}} dx \quad (5.27)$$

Make the following change of variable:

$$ik = x \quad (5.28)$$

Eq. (5.27) becomes:

$$\begin{aligned}
 F(|X|, E) &= c_i \frac{g(E)}{2\pi} \int_{+i\infty}^{-i\infty} \left\{ G_e(k^2) \right\}^2 e^{[u c_i G_e(k^2) - kx]} i dk \\
 &= c_i \frac{g(E)}{2\pi i} \int_{-i\infty}^{+i\infty} \left\{ G_e(k^2) \right\}^2 e^{[u c_i G_e(k^2) - kx]} dk
 \end{aligned} \tag{5.29}$$

Where

$$\begin{aligned}
 G_e(k^2) &= \frac{dk_e^2}{dc_e} \frac{1}{k_e^2 - k^2} + \int_0^1 \frac{d\mathcal{V}}{(1 - k^2 \mathcal{V}^2) g(c_e, \mathcal{V}^2)} \\
 &= \frac{dk_e^2}{dc_e} \frac{1}{k_e^2 - k^2} + \Omega(k^2)
 \end{aligned} \tag{5.30}$$

( $k_e$  being the root of Eq. (5.17b)).

Equation (5.29) involves a contour integral along the imaginary axis for a function of the complex variable  $k$ ; this function is analytic everywhere, except for:

(A) The cuts  $[+1, +\infty]$  and  $[-\infty, -1]$  on the real axis, since these are cuts for  $\Omega(k^2)$  in Eq. (5.30).

(B) The isolated singularities  $k = \pm k_e$  on the real axis, since these are poles for  $G_e(k^2)$  in Eq. (5.30). However,  $\pm k_e$  are essential singularities for the function involved in the contour-integral; this is due to the exponential blow-up of the term

$$e^{u c_i G_e(k^2)}$$

which behaves as  $e^{1/k \pm k_e}$  in the neighborhood of the essential singularities  $\pm k_e$ .

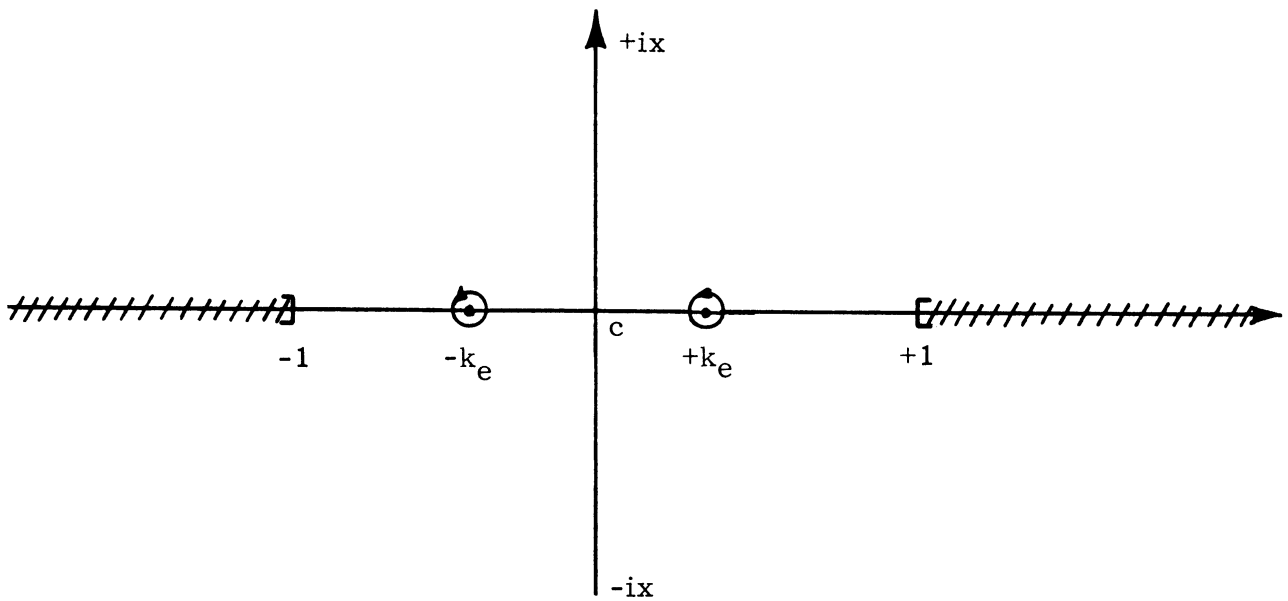


Fig. 9. Domain of analyticity for the Fourier-transform of  $F(|x|, E)$  in the  $k$ -complex plane.

Let us now shift the integration contour in Eq. (5.29) from the imaginary axis to the real axis. If we consider  $x > 0$ , the corresponding Bromwich contour will lie in the positive half-plane, since for  $\text{Re}(k) > 0$  and  $x > 0$  we have  $|e^{-kx}| \rightarrow 0$ . The Bromwich contour includes a contour  $D$  along the cut  $[+1, +\infty]$  and a circle  $C$  centered on  $k = +k_e$ . Things are of course symmetrical for  $x < 0$ .

Then, for  $x > 0$ :

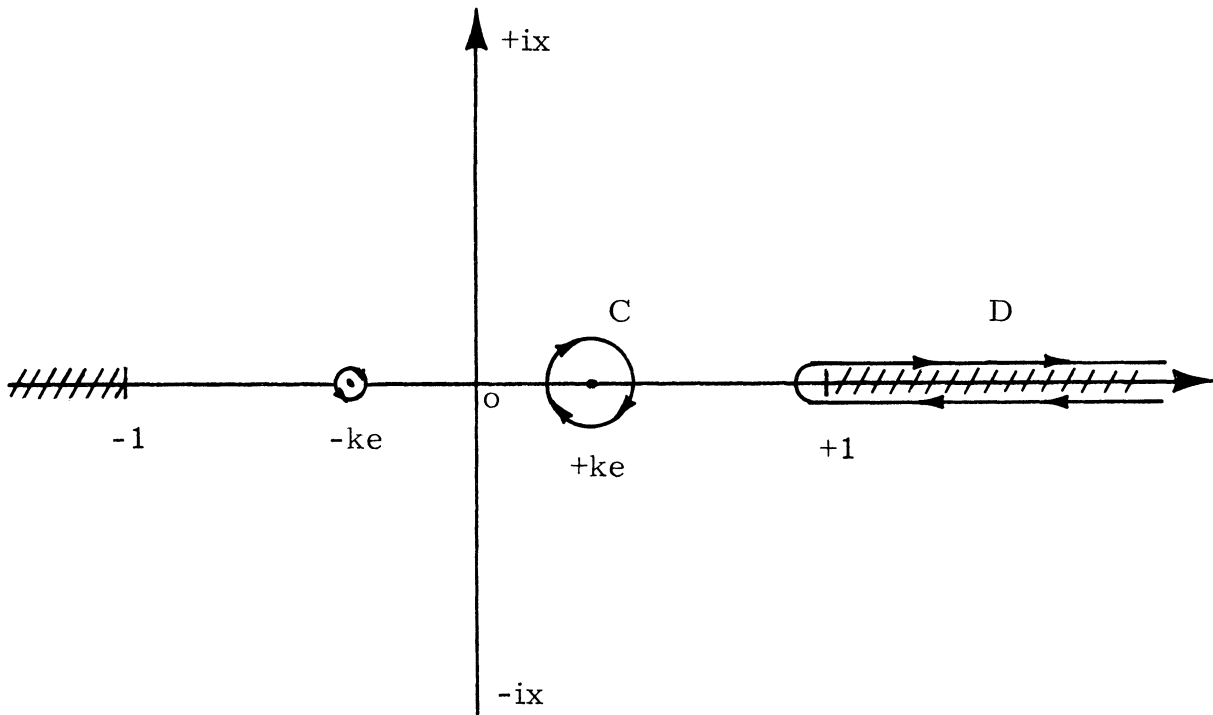


Fig. 10. The Bromwich contour for  $F(x, E)$  (Case  $x > 0$ ) in the  $K$ -complex plane.

$$F(x, E) = a_i \frac{g(E)}{2i\pi} \left\{ \int_D + \int_C \{G_e(k^2)\}^2 e^{[u_{ci} G_e(k^2) - kx]} dk \right\} \quad (5.31)$$

From Eq. (5.31), it is clear that the contribution of the contour  $D$  involves modes all decaying faster than  $e^{-x}$ ; these are all transport-spatial transients.

Any spatial mode decaying slower than  $e^{-|x|}$  will be yielded by the contour integral  $C$ : this is indeed the spatial asymptotic-transport component we are looking for.

However, the circle-contour  $C$  surrounds an essential singularity: classical residue-calculations do not hold. This is typical of a slowing-down problem, where we do not have discrete spatial relaxation lengths. The

contour  $C$  around the essential singularity  $k_e$  includes, in fact, the continuum of discrete regular Case's modes introduced in Section 2.5, Eq. (2.45b), and used in completeness theorems (Eq. (2.53a) and (2.53b)).

So define:

$$F_{AS}(x, E) = \frac{c_i g(E)}{2i\pi} \oint_C \{G_e(k^2)\}^2 e^{[uc_i G_e(k^2) - kx]} dk \quad (5.32)$$

From Eq. (5.30),  $\{G_e(k^2)\}^2$  is:

$$\begin{aligned} \{G_e(k^2)\}^2 &= \left(\frac{dk_e^2}{dce}\right)^2 \frac{1}{(k_e^2 - k^2)^2} \\ &+ \frac{dk_e^2}{dce} \frac{2\Omega(k^2)}{k_e^2 - k^2} + \{\Omega(k^2)\}^2 \end{aligned} \quad (5.33)$$

$\Omega(k^2)$  is an analytic function on the contour  $C$  and within the domain surrounded by  $C$ .

Using the three components of  $\{G_e(k^2)\}^2$  in Eq. (5.33), we can split

$F_{as}(x, E)$  into three parts:

$$F_{AS}(x, E) = F_{AS}^{(1)}(x, E) + F_{AS}^{(2)}(x, E) + F_{AS}^{(3)}(x, E) \quad (5.34)$$

Where:

$$F_{AS}^{(1)}(x, E) = \frac{c_i g(E)}{2\pi i} \oint_C \left(\frac{dk_e^2}{dce}\right)^2 \frac{1}{(k_e^2 - k^2)^2} e^{[uc_i G_e(k^2) - kx]} dk \quad (5.35a)$$

$$F_{AS}^{(2)}(x, E) = \frac{c_i g(E)}{2\pi i} \oint_C \frac{dk_e^2}{dc_e} \frac{2\Omega(k^2)}{k_e^2 - k^2} e^{[uc_i G_e(k^2) - kx]} dk \quad (5.35b)$$

$$F_{AS}^{(3)}(x, E) = \frac{c_i g(E)}{2\pi i} \oint_C \left\{ \Omega(k^2) \right\}^2 e^{[uc_i G_e(k^2) - kx]} dk \quad (5.35c)$$

Since the procedure is quite similar for Eqs. (5.35b) and (5.35c), we concentrate our attention on Eq. (5.35a).

More precisely:

$$F_{AS}^{(1)}(x, E) = \frac{c_i g(E)}{2i\pi} \oint_C L(k, u) \frac{e^{[ \frac{uc_i}{2k_e} \frac{dk_e^2}{dc_e} \frac{1}{k_e - k} - kx ]}}{(k_e - k)^2} dk \quad (5.36)$$

where we define

$$L(k, u) = \left\{ \frac{dk_e^2}{dc_e} \right\}^2 \frac{1}{(k_e + k)^2} e^{\left\{ \frac{uc_i}{2k_e} \frac{dk_e^2}{dc_e} \frac{1}{k_e + k} + uc_i \Omega(k^2) \right\}} \quad (5.37)$$

$L(k, u)$  is an analytic function of the complex-variable  $k$  on the contour  $C$  and within the domain surrounded by  $C$ . Then the asymptotic behavior (for

large  $x$ ) of the inverse Laplace transform is obtained by replacing  $L(k)$  by its value at  $k = k_e$ , in the contour integral (5.36):

$$L(k_e, u) = \left\{ \frac{dk_e^2}{dc_e} \right\}^2 \frac{1}{4k_e^2} e^{uc_i \left\{ \frac{1}{4k_e^2} \frac{dk_e^2}{dc_e} + \Omega(k_e^2) \right\}} \quad (5.38)$$

Then Eq. (5.36) becomes:

$$F_{AS}^{(1)}(x, E) = \frac{c_i g(E)}{2\pi i} \oint_C L(k_e, u) \frac{e^{\left[ \frac{uc_i}{2k_e} \frac{dk_e^2}{dc_e} \frac{1}{k_e - k} - kx \right]} dk}{(k_e - k)^2} \quad (5.39)$$

The idea is then to reduce the contour integral (5.39) to a classical inverse-Laplace transform in  $x$ ; for this purpose, put:

$$k_e - k = p \quad (5.40)$$

Then Eq. (5.39) reduces to:

$$F_{AS}^{(1)} = c_i g(E) L(k_e, u) e^{-k_e x} \\ (x) \frac{1}{2\pi i} \oint_C \frac{e^{\left\{ \frac{uc_i}{2k_e} \frac{dk_e^2}{dc_e} \frac{1}{p} \right\}} e^{px} dp}{p^2} \quad (5.41)$$

(with counter-clockwise integration, this time).



Equation (5.41) is nothing but the Bromwich contour for the inverse-Laplace transform of  $\frac{e^{\alpha/P}}{P^2}$ , where:

$$\alpha = \frac{u c i}{2 k e} \frac{d k e^2}{d c e} \quad (5.42)$$

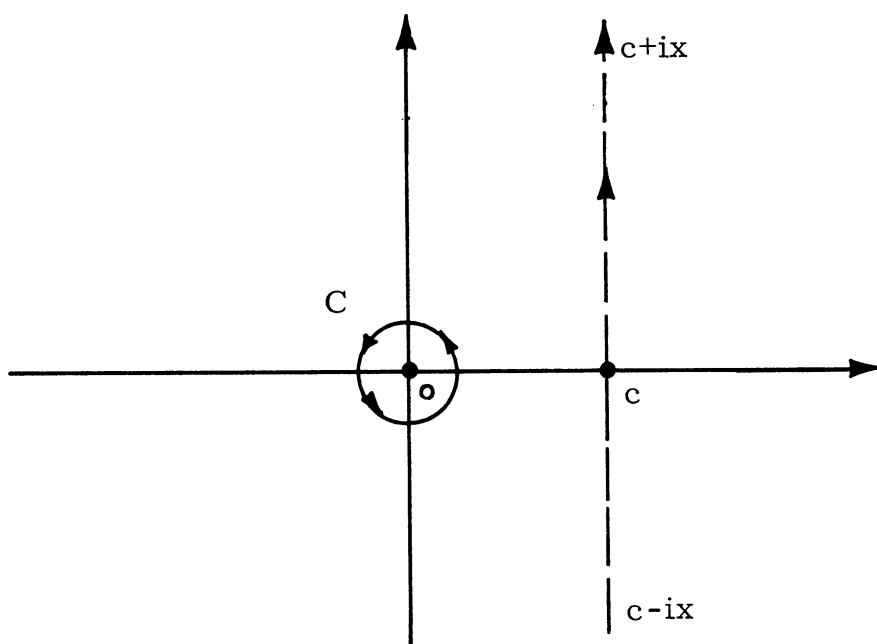


Fig. 11. The Bromwich contour  $C$  in the complex  $P$ -plane.

We have indeed:

$$\frac{1}{2\pi i} \int_{c-i\infty}^{c+i\infty} \frac{e^{\alpha/P}}{P^2} e^{PX} dp = \frac{1}{2\pi i} \oint_C \frac{e^{\alpha/P}}{P^2} e^{PX} dp \quad (5.43)$$

But, from Bateman's table of integral transforms<sup>44</sup> (p. 245):

$$\frac{1}{2\pi i} \int_{c-i\infty}^{c+i\infty} p^{-\nu-1} e^{\alpha/p} e^{pX} dp = \alpha^{-\frac{\nu}{2}} x^{\frac{\nu}{2}} I_{\nu}(2\sqrt{\alpha x}) \quad (5.44)$$

where  $\text{Re}(\nu) > 1$ , and  $I_{\nu}$  is the hyperbolic Bessel function of order  $\nu$ . In Eq. (5.33), we have  $\nu = 1$ . Then, for positive  $x$ , Eq. (5.41) reduces to:

$$F_{AS}^{(1)}(x, E) = c_i g(E) L(k_e, u) \left\{ e^{-k_e X} \sqrt{\frac{x}{\alpha}} I_1(2\sqrt{\alpha x}) \right\} \quad (5.45)$$

So, we successfully have evaluated the contour-integral for  $F_{as}^{(1)}(x, E)$ . A similar procedure can be applied to  $F_{as}^{(2)}(x, E)$  and  $F_{as}^{(3)}(x, E)$  (Eqs. (5.35b) and (5.35c)): namely, the isolation of a term  $L(k, u)$  analytic within the contour  $C$ ; its replacement by  $L(k_e, u)$  in the contour integral; the reduction of the remaining contour integral to an inverse Laplace-transform formula, using the change of variable  $p = k_e - k$ ; the evaluation of this inverse Laplace transform with the help of the following formulae:

$$\frac{1}{2\pi i} \int_{c-i\infty}^{c+i\infty} \frac{1}{p} e^{\alpha/p} e^{pX} dp = I_0(2\sqrt{\alpha x}) \quad (5.46a)$$

$$\frac{1}{2\pi i} \int_{c-i\infty}^{c+i\infty} e^{\alpha/p} e^{pX} dp = \delta(x) + \sqrt{\frac{\alpha}{x}} I_1(2\sqrt{\alpha x}) \quad (5.46b)$$

Formula (5.46a) is used in the evaluation of  $F_{as}^{(2)}(x,E)$  and formula (5.46b) in the evaluation of  $F_{as}^{(3)}(x,E)$  (from page 244, Bateman's project).<sup>44</sup>

So, skipping over the detailed calculations, we write the final expression for  $G_{as}(|x|,E)$ , the spatial asymptotic part of the infinite-space, energy-Green's function:

$$\begin{aligned}
 G_{AS}(|x|,E) &= \frac{1}{2} \frac{dk_e^2}{dc_e} \frac{e^{-k_e x}}{k_e} \cdot \delta(u) \\
 &+ c_i g(E) e^{uc_i} \left\{ \frac{1}{4k_e^2} \frac{dk_e^2}{dc_e} + \Omega(k_e^2) \right\} e^{-k_e |x|} \\
 (x) &\left\{ \frac{1}{4} \left( \frac{1}{k_e} \frac{dk_e^2}{dc_e} \right)^2 \sqrt{\frac{|x|}{\alpha}} I_1(2\sqrt{\alpha}|x|) \right. \\
 &\quad + \frac{1}{k_e} \frac{dk_e^2}{dc_e} \Omega(k_e^2) I_0(2\sqrt{\alpha}|x|) \\
 &\quad \left. + \left( \Omega(k_e^2) \right)^2 \sqrt{\frac{\alpha}{|x|}} I_1(2\sqrt{\alpha}|x|) \right\}
 \end{aligned} \tag{5.47}$$

Where  $u = -\text{Log } h(E)$ , and  $I_0, I_1$  are the hyperbolic Bessel functions of order zero and one.<sup>44</sup>  $\Omega(k^2)$  is defined in Eq. (5.30) and  $\alpha$  in Eq. (5.42):

$$\alpha = \frac{uc_i}{2k_e} \frac{dk_e^2}{dc_e} \tag{5.42}$$

$k_e$  is the root of Eq. (5.17b): it is the inverse of the discrete relaxation length for the monokinetic elastic-scattering equation (5.16a).

It is readily seen that  $G_{as}(|x|, E)$  is split into two parts: one which decays exactly as  $e^{-k_e|x|}$  and corresponds to pure elastic-scattering of the source term; the second one, namely  $F_{as}(|x|, E)$ , includes all inelastic slowing-down effects; recalling that:

$$I_0(0) = 1$$

$$I_1(0) = 0$$

and that hyperbolic Bessel functions are monotonically increasing, we see that  $F_{as}(|x|, E)$  decays more slowly than  $e^{-k_e|x|}$ . We can make this point more precise by making an asymptotic expansion of the hyperbolic Bessel functions:

$$I_n(2\sqrt{\alpha|x|}) \underset{|x| \rightarrow \infty}{\sim} \frac{1}{\sqrt{4\pi} (\alpha|x|)^{\frac{1}{4}}} e^{2\sqrt{\alpha|x|}} \quad (5.48)$$

Then an asymptotic expression for  $F_{as}(|x|, E)$  follows:

$$F_{As}(|x|, E) \underset{|x| \rightarrow \infty}{\sim} c_i g(E) e^{uc_i \left\{ \frac{1}{4k_e^2} \frac{dk_e^2}{dce} + \Omega(k_e^2) \right\}}$$

$$(x) \frac{1}{\sqrt{4\pi} (\alpha|x|)^{\frac{1}{4}}} e^{-k_e|x| + 2\sqrt{\alpha|x|}}$$

$$(x) \left\{ \frac{1}{4} \left( \frac{1}{k_e} \frac{dk_e^2}{dce} \right)^2 \sqrt{\frac{|x|}{\alpha}} + \frac{1}{k_e} \frac{dk_e^2}{dce} \Omega(k_e^2) + \left( \Omega(k_e^2) \right)^2 \sqrt{\frac{\alpha}{|x|}} \right\}$$

(5.49)

Equation (5.39), valid of course for very large  $|x|$ , shows clearly to what extent the decay of  $F_{as}(|x|, E)$  is slower than  $e^{-k_e|x|}$ ; the leading term is:

$$e^{-k_e|x| + 2\sqrt{\alpha}|x|} \quad (5.50)$$

Since  $\alpha$  is linearly increasing with the "lethargy"  $u$  (see Eq. (5.42)),  $F_{as}(|x|, E)$  will decay into space more slowly for low energies than for high energies: this reflects the physical fact of accumulation of slowed-down neutrons with increasing distances.

Anyway, Eq. (5.47) for  $G_{as}(|x|, E)$  is valid for all energies (and "lethargies"), and is spatially "asymptotic" only to the extent that we rejected all transport-transients decaying faster than  $e^{-|x|}$ . This enables us to make unrestricted use of the convolution Theorem 5.2.1 (see Eq. (5.6a)) to obtain an asymptotic expression for the slowing-down transients, valid for all energies.

## 5.6. ASYMPTOTIC EXPRESSION FOR THE GREEN'S FUNCTION OF THE INFINITE MULTIPLYING MEDIUM

Turning-back to the transport equation with fission, heavy elastic scattering, and inelastic slowing-down, we can now write the asymptotic expression  $\Delta_{as}(|x|, E)$  for the infinite-space Green's function  $\Delta(|x|, E)$  solution of Eq. (5.7). The exact expression for  $\Delta(|x|, E)$  has been given in Eq. (3.33a), providing one uses a source term  $1/2 \delta(x) \cdot \chi(E)$  with a fission energy-spectrum. We have, referring to Eqs. (3.33), (5.6), and (5.47):

$$\begin{aligned}
\Delta_{AS}(|x|, E) = & \mathcal{H}(E) \cdot \frac{1}{2} \frac{e^{-\frac{|x|}{v_0}}}{N_0} \\
& + \left( \chi(E) - \mathcal{H}(E) \right) \cdot \frac{1}{2} \frac{dk_e^2}{dce} \cdot \frac{e^{-K_e|x|}}{K_e} \\
& + c_i g(E) e^{-K_e|x|} \int_0^{-\log[h(E)]} \left\{ \left[ \frac{\chi - \mathcal{H}}{g} \right](u') \cdot e^{[u-u']c_i} \left\{ \frac{1}{4K_e^2} \frac{dk_e^2}{dce} + \Omega(k_e^2) \right\} \right. \\
& \quad (X) \left[ \frac{1}{4} \left( \frac{1}{K_e} \frac{dk_e^2}{dce} \right)^2 \sqrt{\frac{|x|}{\alpha}} I_1(2\sqrt{\alpha|x|}) \right. \\
& \quad \left. \left. + \frac{1}{K_e} \frac{dk_e^2}{dce} \Omega(k_e^2) I_0(2\sqrt{\alpha|x|}) + \left( \Omega(k_e^2) \right)^2 \frac{\alpha}{\sqrt{|x|}} I_1(2\sqrt{\alpha|x|}) \right] \right\} du'
\end{aligned}$$

(5.51a)

Recalling that:

$$\alpha = \frac{(u-u')}{2K_e} \frac{dk_e^2}{dce} \quad (5.51b)$$

$$u = -\log\{h(E)\} \quad (5.51c)$$

And that  $(\chi - \mathcal{H}/g)(u')$  is the value of  $\frac{\chi(E') - \mathcal{H}(E')}{g(E')}$  for  $E'$  such that:

$$h(E') = e^{-u'} \quad (5.51d)$$

Let us consider  $\Delta_{as}(|x|, E)$  more closely; Eq. (5.51) is the sum of three components, each of them having a major physical significance. The first one is space-energy separable, characteristic of neutron regeneration; the second merely represents the elastic scattering of the "slowing-down transients" source without any energy change; the third truly represents slowing-down transients characterizing the adjustment of the neutron field by inelastic slowing-down from the initial high-energy source  $\chi(E)$  to the final asymptotic energy-spectrum  $H(E)$ .

The spatial decay of these three components is representative of their relative importance: the first one decays as  $e^{-|x|/\nu_0}$ , where  $\nu_0$  is the fundamental mode of the multiplying medium; the second, as  $e^{-k_e|x|}$ , with  $k_e \gg 1/\nu_0$ ,\* and the third corresponds to a continuum decaying more slowly than  $e^{-k_e|x|}$ , though faster than the fundamental mode. Let us also point that the slowing-down transients correspond to a source term  $\chi(E) - H(E)$  which is positive at high energies and negative at low energies characteristic of the asymptotic spectrum; this is physically natural, since it reflects an excess of high-energy neutrons (positive source) and a deficit of low-energy neutrons (sink-source) at distances close to the origin. The overall neutron density is, of course, positive everywhere.

For further numerical purpose, we can improve the validity of Eq. (5.51) for small values of  $|x|$  by adding two spatial-transport transients:

---

\*As it may be easily seen from Eqs. (3.33b) and (5.17).

$$\begin{aligned}
\Delta'(|x|, E) &= \Delta_{As}(|x|, E) \\
&+ \frac{\chi(E)}{2} \int_0^1 \frac{e^{-\frac{|x|}{v}}}{N(v)} dv \\
&+ \frac{\chi(E) - \chi(E)}{2} \int_0^1 \frac{e^{-\frac{|x|}{v}}}{v g(c_e, v)} dv
\end{aligned} \tag{5.52}$$

The numerical evaluation of these two transport-transients (defined in Eq. (5.17) and (3.33)) is well known from previous works on monokinetic transport theory.<sup>33</sup> This way, the only approximation in the improved formula (5.52) consists in omitting terms which are simultaneously inelastic slowing-down transients and spatial transport-transients (namely, modes coming from the contour integral D in Eq. (5.31)). From further numerical calculations, it will turn out that the improved formula (5.52) for the Green's function  $\Delta(|x|, E)$  is rigorous for distances equal and greater than two mean free paths from the source.

At this stage, the energy-dependent transport theory, presented in this work, has been developed to a point where one can do more than merely interpret analytical formulae. We are now in a position to obtain numerical results and to try to adjust our model to experimental situations. Since our foremost theoretical predictions concern possible competition of slowing-down transients with space-energy separable modes, we may try to investigate



experimental situations where such a phenomenon has been pointed out by investigators. This is indeed the case with fast exponential experiments in both natural and enriched uranium.<sup>36-42,45-47</sup>

These experimentalists have been trying to measure a well-defined relaxation length associated with an asymptotic energy distribution. However, because of the systematical discrepancies between the results yielded by a wide range of experimental and analytical devices, it has been suggested by the investigators themselves that a true equilibrium spectrum might not have been attained in these exponential experiments.

So, we will try to make a semi-quantitative study of the approach to equilibrium in such experiments.

## CHAPTER VI

### THE APPROACH TO EQUILIBRIUM IN THE FAST EXPONENTIAL EXPERIMENT. APPLICATION TO THE ZPR-IV SYSTEMS

#### 6.1. AN EXPERIMENTAL CHALLENGE: IS COMPLETE SPECTRAL EQUILIBRIUM ATTAINED IN THE FAST EXPONENTIAL EXPERIMENT?

The purpose of the fast exponential experiment is to study the propagation of neutrons in a natural or enriched uranium assembly, using a plane source. It is designed to obtain fundamental information about the physics of dilute fast-reactors—such as bucklings, diffusion lengths, and asymptotic energy spectra. Such an integral experiment is particularly attractive since it combines a low investment of fuel, with a high-degree of safety. Related interests are the design of improved devices measuring differential fast neutron spectra in the energy-range 1 keV - 3 MeV and the check of multigroup calculation methods and multigroup cross-sections.

Measurements have been performed on natural uranium by many experimental teams<sup>36-42</sup>; they have yielded a wide range of information on the diffusion length and the behavior of equilibrium neutrons in natural uranium.

In Argonne National Laboratory,<sup>36,37,45</sup> measurements have been performed on systems with various mixtures of enriched fuel and diluent materials and with isotopic ratios of  $U^{238}$  and  $U^{235}$  in the range 3:1 to 7:1. As opposed to natural uranium (for which the infinite medium is subcritical), such systems could achieve criticality and were representative of dilute fast-reactor media. Measurements on these "ZPR-IV" systems have given values for the bucklings and indications of the asymptotic spectra.<sup>45</sup>

Typically, an exponential assembly consists of a cube of natural uranium in sizes varying from 24 in. to 80 cm, or, for ZPR-IV, a rectangular stack of cans filled with the appropriate mixture of fuel and diluent materials: typical sizes were 24 x 24 x 18 in. (see Fig. 12).

The source of neutrons for the fast exponential experiment is usually the thermal column of thermal reactor. The whole system is carefully shielded in order to prevent undesirable leakage of internal neutrons or parasitic scattering of external neutrons. The leakage spectrum of the thermal source reactor gives birth to a fast-fission spectrum on the front-face of the exponential assembly.

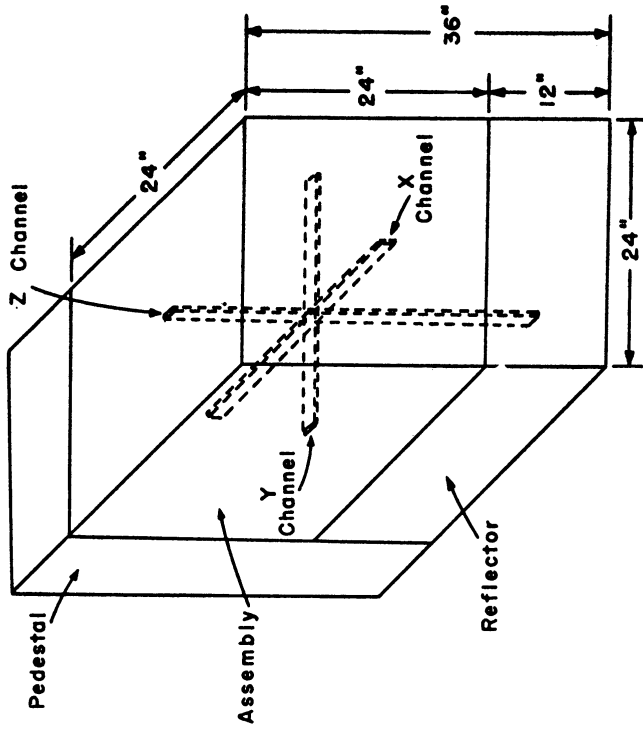
Within the assembly, in a region where only the fundamental mode is present, the spatial and energy variations of the flux are separable. This has been justified theoretically in Section 3.4 of the present work, and corresponds to the damping of energy and spatial transients. The fundamental mode is characteristic of the fast multiplying medium; call it:

$$\phi_E(\underline{r}) \cdot \mathcal{H}(E) \quad (6.1)$$

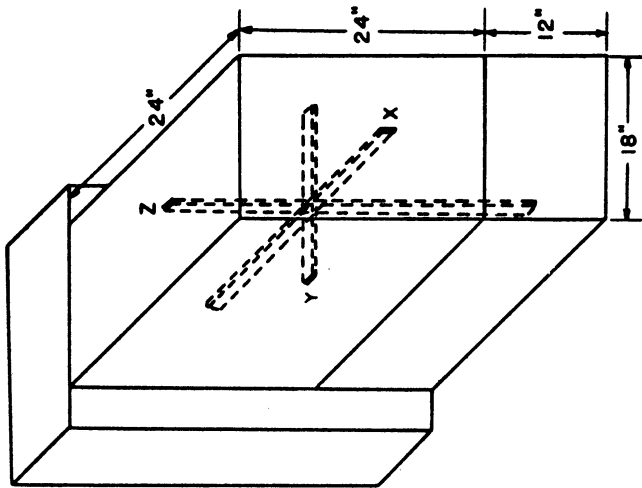
where  $\mathcal{H}(E)$  is the asymptotic energy-spectrum (see Chapter III) and  $\phi_E(\underline{r})$  obeys the asymptotic source-free transport equation:

$$\nabla^2 \phi_E(\underline{r}) + B^2 \phi_E(\underline{r}) = 0 \quad (6.2)$$

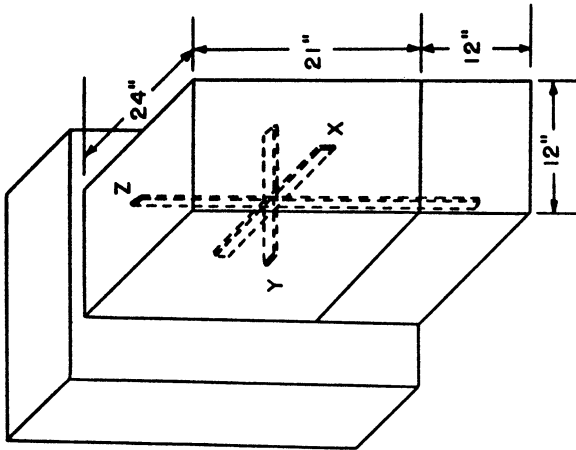
(for a subcritical medium such as ZPR-IV). And:



7:1 URANIUM MIXTURE.



5:1 URANIUM MIXTURE.



3:1 URANIUM MIXTURE.

Fig. 12. Exponential geometries for ZPR-IV.

$$\nabla^2 \phi_E(\underline{r}) - \chi^2 \phi_E(\underline{r}) = 0 \quad (6.3a)$$

(for a subcritical medium such as natural uranium).  $B^2$  is the buckling of the multiplying medium;  $L^2$  defined by:

$$L^2 = \frac{1}{\chi^2} \quad (6.3b)$$

is the diffusion length of the subcritical medium.  $\phi_E(\underline{r})$  corresponds to discrete fundamental modes of the transport equation, and therefore, obeys the diffusion-like equations (6.2) and (6.3). For the boundary conditions of the experiment, the spatial distribution of the fundamental mode is expressed as:

$$\phi_E(\underline{r}) = X(x) Y(y) Z(z) \quad (6.4)$$

The convention is to label the exponential direction as  $x$ , the vertical direction as  $z$ , and the remaining direction as  $y$  (see Fig. 12).

Then:

$$X(x) = A_1 (e^{-\chi_x x} + \gamma e^{+\chi_x x}) \quad (6.5)$$

$$Y(y) = A_2 \cos B_y (y - y_0) \quad (6.6)$$

$$Z(z) = A_3 \cos B_z (z - z_0) \quad (6.7)$$

Where we have the fundamental relations:

$$B_y^2 + B_z^2 - \kappa_x^2 = B^2 \quad (6.8)$$

(for a multiplying medium such as ZPR-IV). Or:

$$\kappa_x^2 - B_y^2 - B_z^2 = \frac{1}{L^2} \quad (6.9)$$

(for a subcritical medium such as natural uranium).

Measurement of the flux direction along the three axes of the assembly in a region where the fundamental mode is asymptotically dominant, enables a determination of  $\kappa_x$ ,  $B_y$ ,  $B_z$ : through Eqs. (6.8) and (6.9), it gives experimental values for the buckling  $B$  (or the diffusion length  $L$ ). A wide range of detectors has been used in practice: fission chambers ( $U^{235}$ ,  $Pu^{239}$ ), fission chambers with an isotope having a high-energy fission threshold ( $U^{238}$ ,  $Pu^{240}$ ,  $Np^{237}$ ,  $Th^{232}$ ), activation detectors with a high energy threshold ( $P(n,p)$ ,  $S(n,p)$  with threshold  $\simeq 3.5$  MeV), activation chambers sensitive to a continuous energy range ( $Mn$ ,  $Au$ ,  $Cu$ ,  $In$ ).

For each experimental flux plot obtained, a least squares method fits a cosine (for  $y$ - and  $z$ -directions) or an exponential curve (for the  $x$ -direction) to the experimental curves. The statistical weight of each curve is considered to be the reciprocal mean square of the residuals. The weighted mean value of  $\kappa_x$  (or  $B_y$ , or  $B_z$ ) from all curves in each direction for a given assembly is then found; finally the buckling  $B$  (from Eq. (6.8)) or the diffusion length  $L$  (from Eq. (6.9)) is deduced from these weighted means.

This seems to be a straightforward procedure; however, it must be heavily emphasized that such fittings have to be made only over those regions where the energy spectrum has reached an actual equilibrium: this requires some information about the differential energy spectrum, which is far from being immediate, since most detectors yield an information integrated over the whole energy spectrum. The classical method to check the equilibrium is to plot the ratio of counts of a detector sensitive to all energies and a threshold detector; for instance, classical equilibrium indexes are the fission ratios of  $U^{235} : U^{238}$ , and  $U^{235} : Np^{237}$  (see Fig. 13).

Typical asymptotic energy spectra in fast dilute media are sharply peaking from 0.1 MeV to 0.15 MeV (see Figs. 14 and 20): this way a  $U^{235}$  fission chamber is most sensitive to this equilibrium distribution; while a fission threshold detector such as  $U^{238}$  is sensitive only to high energy neutrons above 0.8 MeV; thus, a threshold detector is most affected by slowing-down transient modes above 0.8 MeV (as introduced in Chapter IV). Typical asymptotic spectra, which witness the strong inelastic degradation of the fission source, have practically no neutrons above 0.8 MeV (see Fig. 20).

So, the most commonly accepted index of equilibrium is the constancy—say within one percent—of the  $U^{235} : U^{238}$  fission ratios. Figure 13 gives a good example of such an experimental plot. However, this is far from being an absolutely reliable criterion since it is insensitive to those slowing-down transients below 0.8 MeV. More evolved techniques have been used, such as proton-recoil spectrometry and nuclear emulsions which give information

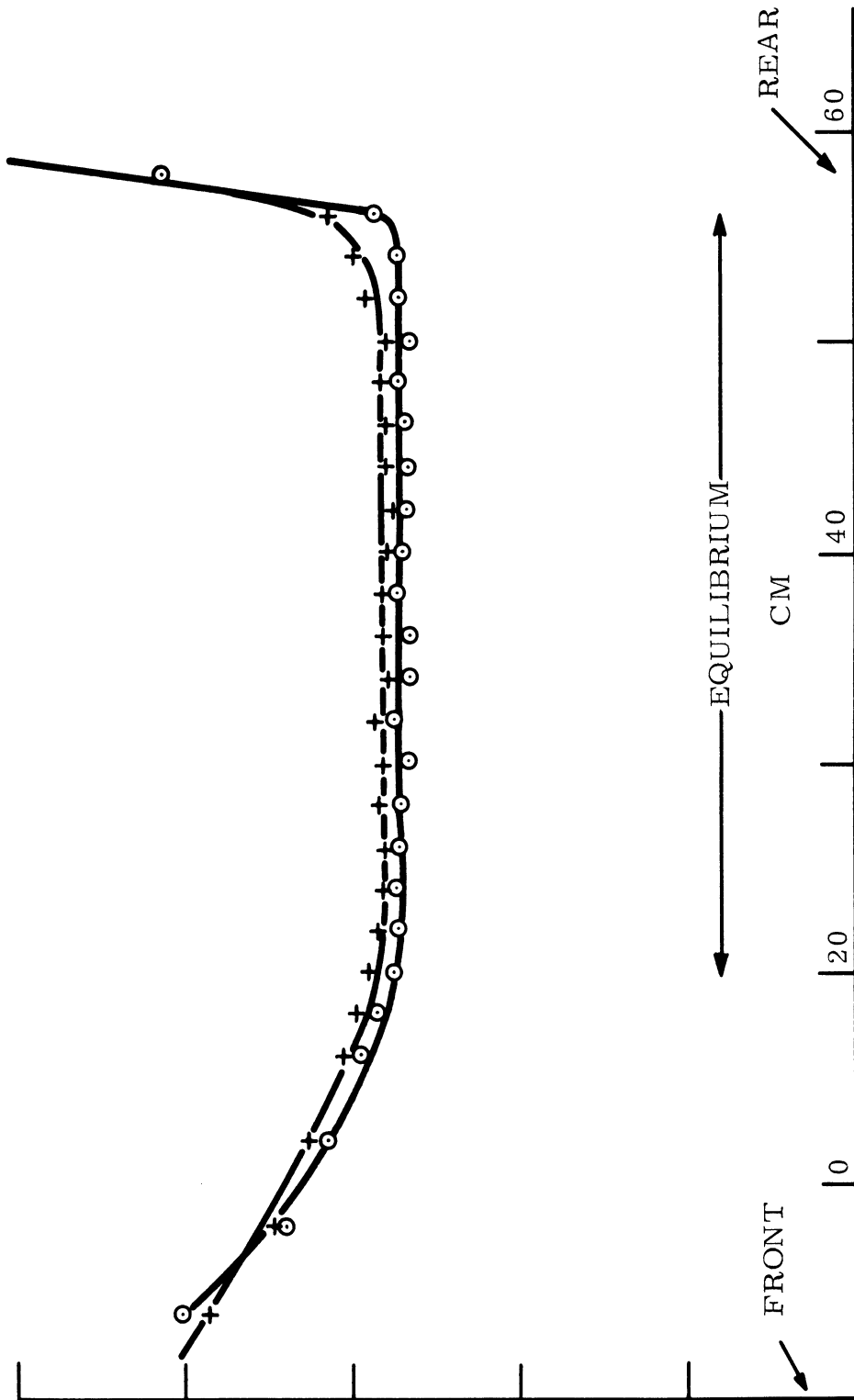


Fig. 13. Fission ratios in the x-direction.



about the differential energy spectrum down to 350 keV<sup>39</sup>; but this is still far above the bulk of neutrons in typical fast reactor spectra. The necessity for more refined devices measuring differential fast neutron spectra has sharply increased with the development of fast reactor studies. Recently successful studies have been done on this subject in Argonne National Laboratory (see ANL Report 7320).

Together with these experimental studies, theoretical calculations have been performed using multigroup diffusion equations. Asymptotic transport theory was also used<sup>37,45</sup> but the deviations from diffusion theory were unimportant in all cases. These calculations were, of course, concerned with the space-energy separable asymptotic mode; they are likely to give reliable results on the buckling and the asymptotic energy spectrum, the computation process being similar to the solution of a criticality problem (successive guesses about the buckling, and successive source-iterations on the energy flux). However, such calculations are unable to make any prediction about the approach to equilibrium. They neglect spatial transport transients (use of an asymptotic transport theory) and they eradicate any kind of slowing-down transients, since the starting assumption of these calculations is space-energy separability. Thus, up to now the problem of approach to equilibrium had to rely only upon experimental data, while theoretical calculations could yield sound values for the asymptotic constants (buckling, equilibrium spectrum, asymptotic  $U^{235}:U^{238}$  fission ratio)—to the extent, of course, that multigroup cross-sections were sufficiently accurate.

However, substantial discrepancies arose between measured and calculated values for the integral constants in the fast exponential experiments.

From the data of Tables I and II for ZPR-IV systems, it may be seen that measured values of the buckling were more than 10% below those calculated.

As to  $U^{235}:U^{238}$  ratios, measured values were more than 20% above those calculated. There are two hypotheses to explain these discrepancies:

- (A) Either the multigroup data used in theoretical calculations are exceedingly poor: too few groups above the  $U^{238}$  fission threshold, erroneous fission cross-section data, purely empirical guesses for inelastic scattering.
- (B) Or true equilibrium has not been reached in the exponential experiment. Detectors have been measuring a mixture of asymptotic and slowing-down transients. This is coherent with the systematical direction of the numerical discrepancies:

- (i) experimental  $B^2$  are consistently smaller than theoretical  $B^2$ ;  
 admitting that the experimental lateral buckling  $B_y^2$  and  $B_z^2$   
 are correct, this gives: experimental  $\kappa_x^2 >$  theoretical  $\kappa_x^2$   
 (through Eq. (6.8)):

$$\kappa_x^2 = B_y^2 + B_z^2 - B^2 \quad (6.8)$$

This means that the experimental distribution is decaying faster along the exponential x-direction than the predicted asymptotic mode, which is typical of the presence of slowing-

TABLE I

Compositions for Typical ZPR-IV Systems

System Designation	$U^{238}:U^{235}$ Atom Ratio	Vol %			
		U	Fe	AL	Void
1	3.13	35.11	10.36	14.76	39.77
2	5.00	34.59	10.36	0	55.05
3	6.82	34.33	10.36	14.76	40.55

TABLE II

Experimental Results and Comparison with a First Set of Theoretical Predictions in ZPR-IV Systems

System Designation	1		2		3	
	Expt	Theory	Expt	Theory	Expt	Theory
Root Buckling B ( $cm^{-1}$ )	0.0512	0.0600	0.0383	0.0423	0.0320	0.0368
$U^{235}:U^{238}$ Fission Ratio per Atom	20.3	16.6	24.0	20.2	34.0	26.5

down transients (see Chapter V, especially the discussion of Eq. (5.51)).

- (ii) experimental  $U^{235}:U^{238}$  ratios are consistently higher than the theoretical; this means that the experimental energy-spectrum is softer than predicted, which is due to an excess of high-energy neutrons leaking out of the system: namely, slowing-down transients are in excess and have a preferential leakage (the diffusion coefficient being an increasing function of energy).

Hypotheses (A) and (B) are not mere "elucubrations de théoriciens"; they have been suggested by experimentalists working on ZPR-IV; quoting<sup>36</sup>:

"It is seen from data of Table I (and II) that values of the Buckling as measured in the experiments are about 10% below those calculated. There are indications that complete spectral equilibrium is not attained in the exponential experiment, which is possible because the criteria used for determining equilibrium are insensitive to changes in the spectrum below about 700 keV. Hence a more detailed study of approach to equilibrium is now being undertaken experimentally.

It is similarly observed that there is a systematic difference between calculated and measured reflector savings, which may be due to the same cause, or may be due to incorrect choices of transport and inelastic scattering-cross sections used in the calculations."

In order to check hypothesis (A), theoretical calculations on ZPR-IV systems were carried on again some time later, using a greatly improved set of multigroup cross-sections: namely, the well-known "Yiftah-Okrent-Moldauer" "YOM" set.<sup>37</sup> Results of these improved calculations are given in Table III. The comments on Table III are left to W. B. Loewenstein and D. Okrent<sup>37</sup>:

TABLE III

Experimental Results and Comparison with a Second Set of Theoretical Predictions in ZPR-IV Systems

System Designation (see Table I)	1		2		3	
	Expt	Theory	Expt	Theory	Expt	Theory
Root Buckling B (cm <sup>-1</sup> )	0.0512	0.0609	0.0383	0.0431	0.0320	0.0368
$\sigma_F U^{238} / \sigma_F U^{235}$	0.0493	0.0529	0.0392	0.0431	0.0292	0.0322
			0.0400		0.0294	

"...Early analyses indicated substantial disagreement between theory and experiment on a variety of integral parameters. The latter included the material Buckling,  $\sigma_F(U^{235})/\sigma_F(U^{238})$  and reflector-savings determination of materials. With the recent

critical-experiment information on assemblies having composition quite similar to those in the exponential columns, it is useful to review the latter experiments. It is evident that calculated values for the material Buckling are consistently higher than observed. This was also reported by previous analyses.<sup>36</sup> Better agreement has been obtained between measured and predicted values for  $\sigma_F(U^{238})/\sigma_F(U^{235})$  than in the past. This can probably be attributed to the inclusion of two energy groups above the  $U^{238}$  fission threshold, where previous analyses utilized only one such group... . However calculated  $\sigma_F(U^{238})/\sigma_F(U^{235})$  are still consistently higher than measured... . ...indicating a softer spectrum in the assembly. Such might be the case if there were an excessive amount of high-energy neutrons leaking out of the system, in other words, a true equilibrium spectrum may not have been attained in the experiment... ."

So, the challenge is still open for the interpretation of ZPR-IV experiments.

As to the exponential experiment in natural uranium, the situation appears even more extreme: most experimental studies concluded that equilibrium was not achieved.<sup>36,39</sup>

From Table IV, it appears clearly that various experimental teams obtained a wide spread of values for the diffusion length in natural uranium. Discrepancies are even more striking for the spectral equilibrium index  $\sigma_F(U^{235})/\sigma_F(U^{238})$ .

The experimental team of Saclay<sup>39</sup> tried to investigate more closely this problem of approach to equilibrium in natural U. special care was given to the acquisition of more detailed information about the differential energy-spectrum of the flux; a fairly wide range of activation detectors and proton-recoil spectrometry were used. Calculations comparing the answers of these various detectors yielded an accurate experimental curve for the asymptotic energy-spectrum (see Fig. 14). However, this did not mean that an actual

TABLE IV

Measurements Made on Natural Uranium

Experiment	Reference	Principle of the Measures	Diffusion Length (cm)	$\frac{\sigma_F(U^{235})}{\sigma_F(U^{238})}$
Saclay	39	fission chambers activation detectors proton-recoil spectr.	9.525 $\pm 0.05$	$230 \pm 10$
Pajarito (Los Alamos)	46	activation detectors fission chambers radiochemical techniques	$9.17 \pm 0.18$	$+238 \pm 6$ $240 \pm 12$ $243 \pm 15$
Oak Ridge	47	activation detectors fission chambers	9.6	336
Argonne	36	fission chambers radiochemical techniques	$10.0 \pm 0.12$	$363 \pm 40$ 220
Pajarito	48	activation detectors radiochemical techniques fission chambers	13.18 10.35	$220 \pm 22$ $200 \pm 10$ $210 \pm 10$

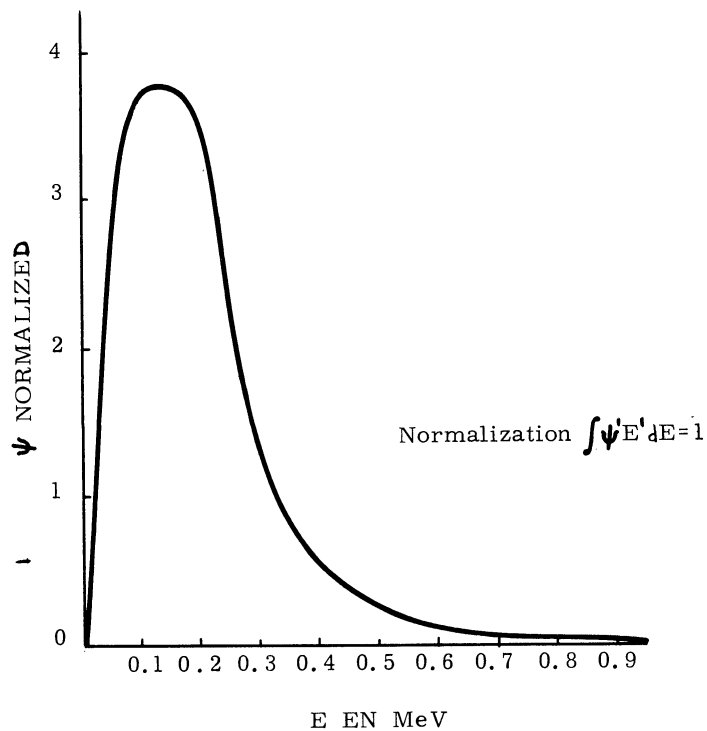


Fig. 14. Asymptotic spectrum in natural uranium: experimental curve.

equilibrium was reached. The system was a cube of 80 cm in size, and apparent equilibrium was obtained for values of  $x$  such that:

$$42 \text{ cm} \leq x \leq 52 \text{ cm}$$

the  $x$ -direction being the exponential one. This turns out to be quite a narrow range of equilibrium (compare with ZPR-IV, Fig. 13). Adjustments of counting data were made within this zone of apparent equilibrium. But it appeared that, even within this restricted range, equilibrium was doubtful; quoting<sup>39</sup>:

"...If we use various detectors  $i$ , the cross-sections of which are varying in very different ways, and if we observe that the apparent relaxation lengths  $L_i$  are equal, then we can assert that the energy-distribution of neutrons is in equilibrium, and we can write:

$$L = \text{relaxation length} = L_i$$

...Results of measurements performed with various detectors are presented in Table V. We realize that the  $L_i$  are not equal, hence the flux energy-distribution is not in equilibrium. The fastest neutrons in the spectrum decay more quickly than the slowest ones... ."

Table V shows the apparent relaxation lengths for various detectors, after careful corrections of measurements made in the restricted zone of apparent equilibrium  $42 \text{ cm} \leq x \leq 52 \text{ cm}$ . There remains, in spite of all corrections and adjustments, an irreducible difference between values given by threshold and "thermal" detectors. This is a striking experimental proof of the behavior and presence of slowing-down transient-modes. As we know from the discussion of Eq. (5.51), these slowing-down transients correspond to a slowing-down source  $\chi(E) - \mathcal{H}(E)$ , where  $\mathcal{H}(E)$  is the asymptotic spectrum, the latter being particularly degraded for natural U (see Fig. 14); this "slowing-

TABLE V

Apparent Relaxation Lengths for Different Detectors in Natural U  
(from Ref. 39)

Detector	Effective Threshold Energy (MeV)	$L_i$ (cm)
P(n,p)	3.0	8.64
S(n,p)	3.0	8.69
Th <sup>232</sup>	1.75	8.82
U <sup>238</sup>	1.45	8.86
Np <sup>237</sup>	0.75	8.53
U <sup>235</sup>		9.02
U <sup>233</sup>		9.12
Pu <sup>239</sup>		9.17
Au(n, $\gamma$ )		9.05

down transients" source is positive and important at fission energies, and the corresponding high energy slowing-down transient modes decay faster than the asymptotic and low-energy transient modes (see Eqs. (5.49) and (5.50)). These facts are faithfully reflected by the behavior of threshold detectors with decreasing threshold energies.

Further calculations from experimental data in Saclay<sup>39</sup> indeed showed that the energy-spectrum was not in equilibrium. Figure 15 gives the evolution of the energy-spectrum along the exponential axis (from experimental data): the equilibrium is not reached even in the zone of apparent asymp-



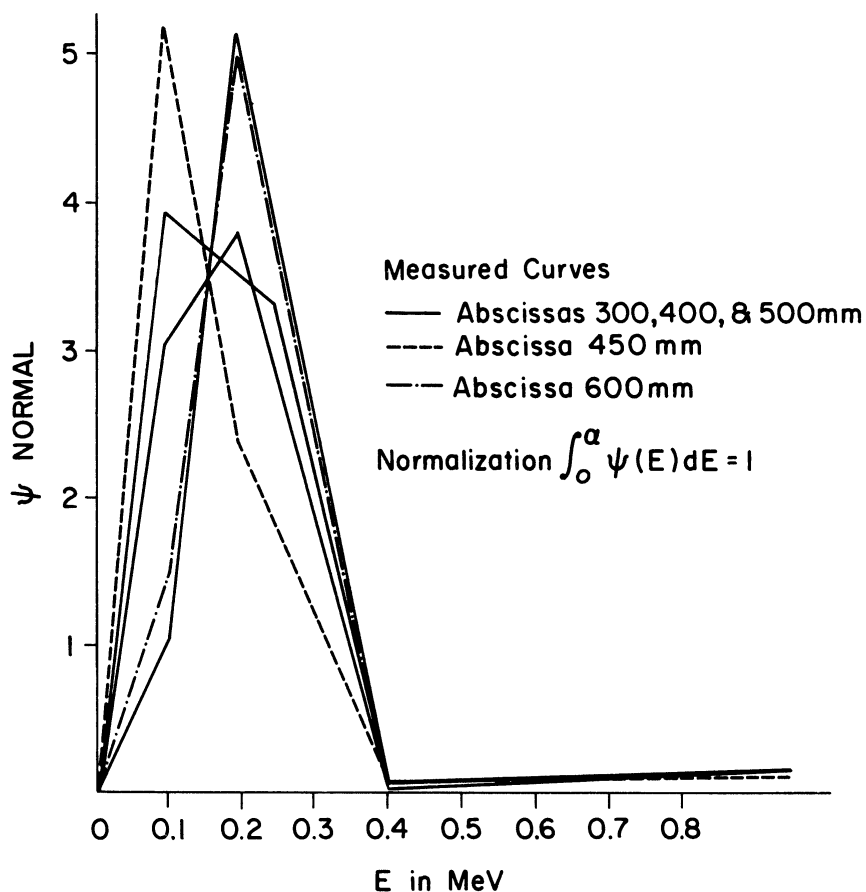


Fig. 15. Evolution of the spectrum along the x-axis in the natural U-exponential system.

toticity (42 cm - 52 cm). There seems to be no doubt that "slowing-down transients" are still important at distances far from the source (roughly 20 m.f.p.) in the natural U-exponential assembly.

Another remarkable study of the slowing-down transients "per se" has been performed by a team of Argonne National Laboratory; noticing the discrepancies between various measured values for the  $U^{235}/U^{238}$  fission ratios in natural uranium, they admitted a priori that equilibrium was not reached; to test experimentally this hypothesis, they measured the fission ratio for blocks of natural uranium, the height and length of which were retained at 24 in., while the thickness was varied from 10 in. to 24 in. For each block,

the  $U^{235}/U^{238}$  fission ratios were carefully measured and corrected in a zone of "apparent equilibrium."<sup>45</sup> From our theory (Chapters III and V), we know that the smaller the block is, the bigger the proportion of slowing-down transients in the neutron flux; since slowing-down transients reflect the adjustment of the neutron spectrum from the initial high-energy fission source to the final degraded asymptotic spectrum, their overall effect is to shift the neutron energy spectrum towards the high-energy range. Figure 16 is a striking experimental verification of this assertion: far from being even approximately constant, the  $U^{235}/U^{238}$  fission ratio decreases steadily with the size of the block, indicating a higher-energy spectrum and an increasing proportion of slowing-down transient modes: these modes are very different from spatial transport transients, since they are still important at distances as far as 20 m.f.p. from the source ( $\approx 40$  cm).

Figure 16, by itself, would justify the theoretical work presented in this thesis as a necessary first step: in spite of many underlying approximations, it is not a mere academic "pièce Parnassienne sur l'Art pour l'Art," but corresponds to an attempt to shed some light upon an actual experimental challenge.

## 6.2. DETAILED DATA ON THE FAST EXPONENTIAL EXPERIMENT IN ZPR-IV SYSTEMS

From this point on, we will focus our attention on the ZPR-IV systems. We will not try to use the theoretical considerations developed in Chapters II, III, and V to predict integral constants in ZPR-IV: on the contrary, we will take for granted the values yielded by experimental measurements or sound

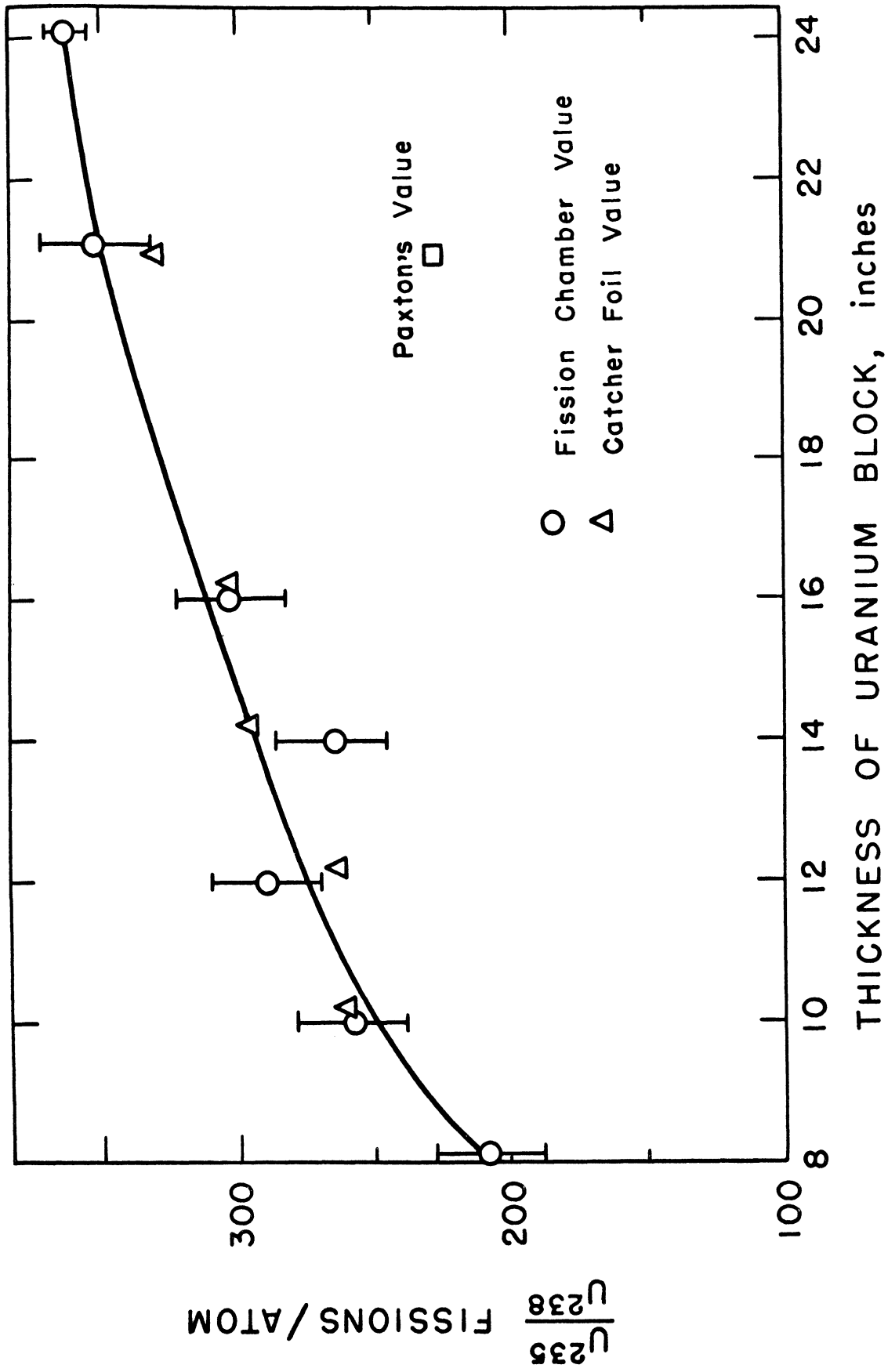


Fig. 16. Effect of uranium block size on fission ratio.

multigroup diffusion calculations for integral parameters such as the buckling  $B$ , the lateral bucklings  $B_y$  and  $B_z$ , the asymptotic energy spectrum  $\chi(E)$ . But we will use our theory to make a semi-quantitative study of the slowing-down transients and the approach to equilibrium—that is, for the very point where an experimental challenge lies and which classical multigroup diffusion theories are totally unable to explain.

We chose to interpret experimental data on ZPR-IV rather than natural uranium; the reasons are multiple:

(i) the experimental situation is not clear in ZPR-IV; discrepancies observed between calculated and measured values could come from a lack of equilibrium as well as from the use of poor multigroup data in calculations (see hypotheses (A) and (B), Section 6.1, p. 132). Yet, a clear answer on this point is crucial, since ZPR-IV systems are highly representative of fast reactor media. If indeed equilibrium were not reached, this would severely limit the validity of asymptotic transport theory commonly used in fast-reactor calculations. On the other hand, if it turned out that equilibrium was practically reached in ZPR-IV systems, then the observed discrepancies could be attributed only to the lack of accuracy of multigroup cross-sections used in calculations, and not to any transport effects: asymptotic transport theory "per se" would be valid.

(ii) On the other hand, the experimental situation is quite clear for natural U: in most cases, equilibrium is undoubtedly not reached.

(iii) The equilibrium spectrum in natural U is much more degraded than in ZPR-IV systems (see Figs. 14 and 20); in the latter, few neutrons are present

below the inelastic scattering threshold, which is one of the hypotheses used in our theoretical work.

(iv) We will study ZPR-IV systems with a wide range of fuel isotopic composition (namely ratios of  $U^{238}/U^{235}$  varying from 3:1 to 7:1). This way, we can get a clear quantitative appraisal of the way slowing-down transients evolve with the enrichment of the system: we can easily extrapolate these effects to natural uranium, in which they will be much more significant.

The basis for further work is to adjust the parameters in our theoretical model, so that the integral constants predicted by our model will be equal to those measured in experiments (or eventually calculated through the use of accurate multigroup codes). By integral constants, we mean the buckling  $B$ , the lateral bucklings  $B_y$ ,  $B_z$ , the exponential relaxation length  $1/\kappa_x$ , the asymptotic energy-spectrum  $\chi(E)$ , such as defined in Section 6.1; all these parameters are considered as constants of the system, with which our theoretical model must agree. Then, through the help of the theoretical model, we may proceed to a consistent study of the approach to equilibrium.

So, at this point, a careful review of available data on ZPR-IV assemblies is necessary.<sup>36,45</sup> These assemblies consisted of a rectangular stack of iron cans, 3 x 3 x 24 in., filled with the appropriate mixture of uranium isotopes ( $U^{235}$ ,  $U^{238}$ ) and diluant materials (Al, Fe). Al was chosen to simulate Na. The volume occupied by Al could be replaced by Na to check the validity of the Al substitution.

The volume fraction of the various constituents of the assemblies are listed in Tables I and VI. The source of neutrons was a light water moderated,

enriched uranium reactor of rectangular geometry. A lead and water reflection shield reduced the leakage from the rear and sides.

From Figure 12, it can be seen that the assembly rests upon a bottom reflector, 12 in. thick, which serves to eliminate the effect of neutrons scattered from the floor and also allows reflector savings data to be obtained. The whole assembly rests on a travelling cart.

In the assemblies, channels of 1-1/4 x 1-1/4 in. cross section are provided through which detectors can be moved to obtain neutron flux distributions. In most cases, these flux traverses were made using miniature fission chambers with external dimensions of 0.2 x 1 x 1 in.

Experimental flux plots were obtained along the exponential x-direction, the vertical z-direction, and the transverse y-direction. For each such flux plot, a least-square fit to a cosine or exponential curve was made, using a computer program. At least one plot was obtained for each of four different chambers (loaded, respectively, with  $U^{235}$ ,  $U^{238}$ ,  $Np^{237}$ , and  $Pu^{240}$ ) in each of the three directions. The fittings were made only over those regions in which the spectrum, as measured by the chambers of varying spectral response, was constant to within one percent in detector ratio. Figures 17 (a), (b), and (c) show typical fitted flux plots. As to Figure 17(c), notice that a knowledge of the position of the maximum in the neutron distribution in the z-direction together with the z-curvature ( $B_z$ ) enables a calculation of the extrapolated end-point of the cosine function located in the reflector.

Finally the weighted mean value of  $\kappa_x$  (or  $B_y$ ,  $B_z$ ) from all curves in each direction is found; from Eq. (6.8), the buckling is deduced from these weighted means.

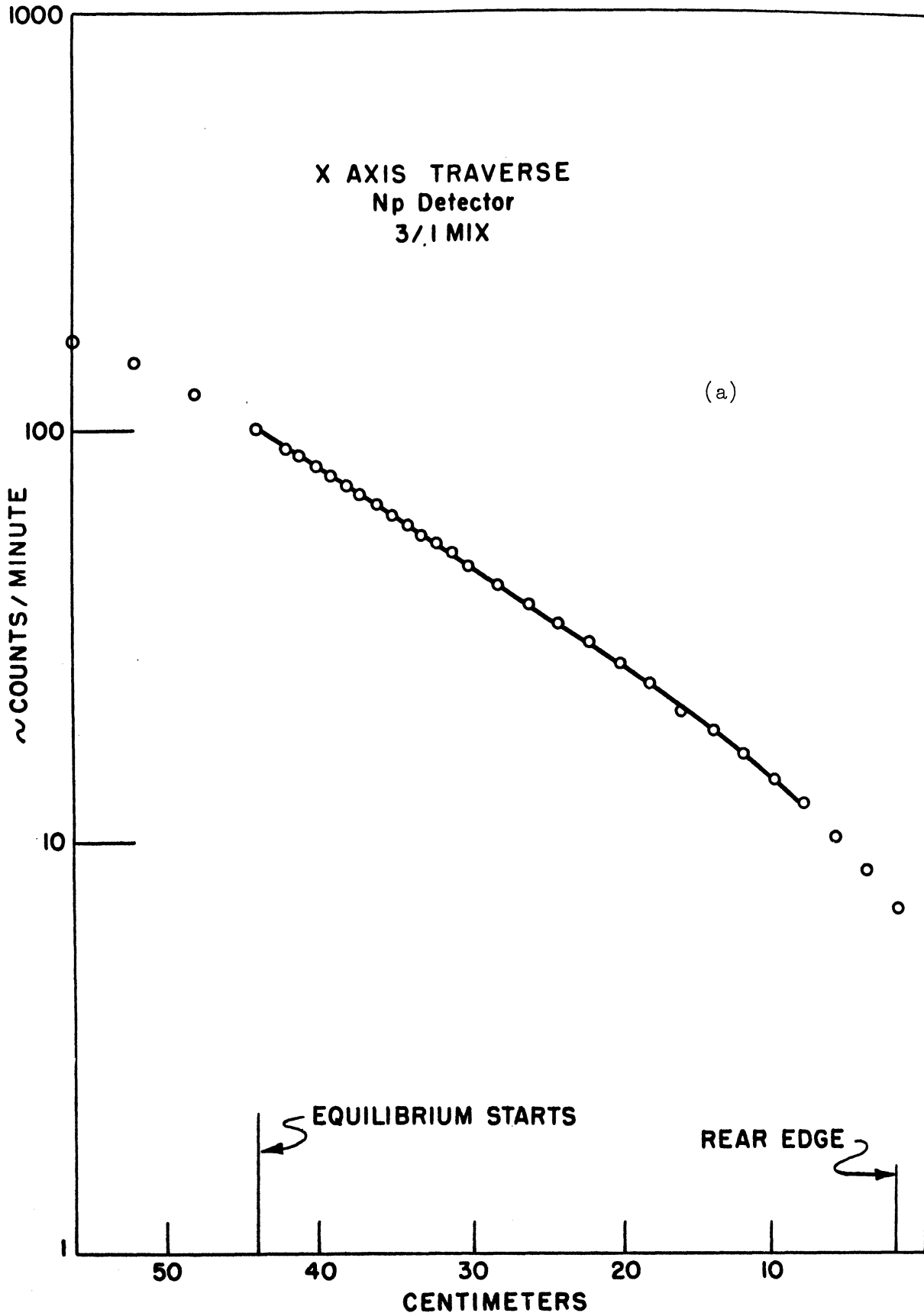


Fig. 17. Experimental neutron distribution in ZPR-IV systems.

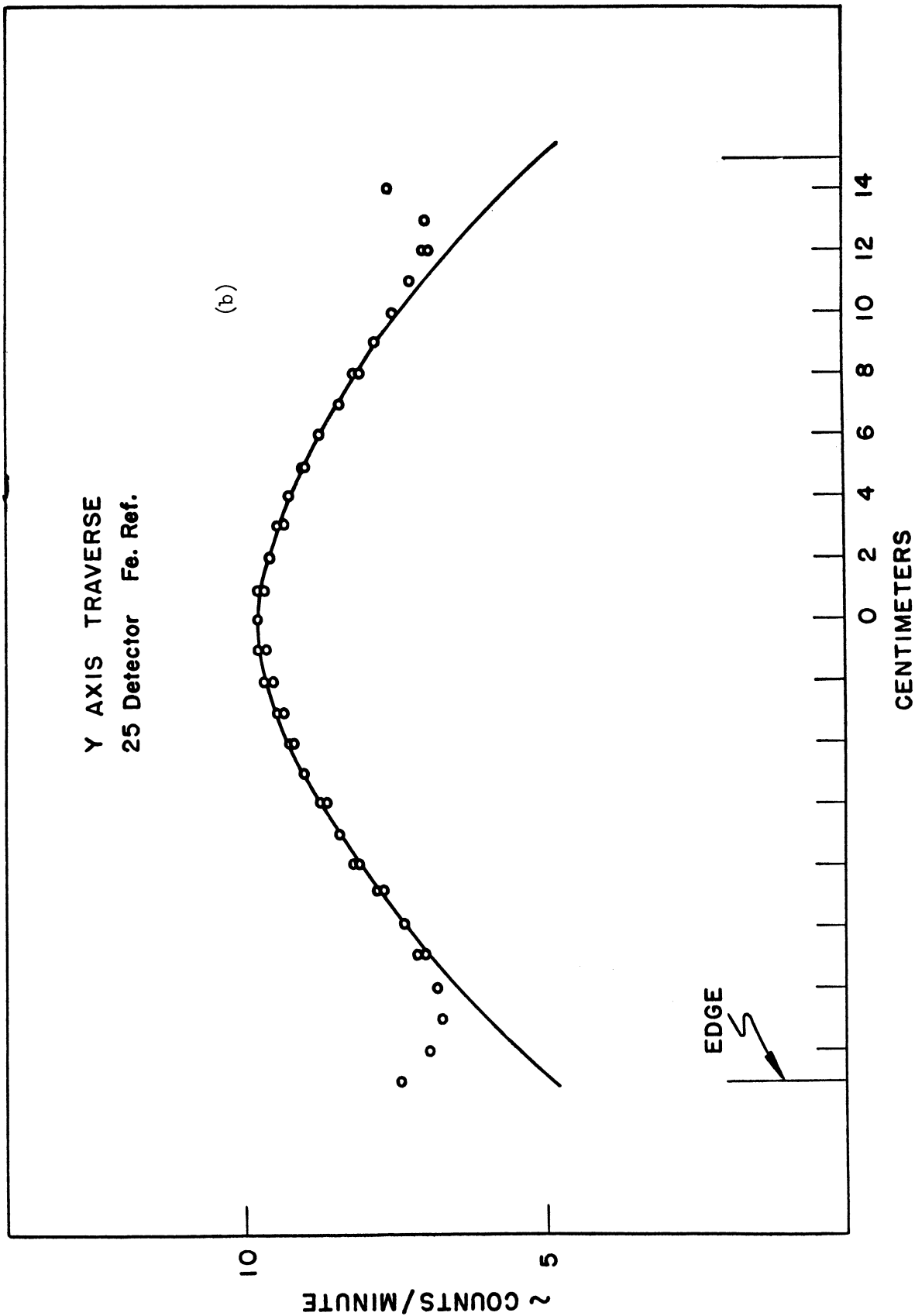


Fig. 17; (Continued).



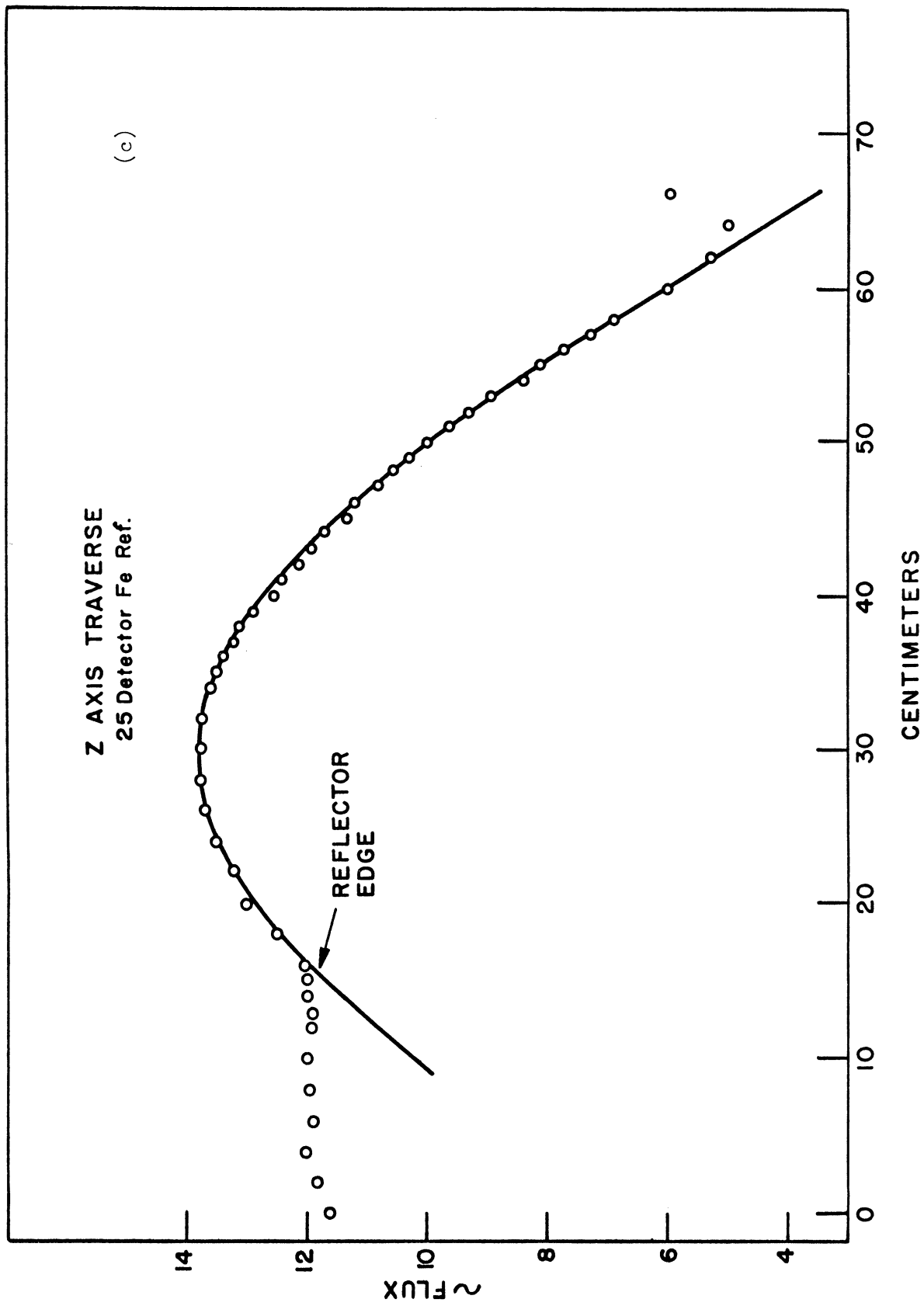


Fig. 17. (Concluded).

Table VI shows the composition and the experimental bucklings of the three ZPR-IV assemblies we will investigate. Bucklings increase of course with the  $U^{235}:U^{238}$  enrichment ratio.

TABLE VI

Composition and Experimental Bucklings for the Studied ZPR-IV Systems

Designation	$U^{238}:U^{235}$ Atom Ratio	Vol %				Buckling	
		U	Fe	Al	Void	B ( $cm^{-1}$ )	B <sup>2</sup> ( $cm^{-2}$ )
1	3.13	35.11	10.36	14.76	39.77	0.0512 $\pm 0.0011$	0.00263 $\pm 0.00011$
2	5.00	34.59	10.36	0	55.05	0.0383 $\pm 0.0007$	0.00147 $\pm 0.00007$
3	6.82	34.33	10.36	14.76	40.55	0.0320 $\pm 0.0003$	0.00102 $\pm 0.00003$

Table VII presents the experimental values for the lateral bucklings  $B_y$  and  $B_z$ , and the exponential relaxation length  $\kappa_x$ . The relaxations lengths do not vary coherently with the uranium enrichment, since the sizes of the assembly, and therefore the lateral bucklings, are not constant from one assembly of given composition to another (see Fig. 12).

Table VIII presents the group energy fluxes for the asymptotic spectra  $\mathcal{H}(E)$ ; these calculations were performed using a 20-group set of diffusion equations; various multigroup cross-section sets were used, and the table presents those results which are the closest to experimental data. The normalization used corresponds to  $\int_0^\infty \mathcal{H}(E)dE = 1$ .

TABLE VII

Experimental Values for the Lateral Bucklings and the  
Relaxation Length in ZPR-IV Systems

System Designation	$\kappa_x^2$ ( $\text{cm}^{-2}$ )	$B_y^2$ ( $\text{cm}^{-2}$ )	$B_z^2$ ( $\text{cm}^{-2}$ )	$B^2 = B_y^2 + B_z^2 - \kappa_x^2$ ( $\text{cm}^{-2}$ )
1	0.00308 $\pm 0.00008$	0.00436 $\pm 0.00007$	0.00135 $\pm 0.00003$	0.00263 $\pm 0.00011$
2	0.00190 $\pm 0.00001$	0.00255 $\pm 0.00004$	0.00082 $\pm 0.00003$	0.00147 $\pm 0.00007$
3	0.00179 $\pm 0.00004$	0.00178 $\pm 0.00002$	0.00103 $\pm 0.00001$	0.00102 $\pm 0.00003$

TABLE VIII

Group Energy Fluxes for the Asymptotic Spectra of ZPR-IV Systems

Group Number	Energy Interval (MeV)	System I	System II	System III
1	1.4 - $\infty$	0.1471	0.1255	0.0956
2	1.0 - 1.4	0.717	0.0699	0.0511
3	.9 - 1.0	0.0296	0.0278	0.0221
4	.8 - .9	0.0315	0.0329	0.0238
5	.7 - .8	0.0448	0.0422	0.0355
6	.6 - .7	0.0563	0.0569	0.0469
7	.55 - .6	0.0314	0.0319	0.0268
8	.50 - .55	0.0343	0.0355	0.0299
9	.45 - .50	0.0373	0.0384	0.0333
10	.40 - .45	0.0395	0.0426	0.0358
11	.35 - .40	0.0523	0.0521	0.0499
12	.30 - .35	0.0618	0.0652	0.0632
13	.25 - .30	0.0677	0.0652	0.0755
14	.20 - .25	0.0579	0.0704	0.0662
15	.15 - .20	0.0679	0.0819	0.0833
16	.10 - .15	0.0787	0.0752	0.1127
17	.050 - .10	0.0599	0.0567	0.0960
18	.025 - .050	0.0205	0.0196	0.0352
19	.010 - .025	0.0073	0.0070	0.0136
20	.000 - .010	0.0013	0.0019	0.0025

The group fluxes corresponding to the group  $i$  are:

$$\int_{E_i}^{E_{i+1}} \mathcal{H}(E) dE$$

where  $E_i$  is the lower energy bound for the group  $i$  and  $E_{i+1}$  the corresponding one for the group  $i+1$ .

### 6.3. ADJUSTMENT OF THE THEORETICAL MODEL TO EXPERIMENTAL CONDITIONS AND DATA IN ZPR-IV SYSTEMS

#### 6.3.1. Introduction

Our major tool for numerical investigation will be the infinite-space Green's function, an elaborate expression of which has been given in Eq. (5.51) and (5.52); this function is solution of the transport equation (5.7), corresponding to an infinite medium along the  $x$ -axis, and a fission isotropic-source at the origin:

$$\begin{aligned} \mu \frac{\partial \Psi}{\partial x}(x, \mu, E) + \Psi(x, \mu, E) &= \frac{c_e}{2} \int_{-1}^{+1} \Psi(x, \mu', E) d\mu' \\ &+ \frac{c_i}{2} q(E) \int_{-1}^{+1} d\mu' \int_E^{\infty} \frac{\Psi(x, \mu', E')}{h(E')} dE' \\ &+ \frac{c_f}{2} \chi(E) \int_{-1}^{+1} d\mu' \int_0^{\infty} \Psi(x, \mu', E') dE' \\ &+ \frac{1}{2} \delta(x-x_0) \chi(E) \end{aligned} \quad (5.7)$$

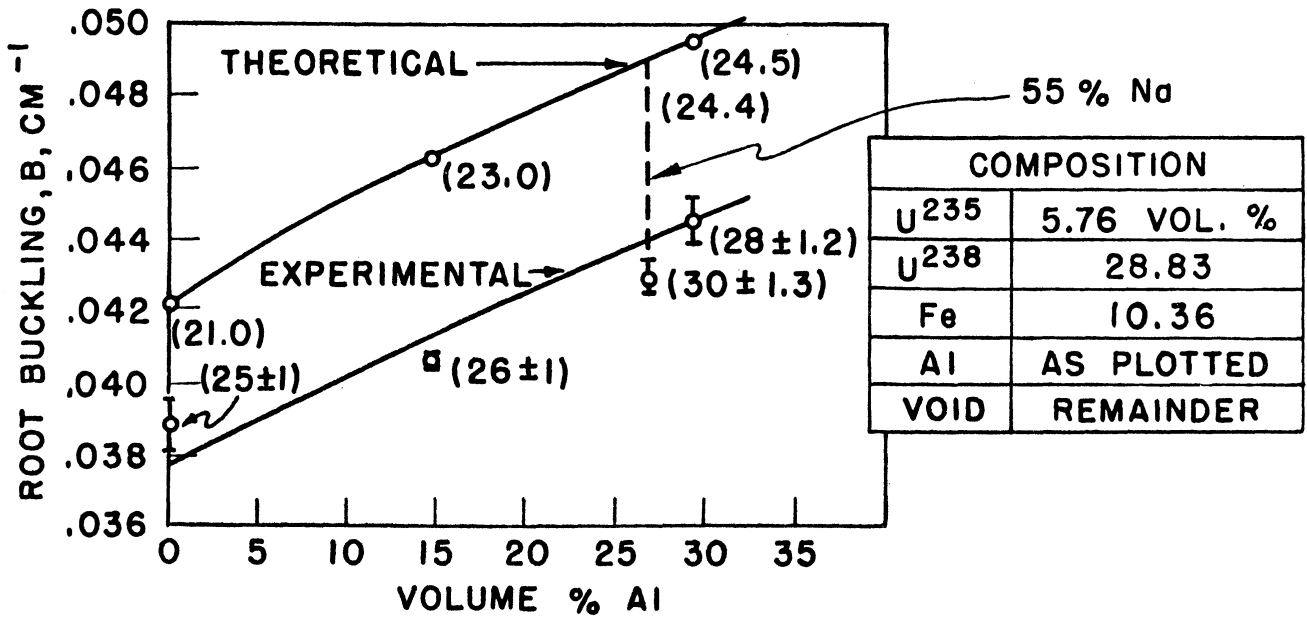
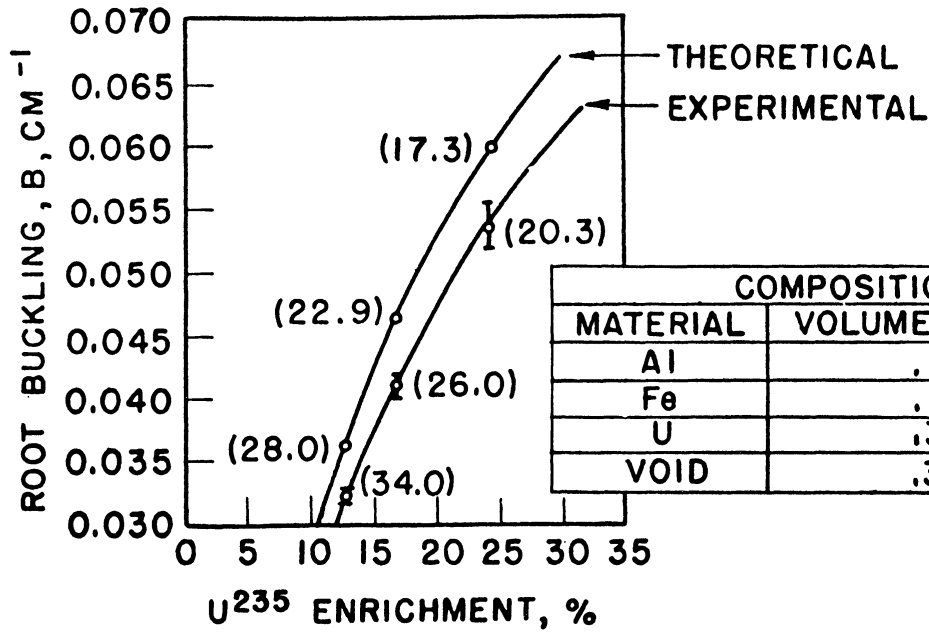


Fig. 18. Bucklings and  $U^{235}/U^{238}$  fission ratios vs. enrichment and Al concentrates.

The experimental system is, of course, a prism bounded along the z- and y-directions; but in Section 6.3.2, we will show how a very elegant method, introduced by M. M. R. Williams,<sup>49</sup> allows us to easily take into account lateral finite dimensions in the solution of Eq. (5.7), while still keeping an infinite dimension along the x-axis of exponential measurements.

Boundary conditions in a fast-exponential experiment are generally poorly defined. The source is usually a stream of thermalized neutrons (see Sections 6.1 and 6.2) but such neutrons do not belong to the energy-range of the neutron field in the fast assembly: by hitting the front-face of the system, they generate isotropic fission sources. As to the thermalized source-stream, it damps out very quickly in the exponential assembly, because of the considerable thermal absorption cross-section for the enriched uranium fuel. So, to some extent, one could consider the following fission source-term for the fast-neutron field:

$$\frac{1}{2} \delta(x-x_0) \chi(E) \quad (6.11)$$

where  $x_0$  is the position of the front-face of the assembly. However, things are much more complex in ZPR-IV systems: located on the front leakage face is a converter plate, or "pedestal" of natural uranium (see Fig. 12), 8 in. thick, which reduces the interaction between the source core and the exponential assembly; it produces an energy spectrum of neutrons which matches the asymptotic spectrum of ZPR-IV more closely than the thermalized leakage spectrums of the thermal source.

So, in regard to these poorly defined boundary conditions, since we are above all interested in making a semi-numerical appraisal of the relative importance of slowing-down transients and space-energy separable modes, we will consider a prism having the composition of ZPR-IV systems, finite along the y- and z-directions, and infinite along the x-direction. We will study numerically the importance of the slowing-down transients generated by a plane-isotropic fission source. The model will be adjusted so that the lateral bucklings, the discrete fundamental relaxation length along the x-axis, and the asymptotic energy spectrum will be those yielded by ZPR-IV experiments.

### 6.3.2. Reduction of the Three-Dimensional Transport Equation to a Single-Dimensional One

Since the system is a prism bounded in the y- and z-directions, the actual transport equation must be reformulated as:

$$\begin{aligned}
 \vec{\Omega} \cdot \overrightarrow{\text{grad}}_r \psi(\vec{r}, \vec{\Omega}, E) + \psi(\vec{r}, \vec{\Omega}, E) \\
 = \frac{C_i}{4\pi} \int d\Omega' g(E) \int_E^\infty \frac{\psi(\vec{r}, \vec{\Omega}', E')}{h(E')} dE' \\
 + \frac{C_f}{4\pi} \int d\Omega' \chi(E) \int_0^\infty \psi(\vec{r}, \vec{\Omega}', E') dE' \\
 + \frac{C_e}{4\pi} \int d\Omega' \psi(\vec{r}, \vec{\Omega}', E) + S(\vec{r}, \vec{\Omega}) \chi(E)
 \end{aligned}
 \tag{6.12}$$

However, along the z-vertical direction, and the y-transverse direction, the dimensions of the ZPR-IV systems are quite large compared to the mean-free path; typically, the dimensions along the y-axis are  $\geq 9$  m.f.p. and along the z-axis,  $\geq 12$  m.f.p.\* Moreover, experimental flux-plots showed that the flux shape was very close to a cosine, over a wide spatial range in the z- and y-directions (see Figs. 17(b) and 17(c)).

Then, the fundamental idea, introduced by M. M. R. Williams,<sup>49</sup> is to assume asymptotic transport theory along the y- and z-axis; that is, we look for solutions of Eq. (6.12) such that:

$$\psi(r, \Omega, E) = \psi(x, \mu, E) e^{-iB_y \cdot y} e^{-iB_z \cdot z} \quad (6.13)$$

where  $B_y$  and  $B_z$  are the lateral "bucklings" (i.e., fundamental modes). This "ansatz" reduces our tri-dimensional transport equation (6.12) to a single-dimensional one which we can solve rigorously. It must be emphasized that the validity of the "ansatz" (6.13) has been verified experimentally in ZPR-IV systems (Figs. 17(b) and 17(c)), and that we have accurate experimental values for the bucklings  $B_y$  and  $B_z$  (see Table VII). There is no need for any kind of "théorie"acrobatique" for an energy-dependent extrapolation length.

Let us proceed to the reduction of Eq. (6.12): from Sections 3.4 and 3.5, we know that Eq. (6.12) can be decomposed into two associated equations, the first one being space-energy separable, hence "de facto" monokinetic; the

---

\*For ZPR-IV systems, 1 m.f.p.  $\simeq 2$  in.



second one being a plain slowing-down equation, which we can also reduce to a "monokinetic" one, through an energy  $\mathcal{M}$ -transformation (Section 2.4): so, instead of tackling with the lengthy formalism of the complete equation (6.12), it is absolutely equivalent to study the reduction of the one-speed transport equation:

$$\vec{\Omega} \cdot \vec{\text{grad}}_{\vec{r}} \psi(\vec{r}, \vec{\Omega}) + \psi(\vec{r}, \vec{\Omega}) = \frac{c}{4\pi} \int d\Omega' \psi(\vec{r}, \vec{\Omega}') + S(\vec{r}, \vec{\Omega}) \quad (6.14)$$

since results can be immediately applied to the two "monokinetic" equations associated with the general equation (6.12). Introducing the ansatz:

$$\psi(\vec{r}, \vec{\Omega}) = \psi(x) e^{-iB_y \cdot y} e^{-iB_z \cdot z} \quad (6.15)$$

And setting:

$$S(\vec{r}, \vec{\Omega}) = \frac{1}{4\pi} \delta(x) \cdot e^{-iB_y \cdot y} e^{-iB_z \cdot z} \quad (6.16)$$

Eq. (6.14) reduces to:

$$\begin{aligned} \mu \frac{\partial \psi}{\partial x}(x, \mu) + \left\{ 1 - i\sqrt{1-\mu^2} (B_y \cos \eta + B_z \sin \eta) \right\} \psi(x, \mu) \\ = \frac{c}{4\pi} \psi_0(x) + \frac{1}{4\pi} \delta(x) \end{aligned} \quad (6.17a)$$

where

$$\psi_0(x) = \int_0^{2\pi} d\eta \int_{-1}^{+1} \psi(x, \mu) d\mu \quad (6.17b)$$

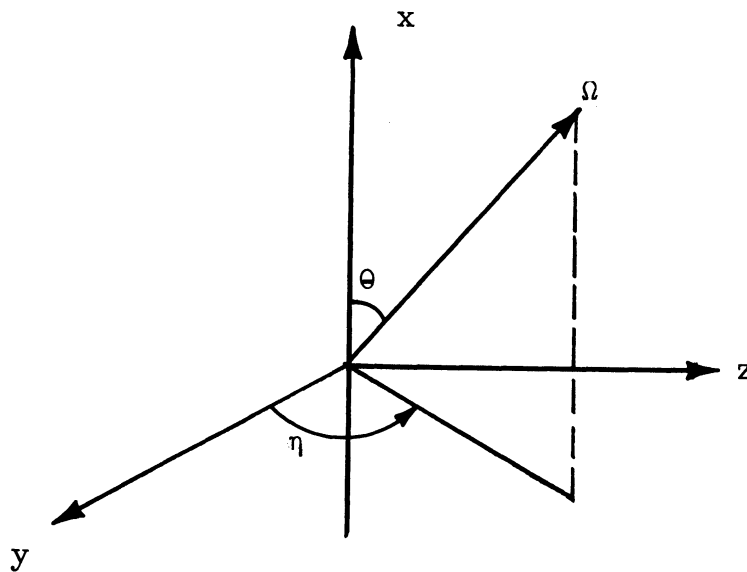


Fig. 19. The angles  $\theta$  and  $\eta$ .

From this point on, our calculation methods will differ from William's.<sup>49</sup>

the final results, of course, will be identical.

Apply a Fourier-transformation to Eqs. (5.17):

$$\bar{\Psi}(k, \mu) = \int_{-\infty}^{+\infty} \psi(x, \mu) e^{-ikx} dx \quad (6.18a)$$

And obtain:

$$\left\{ 1 + ik\mu - i\sqrt{1-\mu^2} (B_y \cos \eta + B_z \sin \eta) \right\} \bar{\Psi}(k, \mu) \\ = \frac{c}{4\pi} \bar{\Psi}_0(k) + \frac{1}{4\pi} \quad (6.18b)$$

Define the lateral buckling  $B_L$ :

$$B_L = \sqrt{B_y^2 + B_z^2} \quad (6.19)$$

Also, define the angle  $\Delta$  such that:

$$B_y = B_L \cos \Delta \\ B_z = B_L \sin \Delta \quad (6.20)$$

Then Eq. (6.18b) becomes:

$$\left\{ 1 + ik\mu - i\sqrt{1-\mu^2} (B_L \cos(\eta - \Delta)) \right\} \bar{\Psi}(k, \mu) \\ = \frac{c}{4\pi} \bar{\Psi}_0(k) + \frac{1}{4\pi} \quad (6.21)$$

Integration of Eq. (6.21) over  $\mu$  and  $\eta$  yields:

$$\bar{\Psi}_0(k) = \left\{ c \bar{\Psi}_0(k) + 1 \right\} \\ (x) \frac{1}{4\pi} \int_{-1}^{+1} d\mu \int_0^{2\pi} \frac{d\eta}{1 + ik\mu - i B_L \sqrt{1-\mu^2} \cos(\eta - \Delta)} \quad (6.22)$$

It will be shown in Appendix C, after lengthy calculations, that in some domain of the complex plane, which includes the strip  $-1 < \text{Im}k < +1$ :

$$\frac{1}{4\pi} \int_{-1}^{+1} d\mu \int_0^{2\pi} \frac{d\eta}{1 + ik\mu - iB_L \sqrt{1-\mu^2} \cos(\eta-\Delta)}$$

$$= \frac{1}{\sqrt{K^2 + B_L^2}} \arctan \sqrt{K^2 + B_L^2} \quad (6.23)$$

Then Eq. (6.22) becomes:

$$\overline{\Psi}_0(k) = \left\{ c \overline{\Psi}_0(k) + 1 \right\} \frac{1}{\sqrt{K^2 + B_L^2}} \arctan \sqrt{B_L^2 + K^2} \quad (6.24)$$

Relations (6.23) and (6.24) are fundamental; they can be expressed in the following way.

In some domain of the complex plane, which includes the strip  $-1 < \text{Im}k < +1$ , the Fourier-transform of the transport kernel of the tri-dimensional equation (6.14) is obtained from the Fourier-transform of the transport kernel of the classical single-dimensional equation, through the replacement of the Fourier variable  $K^2$  by  $K^2 + B_L^2$ , where  $B_L^2$  is the lateral buckling defined by:

$$B_L^2 = B_y^2 + B_z^2 \quad (6.25)$$

(By transport kernel, we mean the kernel of the integral form of the transport equation, see Ref. 30.)

It follows that the Fourier-transform of the infinite-medium Green's function is immediately obtained from the corresponding one for the classical one-dimensional problem, through the mere replacement of  $K^2$  by  $K^2 + B_L^2$ , in

some domain of the complex  $k$ -plane:

$$\overline{\Psi}_0(k^2) = \frac{\frac{1}{\sqrt{k^2 + B_L^2}} \arctan \sqrt{k^2 + B_L^2}}{1 - \frac{c}{\sqrt{k^2 + B_L^2}} \arctan \sqrt{k^2 + B_L^2}} \quad (6.26)$$

Then, it is easily verified that the asymptotic part of the Green's function is given by:

$$\overline{\Psi}_0(k^2) = \frac{dK_0^2}{dc} \frac{1}{(K_0^2 + B_L^2) + k^2} \quad (6.27)$$

where  $K_0$  is the root of:

$$1 = \frac{c}{K_0} \operatorname{arctgh} K_0 \quad (6.28)$$

provided that the corresponding pole belongs to the strip of analyticity for which (6.24) is valid:

$$\begin{aligned} |K_0^2 + B_L^2| < 1 \text{ if } c < 1, \quad K_0 \text{ real} \\ |B_0^2 + B_L^2| < 1 \text{ if } c > 1, \quad K_0 = iB_0 \end{aligned} \quad (6.29)$$

And, after an elementary inverse Fourier-transformation, we find, for the asymptotic component, and for  $B_L^2$  such that (6.29) is verified:

$$\Psi_0(|x|) = \frac{1}{2} \frac{dk_0^2}{dc} \cdot \frac{e^{-|x| \sqrt{K_0^2 + B_L^2}}}{\sqrt{K_0^2 + B_L^2}} \quad (6.30)$$

The Green's function (6.30), solution of Eq. (6.14), is quite interesting: the decay constant  $K_0$  of the discrete mode of the single-dimensional equation is merely replaced by  $\sqrt{K_0^2 + B_L^2}$  for sufficiently small  $B_L^2$ . As to the

transient part of Eq. (6.30), an approximate expression consists in taking the formula for the classical single-dimensional case, which is not too bad if:

$$B_L^2 \ll 1 \quad (6.31)$$

this is generally verified for sufficiently large systems.

These results are of course in agreement with the classical diffusion theory; calling  $\kappa_x$  the fundamental decay constant along the x-axis, we have:

$$\kappa_x^2 = K_o^2 + B_L^2 = K_o^2 + B_y^2 + B_z^2 \quad (6.32)$$

Notice that the "material buckling" is  $-K_o^2$ :

$$B^2 = -K_o^2 \quad (6.33)$$

And obtain the well-known diffusion theory relation:

$$B^2 = -\kappa_x^2 + B_y^2 + B_z^2 \quad (6.34)$$

Using the modified monokinetic Green's function (6.30), we can now proceed to the reduction of the three-dimensional polyenergetic equation (6.12). We can easily obtain the modified expressions for the asymptotic solution of this equation, namely:

$$\Delta'(|x|, E) \cdot e^{-i B_y \cdot y} \cdot e^{-i B_z \cdot z} \quad (6.35)$$

from the corresponding  $\Delta'(|x|, E)$  developed in Chapter V for the single-dimen-

sional case, the expression of which is given in Eq. (5.52). We just have to keep in mind that:

(A) We must replace everywhere the Fourier variable,  $K^2$  by  $K^2 + B_L^2$ , in the calculations carried in Sections 5.4 and 5.5, in order to obtain an asymptotic expression for the slowing-down transients; this is valid if the essential singularity involved is such that  $|K_e^2 + B_L^2| < 1$ .

(B) The Green's function  $G_e(|x|)$  for the monokinetic transport equation with plain elastic-scattering, as introduced in Eqs. (5.16), (5.17), and (5.22), has to be modified as follows:

$$G_e(|x|) e^{-iB_y \cdot y} e^{-iB_z \cdot z} = e^{-iB_y \cdot y - iB_z \cdot z} \left\{ \frac{1}{2} \frac{dK_e^2}{dc} \cdot \frac{e^{-\sqrt{K_e^2 + B_L^2} |x|}}{\sqrt{K_e^2 + B_L^2}} \right\} \quad (6.36a)$$

provided that  $|K_e^2 + B_L^2| < 1$  where  $K_e$  is the root of:

$$1 = c_e \frac{1}{K_e} \operatorname{argth} K_e \quad (6.36b)$$

(C) The space-energy separable component of  $\Delta'(|x|, E)$  in Eqs. (5.51) and (5.52), which corresponds to self-sustaining modes of the fast multiplying medium, has to be modified as follows:

$$\Phi_E(|x|) \cdot \chi(E) \cdot e^{-iB_y \cdot y - iB_z \cdot z} = \frac{\chi(E)}{2} \cdot e^{-iB_y \cdot y - iB_z \cdot z} \cdot (x) \left\{ \frac{dB^2}{dc} \cdot \frac{e^{-\sqrt{B_L^2 - B^2} |x|}}{\sqrt{B_L^2 - B^2}} \right\} \quad (6.37a)$$

Provided that  $|B_L^2 - B^2| < 1$  when B is the "buckling" of the system, solution of:

$$l = (C_F + C_i + C_e) \frac{1}{B} \arctan B \quad (6.37b)$$

and

$$C = C_F + C_i + C_e \quad (6.37c)$$

In experimental systems such as ZPR-IV, we have (see Table VII):

$$B_L^2 = B_Y^2 + B_Z^2 > B^2 \quad (6.37d)$$

Finally, we obtain the following asymptotic expression for the Green's function solution of Eq. (6.12), corresponding to a prism infinite along the x-axis, finite along the y- and z-axes, and a fission plane source at the origin; this expression includes only poles and essential singularities belonging to the strip of analyticity where Eqs (6.23) and (6.24) are valid; it will turn out (see Table IX) that in ZPR-IV systems, the conditions

$$|K_e^2 + B_L^2| < 1$$

$$|B_L^2 - B^2| < 1$$

are fulfilled in all cases. In fact;  $|B_L^2 - B^2| \ll 1$ , and  $\sqrt{-K_e^2 - B_L^2} \simeq 0.76i$ .

This corresponds to well separated poles and essential singularities.



$$\Delta'(|x|, E) e^{-iB_y \cdot y - iB_z \cdot z} = e^{-iB_y \cdot y - iB_z \cdot z}$$

$$(x) \left\{ \frac{\chi(E)}{2} \left[ \frac{dB^2}{dc} \frac{e^{-\sqrt{B_L^2 - B^2} |x|}}{\sqrt{B_L^2 - B^2}} \right] \right.$$

$$+ \frac{\chi(E) - \chi(E)}{2} \left[ \frac{dK_e^2}{dce} \frac{e^{-\sqrt{B_L^2 + K_e^2} |x|}}{\sqrt{B_L^2 + K_e^2}} \right]$$

$$+ c_i g(E) \cdot e^{-\sqrt{B_L^2 + K_e^2} |x|}$$

$$(x) \int_0^{-\text{Log}[h(E)]} \left[ \frac{\chi - H}{g} \right] (u') \cdot e^{\{u - u'\} \cdot c_i \cdot \left\{ \frac{1}{4} \frac{dK_e^2}{dce} \cdot \frac{1}{K_e^2 + B_L^2} + \Omega(K_e^2 + B_L^2) \right\}}$$

$$(x) \left\{ \frac{1}{4} \left( \frac{1}{\sqrt{K_e^2 + B_L^2}} \cdot \frac{dK_e^2}{dce} \right)^2 \sqrt{\frac{|x|}{\alpha}} \cdot I_1(2\sqrt{\alpha|x|}) \right.$$

$$+ \frac{1}{\sqrt{K_e^2 + B_L^2}} \cdot \frac{dK_e^2}{dce} \cdot \Omega(K_e^2 + B_L^2) \cdot I_0(2\sqrt{\alpha|x|})$$

$$\left. + \left( \Omega(K_e^2 + B_L^2) \right)^2 \sqrt{\frac{\alpha}{|x|}} \cdot I_1(2\sqrt{\alpha|x|}) \right\} du'$$

with:

$$\alpha = \frac{(u-u')}{2} \frac{C_i}{\sqrt{K_e^2 + B_L^2}} \cdot \frac{dK_e^2}{dc_e} \quad (6.38b)$$

$$\Omega(K_e^2 + B_L^2) = \int_0^1 \frac{d\nu}{(1 - (K_e^2 + B_L^2)\nu^2) g(c_e, \nu)} \quad (6.38c)$$

$K_e$  is defined in Eq. (6.36b),  $B^2$  in Eq. (6.37b),  $\lambda(E)$  in Eq. (3.29),  $g(c, \nu)$  in Eq. (6.29),  $B_L^2$  in Eq. (6.25), the "lethargy"  $u$  in Eq. (5.3).

Equation (6.38a) will be our final tool for numerical investigation; this is an asymptotic expression for the neutron flux due to a plane fission-source in a prism of fast-multiplying medium, which is finite along the  $z$ - and  $y$ -directions and infinite along the  $x$ -direction; this expression is valid for all energies, and is spatially asymptotic only to the extent that we neglected all transport transients decaying faster than  $e^{-|x|}$ . As a matter of numerical check we may include some transport transients (i.e., decaying faster than  $e^{-|x|}$ ), approximated by a one-dimensional expression for Eqs. (6.36a) and (6.37a), with  $B_L^2 = 0$ . The corresponding formula is likely to be valid for points close to the plane source, provided that  $B_L^2 \ll 1$ , and that we are sufficiently far away from the lateral boundary faces ( $x$ -axis, for  $y = z = 0$ ).

### 6.3.3. Adjustment of the Parameters in the Theoretical Formula for the Neutron Distribution

The next step is to adjust the parameters in Eq. (6.38) to the experimental data and results on ZPR-IV systems.

For the synthetic inelastic scattering kernel introduced in Section 2.2, we will use the following shape:

$$g(E) = \frac{E}{T^2} e^{-\frac{E}{T}} \quad (6.39a)$$

$$h(E) = 1 - \left(1 + \frac{E}{T}\right) e^{-\frac{E}{T}} \quad (6.39b)$$

where  $T$  is the nuclear temperature, and

$$h(E) = \int_0^E g(E') dE' \quad (6.39c)$$

This shape is, of course, directly inspired from Weisskopf's statistical evaporation model (see Eq. (2.8a)). Improved synthetic kernels are being worked on,<sup>29</sup> but the results were not available in the literature, at the time of the present work. We keep the nuclear temperature  $T$  as an arbitrary parameter.

There are three basic principles to be followed in adjusting the parameters:

(A) Average those macroscopic cross-sections, which are varying smoothly enough, over the "experimental" asymptotic flux  $\chi(E)$  tabulated in Table VIII (see also Figs. 20). This method is justified to the extent that the bulk of

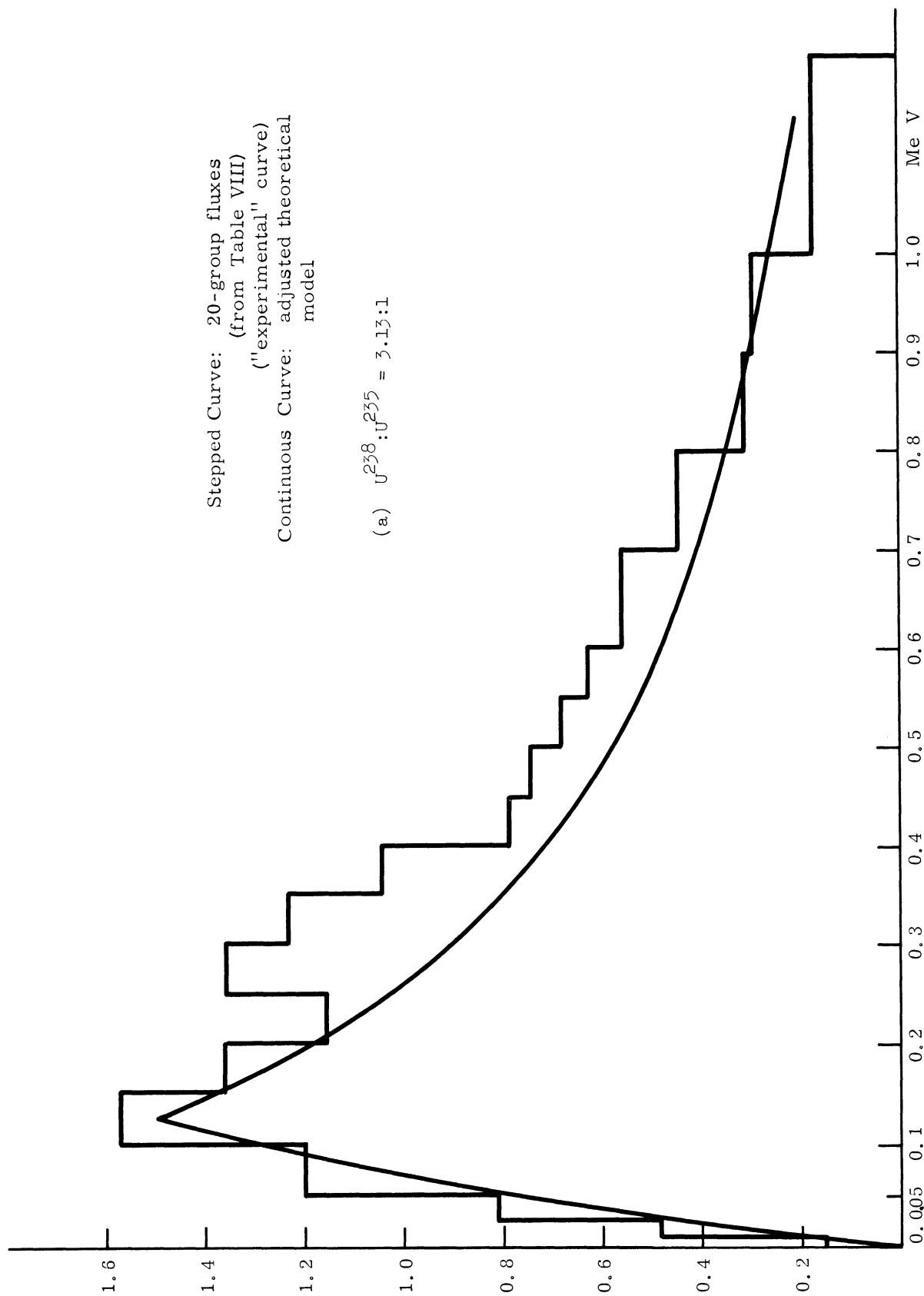


Fig. 20. Asymptotic spectra for ZPR-IV.

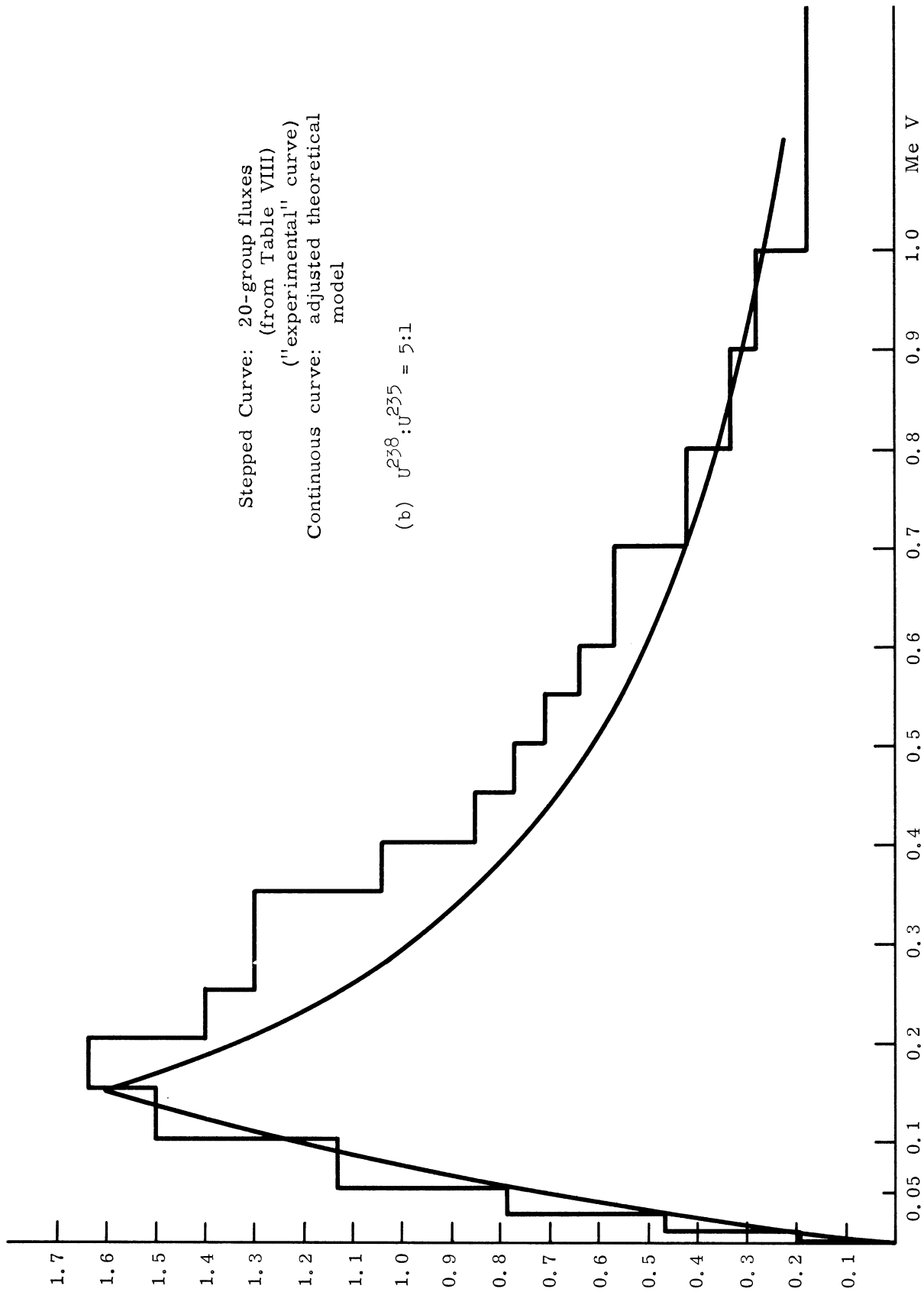


Fig. 20. (Continued).

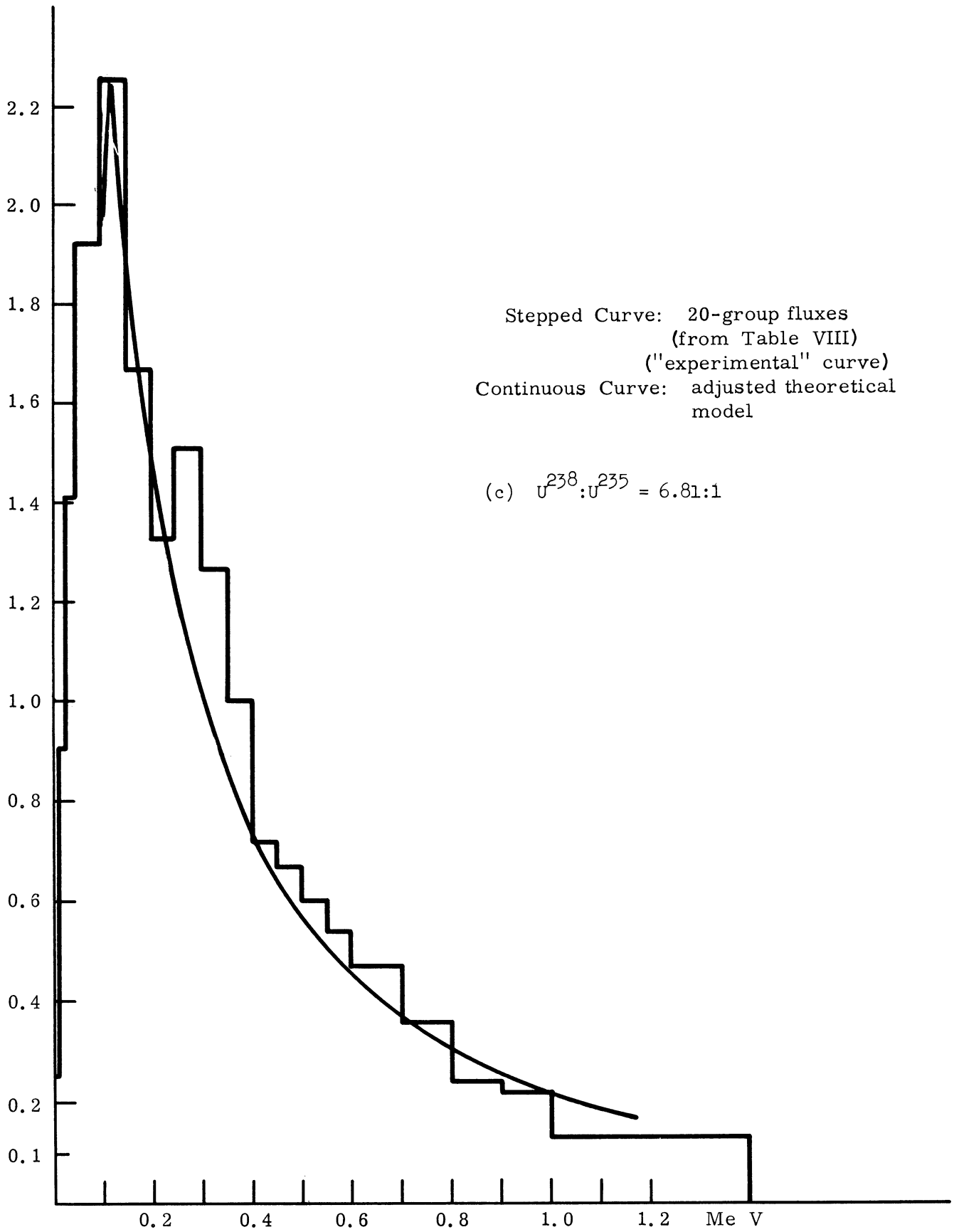


Fig. 20. (Concluded).

neutrons in ZPR-IV systems is well above the inelastic-threshold energy (see Figs. 20); in this energy range, the macroscopic total, fission\* and elastic cross-sections are varying smoothly enough to allow the following averaging scheme:

$$\overline{\Sigma_T} = \int_0^{\infty} \Sigma_T(E) \cdot \mathcal{H}(E) dE \quad (6.40a)$$

$$\overline{\nu \Sigma_F} = \int_0^{\infty} \nu(E) \Sigma_F(E) \cdot \mathcal{H}(E) dE \quad (6.40b)$$

$$\overline{\Sigma_e} = \int_0^{\infty} \Sigma_e(E) \cdot \mathcal{H}(E) dE \quad (6.40c)$$

which yields for  $c_F$  and  $c_e$ , average number of secondaries resulting respectively from a fission and an elastic collision:

$$c_F = \frac{\overline{\nu \Sigma_F}}{\overline{\Sigma_T}} \quad (6.41a)$$

$$c_e = \frac{\overline{\Sigma_e}}{\overline{\Sigma_T}} \quad (6.41b)$$

The cross-sections in Eq. (6.40) were averaged using the isotopic compositions given in Table VI, the list of values for  $\mathcal{H}(E)$  in Table VIII, and the graphs of microscopic cross-sections in BNL 325.

---

\*Since the fuel is notably enriched in  $U^{235}$ , the fission macroscopic cross-section varies smoothly enough.

This allows us to define a new unit of length, namely the mean-free path  $\Lambda$  defined as:

$$\Lambda = \frac{1}{\sum_T} \quad (6.42)$$

(B) The second principle in adjusting the parameters, is to set the "material" buckling  $B^2$  and the lateral buckling  $B_L^2$  equal to their experimental values (see Tables VI and VII). They are, however, normalized to the new unit of length defined in Eq. (6.42), so that they become dimensionless. This implies, of course, that the exponential fundamental mode  $\kappa_x$  is kept to its experimental value, since:

$$\kappa_x^2 = B_L^2 - B^2$$

(see comments on Eq. (6.34)).

The adjustment of the "material" buckling  $B^2$  immediately yields a value for the overall multiplication coefficient  $c$  defined by

$$c = c_F + c_e + c_i \quad (6.43a)$$

through the formula:

$$c = \frac{1}{B} \arctan B \quad (6.43b)$$

(C) The only remaining parameters to be adjusted are  $c_i$ , the average number of secondaries from an inelastic collision, and the nuclear temperature



T. Here, an averaging process would be far too delicate, since the macroscopic inelastic cross-section is varying sharply with the energy, and the nuclear temperature  $T$  is a complex function of the incident neutron energy.

The right approach is to require that the theoretical asymptotic energy spectrum should coincide with the "experimental" one described in Table VIII,

Figs. 20; we have to adjust  $c_i$  and  $T$  in the theoretical expression:

$$H(E) = \frac{c_F}{c_F + c_i} \chi(E) + \frac{c_i}{c_F + c_i} g(E) \cdot h(E) \frac{-c_i}{c_F + c_i} \int_E^\infty \frac{\frac{c_F}{c_F + c_i} \cdot \chi(E') dE'}{h(E') \left\{ 1 - \frac{c_F}{c_F + c_i} \right\}}$$

(from Eq. (3.29)).

A computer program has consequently been written for the formula (3.29), with the input parameters  $c_i$  and  $T$ . It turned out that one must slightly modify the theoretical expression for  $H(E)$ , in order to greatly improve the adjustment of the theoretical curve to the "experimental" one; details are presented in Appendix D.\*

Results of these curve-fittings are shown in Figs. 20: emphasis has been put on a good agreement in the higher-energy-part of the spectrum: we are above all interested in high-energy slowing-down transients (say,  $\geq 0.4$  MeV), and the corresponding source of slowing-down transients is  $\chi(E) - H(E)$ , which means that we must have a particularly good accuracy on  $H(E)$  for  $E \geq 0.4$  MeV (see Eq. (6.38a)).

---

\*In particular, relation (6.43a) turns out to be only a first approximation for  $c_i$ .

Results of all these computations are shown in Table IX, which presents the adjusted values for all the basic parameters we need in the numerical evaluation of the Green's function (6.38).

Let us conclude with the following remark: we assumed that elastic scattering did not involve any energy change. This is quite valid in ZPR-IV systems, in spite of the presence of Al and Fe, since the bulk of neutrons in the asymptotic spectrum occurs well above the inelastic scattering threshold (see Figs. 20). Therefore, most of the slowing-down in ZPR-IV takes place in the high-energy domain, where inelastic scattering is overwhelmingly dominant; the majority of neutron degradation is due to inelastic scattering in the highly concentrated, enriched fuel, and we are allowed to consider that elastic scattering does not involve any appreciable energy change. This point has even been verified by numerical computations in Refs. 36 and 45, where it was found that elastic energy degradation had a minor effect on the energy-spectrum, while the latter was very sensitive to any variation in the parameters of the inelastic scattering matrix.

#### 6.4. SLOWING-DOWN TRANSIENTS AND THE APPROACH TO EQUILIBRIUM IN ZPR-IV LIKE SYSTEMS: A NUMERICAL STUDY

##### 6.4.1. The Computational Procedure

Using the theoretical model adjusted in Section 6.3, we computed the distance and energy for the following physical situation: a prism finite along the transverse y- and z-directions,

TABLE IX

Adjusted Values for the Parameters of the Green's Function

System Designation (see Table VI)	1	2	3
$U^{238}:U^{235}$ ratio	3.13:1	5.0:1	6.82:1
$\overline{\Sigma_T}$ averaged ( $\text{cm}^{-1}$ )	0.208	0.176	0.219
$\overline{\nu\Sigma_f}$ averaged ( $\text{cm}^{-1}$ )	0.171	0.0127	0.00981
$\overline{\Sigma_e}$ averaged ( $\text{cm}^{-1}$ )	0.176	0.146	0.190
$c_F = \overline{\nu\Sigma_f}/\overline{\Sigma_T}$	0.0823	0.0724	0.0448
$c_e = \overline{\Sigma_e}/\overline{\Sigma_T}$	0.845	0.828	0.868
$\Lambda = 1/\overline{\Sigma_T}$ (cm) (new unit of length)	4.795	5.677	4.570
B "material" buckling (experimental value, normalized to the unit of length $\Lambda$ )	0.245	0.217	0.146
$B^2$ (normalized experimental value)	0.0605	0.0473	0.0213
$B_L^2$ , lateral buckling (normalized experimental value)	0.1313	0.1086	0.0587
$\kappa_x$ (fundamental mode along the x- axis) (normalized experimental value)	0.266	0.247	0.193
c - overall multiplication coef- ficient (from the normalized experimental value of B)	1.0198	1.0155	1.00709
$c_i$ (from the adjustment of the theo- retical asymptotic spectrum to the experimental one)	0.104	0.128	0.113
T (MeV) (from the adjustment of the theo- retical asymptotic spectrum to the experimental one)	0.34	0.41	0.36

infinite along the "exponential" x-direction, having the isotopic composition of ZPR-IV systems; a fission source is located on the plane  $x = 0$ , and the neutron distribution is calculated along the axis  $y = z = 0$ .

Rather than giving a mass of flux plots, we preferred to focus on a single parameter, namely the ratio  $\rho(x,E)$  of the asymptotic space-energy separable fundamental mode to the overall neutron flux, for a given point and energy. From Eq. (6.38a),  $\rho(x,E)$  is defined by\*:

$$\rho(x,E) = \frac{\frac{1}{2} \cdot H(E) \cdot \left\{ \frac{dB^2}{dc} \cdot \frac{e^{-\kappa_x |x|}}{\kappa_x} \right\}}{\Delta'(|x|, E)} \quad (6.44)$$

where  $\Delta'(|x|, E)$  is the expression for the global neutron flux, established in Section 5.6 and improved in Section 6.3.2;  $H(E)$  is the asymptotic energy spectrum.

$\rho(x,E)$  has a foremost physical importance: it is an index of asymptotic equilibrium and its deviations from the unity yield the proportion of transport transients and slowing-down transients in the global neutron distribution for a given energy and distance from the source. Through  $\rho(x,E)$  we can study, in depth, the approach to equilibrium for various energy ranges in ZPR-IV like systems. The number of mean-free-paths necessary to obtain complete equilibrium at all energies, is a good criterion for the minimum size that an experimental system should have for an integral experiment. Spe-

---

\*Of course,  $\kappa_x = \sqrt{B_L^2 - B^2}$ .

cifically, the minimum size beyond which space-energy separable modes are sufficiently well established to allow meaningful measurements of integral constants and (last but not least) meaningful calculations with multigroup asymptotic transport theories.

Another outstanding interest of  $\rho(x,E)$  is to shed light upon slowing-down transients: the detailed behavior of  $\rho(x,E)$  in the space and energy domains where it is markedly different from its unit asymptotic value, gives a rich information on the corresponding behavior of slowing-down transients in the same spatial and energetic domains.

So, using the theoretical formula (6.38) and the corresponding parameters adjusted in Section 6.3.3, a computer program has been written for  $\rho(x,E)$ ; numerical values have been obtained for the three ZPR-IV systems (defined in Table VI), and for energies ranging from 0.4 MeV to 3 MeV, and abscisses from 2 m.f.p. to 15 m.f.p. The corresponding results are tabulated in Appendix E.

In order to make a clear cut between spatial-transport transients (i.e., decaying faster than  $e^{-|x|}$ ) and slowing-down transients (decaying more slowly than  $e^{-|x|}$ ), we calculated, in fact, two values for  $\rho(x,E)$ ; specifically, we defined  $\rho_{as}(x,E)$  such as:

$$\rho_{AS}(x,E) = \frac{\frac{1}{2} \cdot \mathcal{H}(E) \left\{ \frac{dB^2}{dc} \cdot \frac{e^{-\kappa_x |x|}}{\kappa_x} \right\}}{\Delta_{AS}(|x|, E)} \quad (6.45)$$

where  $\Delta_{as}(|x|, E)$  has been defined in Eq. (5.51), and the difference between  $\Delta'(|x|, E)$  and  $\Delta_{AS}(|x|, E)$  is explained in Eq. (5.52): explicitly,  $\Delta'(|x|, E)$  includes an one-dimensional approximation for some spatial transport transient modes,\* while the latter are omitted in  $\Delta_{AS}(|x|, E)$ , which includes all modes decaying more slowly than  $e^{-|x|}$ . While  $\rho(|x|, E)$  defined in Eq. (6.44) is the correct physical expression, the difference between  $\rho_{AS}(|x|, E)$  and  $\rho(|x|, E)$  gives an excellent check of the relative importance of slowing-down transients and spatial transport transients.

Detailed curves for  $\rho(|x|, E)$  are given in Figs. 21, 22, and 23. Figure 21 is a plot of  $\rho(|x|, E)$  as a function of energy for a fixed distance—5 m.f.p.—from the source, in the three systems.

Figure 22(a) is a plot of  $\rho(|x|, E)$  as a function of the distance from the plane source, in the three systems, for a constant high-energy  $E = 1.5$  MeV; Fig. 22(b) is a similar plot for the intermediate energy  $E = 0.8$  MeV, and Fig. 22(c), a similar one for the low energy  $E = 0.4$  MeV.

Figure 23 is an outline of results for the most interesting system—with a  $U^{238}:U^{235}$  ratio equal to 6.81, where slowing-down transients take a remarkable importance.

A careful study of these curves reveals many outstanding features of the approach to equilibrium in ZPR-IV systems.

#### 6.4.2. Relative Importance of Spatial Transport Transients and Slowing-Down Transients

From the inspection of the tables in Appendix F, it turns out that the

---

\*Keep in mind that in ZPR-IV systems,  $B_L^2 \ll 1$ .

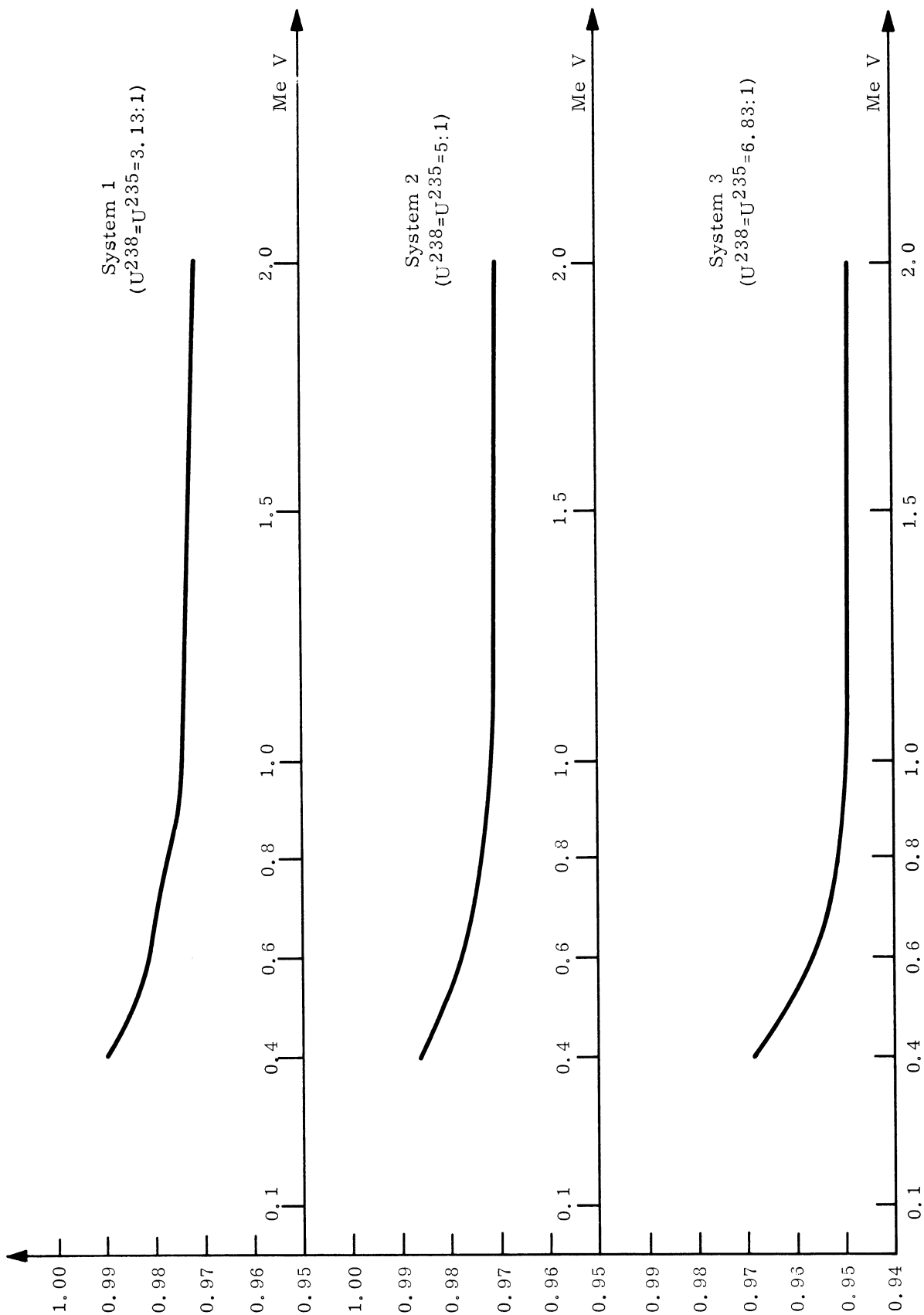


Fig. 21.  $\rho$  as a function of energy for  $x = 5$  m.f.p.

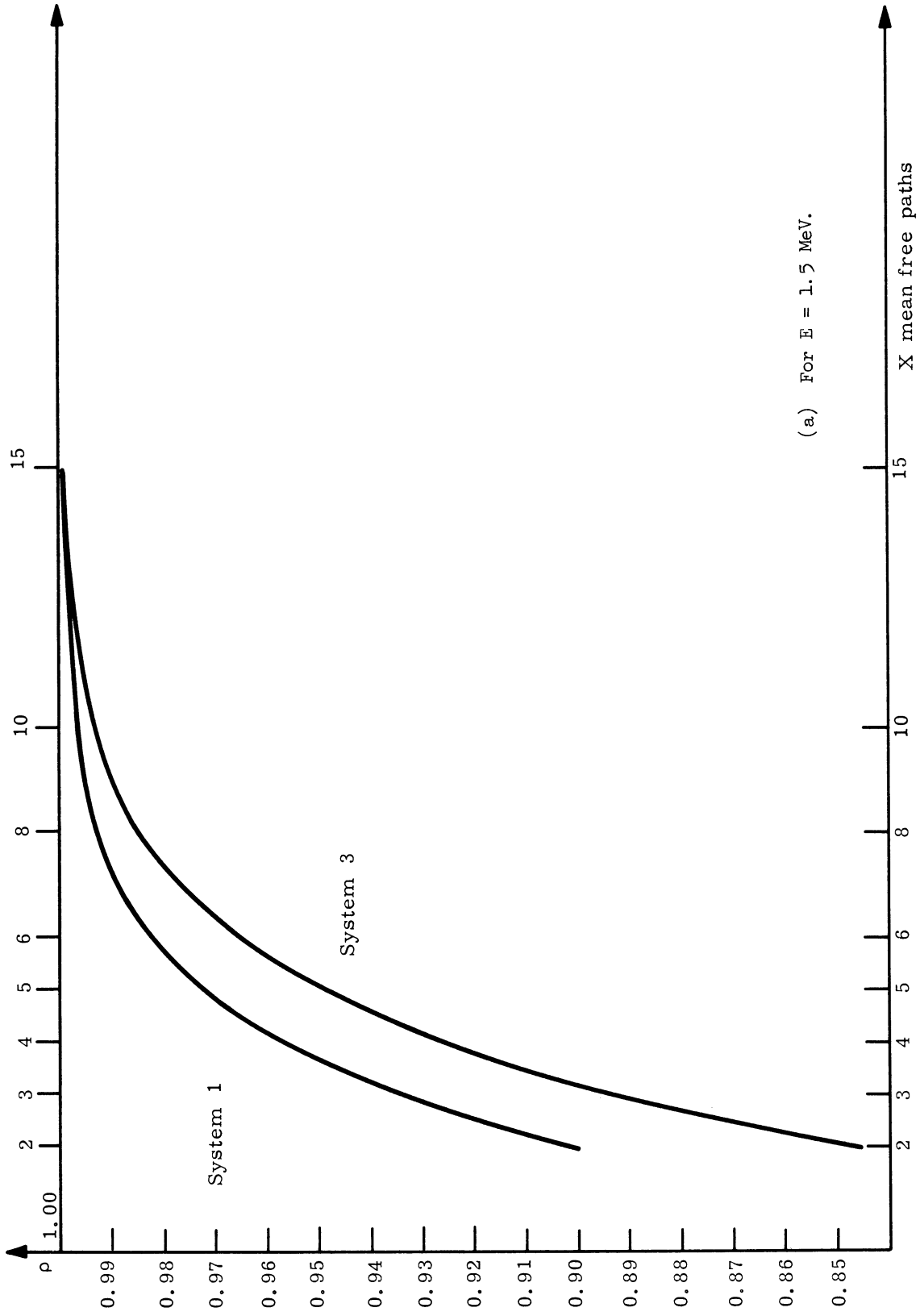
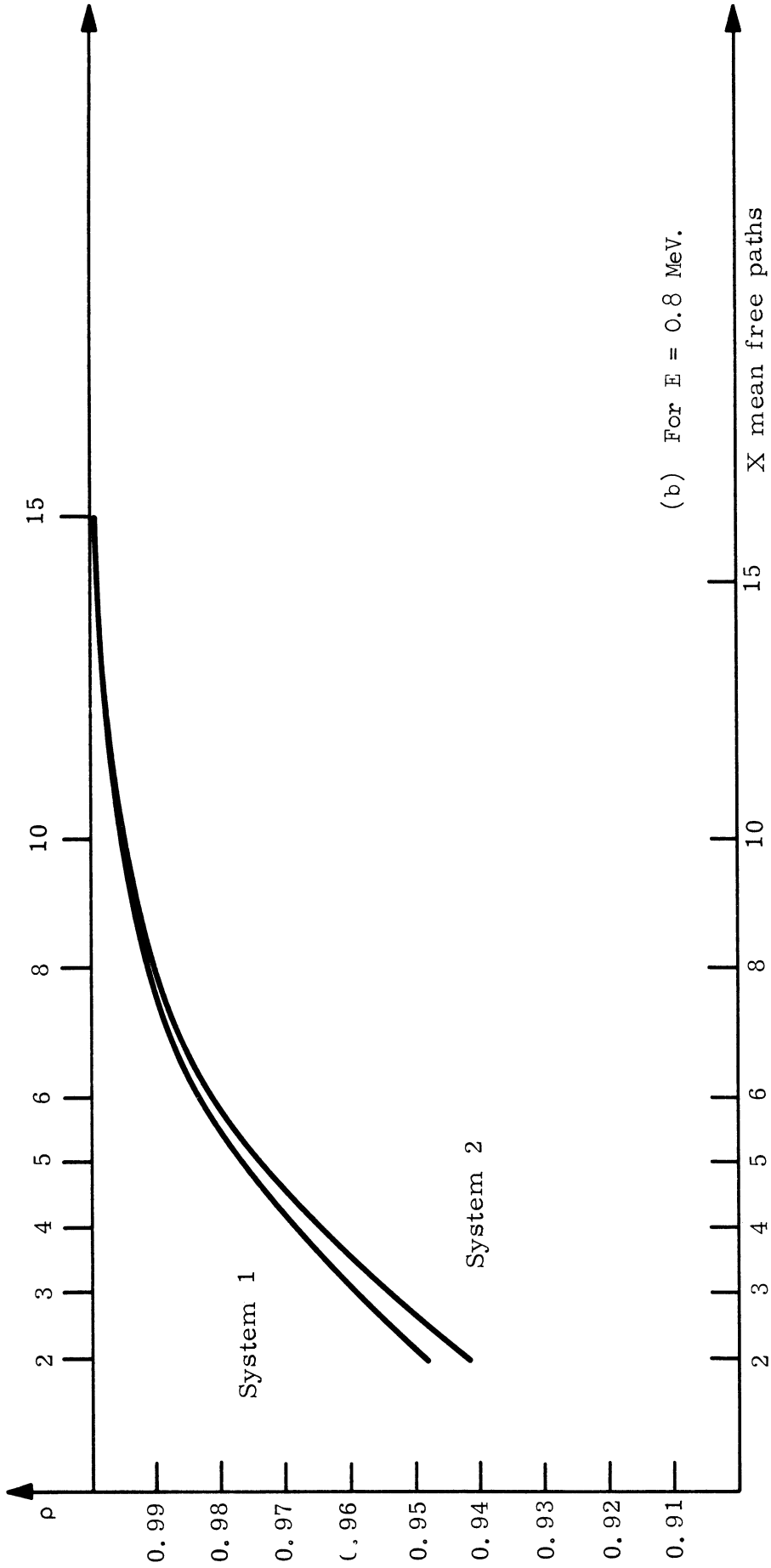


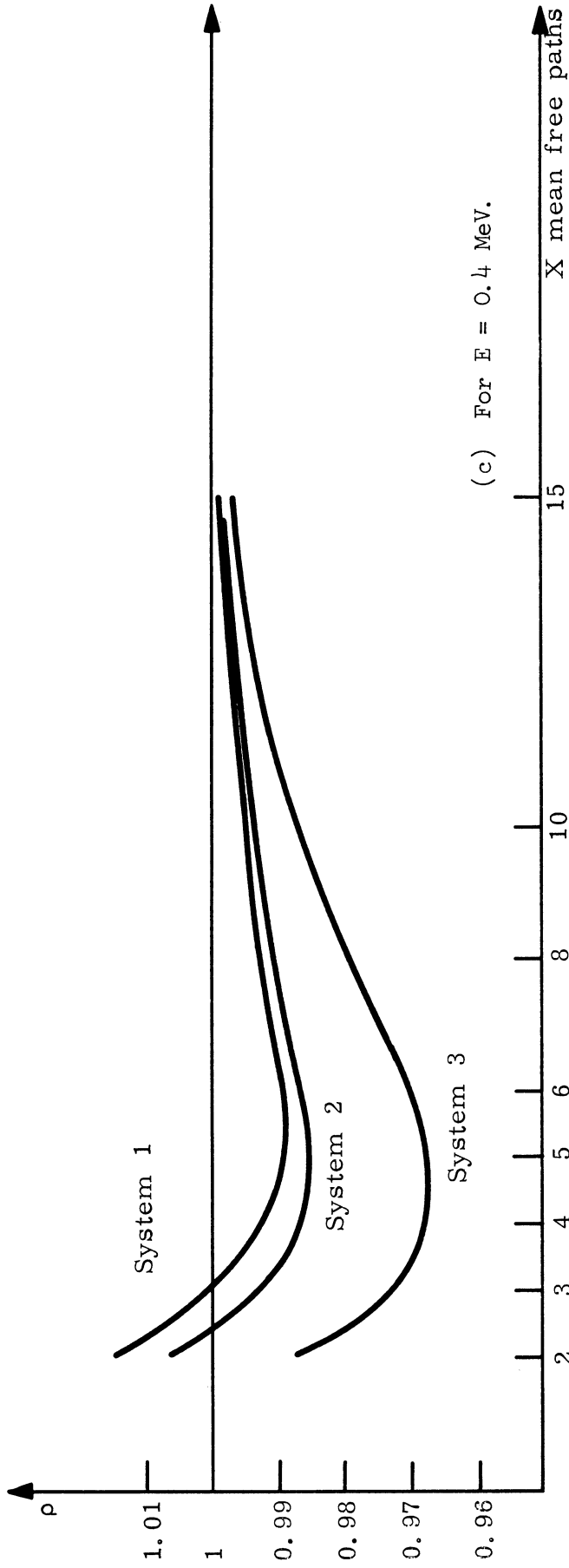
Fig. 22.  $\rho$  as a function of distance.





(b) For  $E = 0.8$  MeV.

Fig. 22. (Continued).



(c) For  $E = 0.4$  MeV.

Fig. 22. (Concluded).

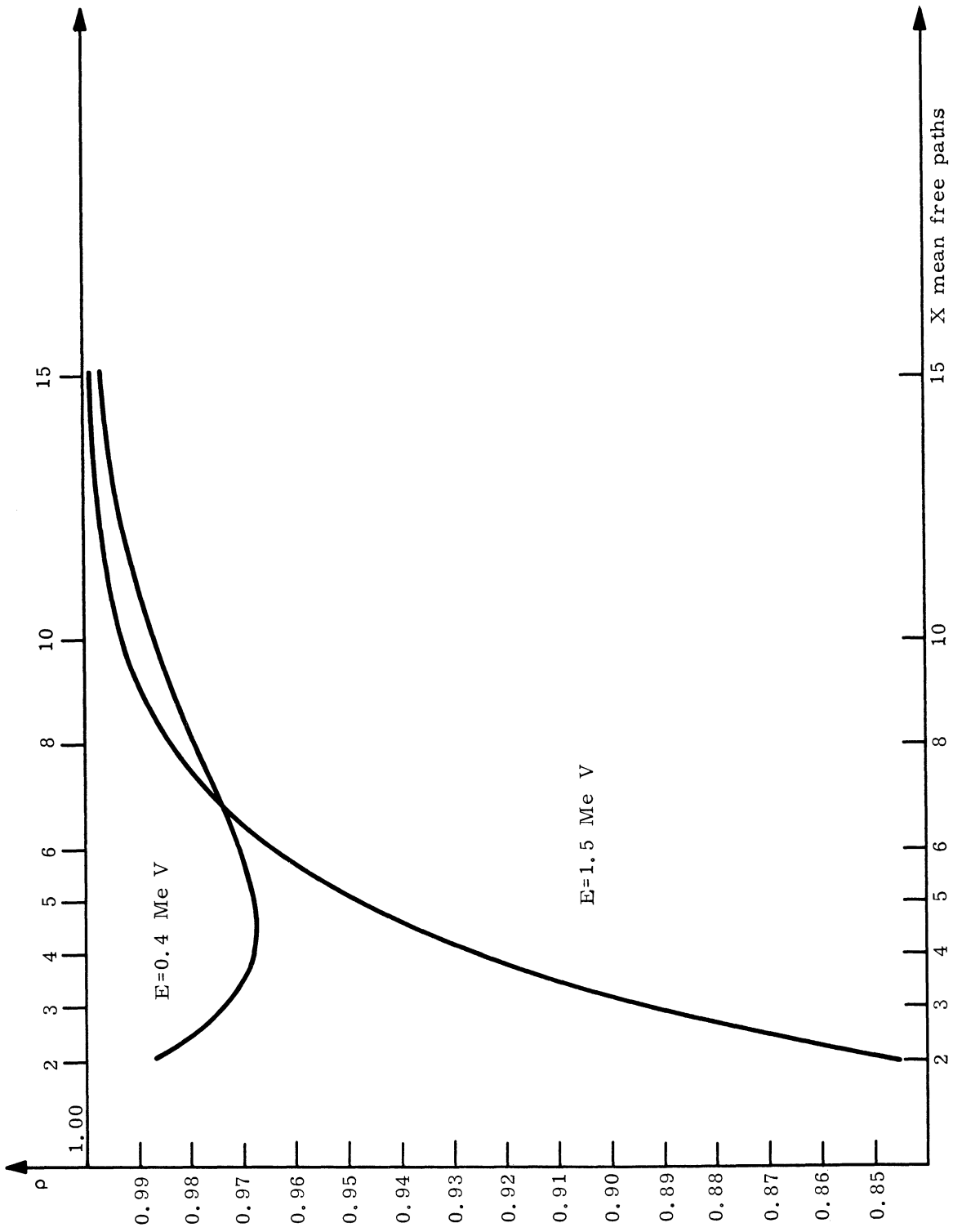


Fig. 23.  $\rho$  as a function of distance for system 3 ( $U^{238}/U^{235} = 6.81/1$ ).

difference between  $\rho_{as}$  and  $\rho$  is quite minimal—less than 1% for all energies and all distances greater than 2 m.f.p. This, of course, gives a good check on the validity of our theoretical formula: in ZPR-IV systems, the formula is correct for all energies and distances as close as 2 m.f.p., which justifies the lengthy mathematical developments of Chapter V. Furthermore, the physical implication is that all spatial transport transients are damped out 2 m.f.p. from the source, for all energies and in all systems. Since curves show that equilibrium is far from being reached at 2 m.f.p., there lies the evidence of the physical importance of slowing-down transients\* which are the only modes responsible for the approach to equilibrium at distances beyond 2 m.f.p. It is indeed surprising that numerically there takes place such a fast spatial uncoupling between genuine transport ("singular") modes and slowing-down transients: the latter having their own identity in further delaying the approach to equilibrium. Since slowing-down transients decay more slowly than transport transients, the damping of the former implies of course the damping of the latter.

#### 6.4.3. Is Equilibrium Reached in the Exponential ZPR-IV Systems?

From Fig. 20, there is a very strong evidence that equilibrium is reached for all energies at distances beyond 5 m.f.p. This preceding figure shows plots of  $\rho$  for all energies, at  $x = 5$  m.f.p. If we choose the following criterion of equilibrium that, for all parts of the energy spectrum,  $\rho$  should be greater than 95%—then Fig. 20 proves that equilibrium is obtained in all ZPR-IV systems for distances greater than 5 m.f.p.

---

\*Decaying more slowly than  $e^{-|x|}$ .

Let us notice that this distance of 5 m.f.p. for equilibrium, corresponds to particularly severe conditions: namely, a high-energy fission source on the boundary plane, the spectrum of which is well above the asymptotic spectra in ZPR-IV systems.

Returning our attention to the exponential ZPR-IV assemblies, where 1 m.f.p. roughly equals two inches,\* the preceding considerations enable us to assert that, the space-energy separable mode is, without a doubt, dominant at distances beyond 10 inches from the front face in all of these exponential assemblies—the size of which was 24 in. along the x-axis. More detailed considerations show that:

(A) in system 1 ( $U^{238}:U^{235} = 3.13:1$ ) the distance for equilibrium is 7 in. (3.5 m.f.p.), which leaves a minimal zone of 10 inches in the central part of the assembly\*\* where the space-energy separable mode is dominant and spectral equilibrium is obtained.

(B) in system 2 ( $U^{238}:U^{235} = 5.0:1$ \*\*\*—the distance is 8 in. (4 m.f.p.) which leaves a minimal equilibrium zone of 8 in. in the central part of the assembly.

(C) in system 3 ( $U^{238}:U^{235} = 6.81:1$ ) the distance is 10 in. (5 m.f.p.) which leaves a minimal equilibrium zone of 4 in.

In fact, in ZPR-IV systems experimental conditions are more relaxed since the flux hitting the front face is rather degraded compared to the fission spectrum: this is due to the presence of a natural uranium pedestal,

---

\*See Table IX.

\*\*This agrees quite well with the experimental plot in Fig. 13.

\*\*\*Since there is no aluminum in system 2, the latter one is much closer to system 1 than system 3.

producing an energy spectrum of neutrons which matches more closely the asymptotic spectrum of ZPR-IV.

So, this work gives an unambiguous answer to the doubts raised by experimentalists (see Section 6.1): the dimensions of ZPR-IV assemblies are large enough to obtain an actual equilibrium. The harsh, but logical consequence is that any kind of discrepancies observed between calculated and measured integral constants are due only to the poor quality of the multi-group constants used.

The use of asymptotic transport theory is completely justified in calculations on ZPR-IV exponential systems. That such great discrepancies arose, reflects pitilessly the inadequacy of the multigroup cross-sections—including the Y.O.M. set—used for the calculations on these assemblies.<sup>36,37,45</sup> It isn't a mystery that many gaps of experimental information were filled up with educated guesses in these multigroup sets. The need for more accurate experimental information yielding improved multigroup constants has been widely acknowledged by teams working on fast reactor physics. We refer, for instance, to the proceedings of the latest Argonne Conference on fast reactor physics (ANL-7320). Since 1960, a considerable effort has been made to obtain experimental data on neutron reaction cross-sections in the high-energy domain, and this should yield greatly improved multigroup sets.

On the other hand, a major interest of our theory is to give a consistent estimate of the minimum size that an experimental system should have in an integral experiment in order to yield consistent measured values for integral constants. This size should be at least twice the distance needed to obtain

complete spectral equilibrium, this allowing the space-energy, separable, fundamental mode to be dominant in at least some section of the assembly. We recall that in most integral experiments, the source term is either a fission source or a high-energy neutron beam produced by a nuclear reaction in an accelerator: therefore, it is justifiable to take into account the equilibrium distance corresponding to the damping of transients from a fission source.

From these considerations, the minimum size of ZPR-IV systems should be at least around 14 in. for system 1, 16 in. for system 2, and 20 in. for system 3.

We realize that in the case of the isotopic system 3, the actual experimental size of 24 in. was just sufficient; so there is absolutely no doubt that equilibrium was not obtained in the exponential experiment on a similar assembly made of natural uranium, keeping in mind that system 3 is 15 times richer in  $U^{235}$  than natural U.

Such an estimate for the minimum size of an assembly gives also information about the domain of validity of asymptotic transport theory, which assumes a priori space-energy separability, and which holds only for the fundamental asymptotic mode.

#### 6.4.4. The Behavior of Slowing-Down Transients in the High-Energy Range

As we know from 6.4.2, slowing-down transients are the only modes responsible for deviation from equilibrium at distances beyond 2 m.f.p.—close examination of our curves and comparison of the cases  $E = 1.5$  MeV, 0.8 MeV,

0.4 MeV, clearly prove that the high-energy slowing-down transients are primarily accountable for the delayed establishment of equilibrium from 2 m.f.p. to 5 m.f.p.

Clearly, the low-energy neutrons ( $< 0.8$  MeV) reach equilibrium much faster than the high-energy neutrons ( $> 1$  MeV). The effect of slowing-down transients is particularly acute for the fastest neutrons, and this enlightens the experimental fact that threshold detectors measure an actual equilibrium spectrum much farther than continuous "thermal" detectors—see Table V; for instance, by considerably affecting the measurements yielded by a  $U^{238}$  fission chamber, the high-energy slowing-down transients have a direct primordial effect on the accuracy of the classical  $U^{238}:U^{235}$  fission ratio. In fact, a careful experimental investigation of this fission ratio can yield data as well for the equilibrium spectrum as for the behavior of high-energy slowing-down transients.

Curves show also that the less enriched the medium is in  $U^{235}$ , the more important are high energy slowing-down transients. Since a decreasing enrichment corresponds to an increasing degradation of the asymptotic spectrum, this clearly explains the physical importance of high-energy slowing-down transients: there is a considerable excess of neutrons in the high-energy domain,\* at distances close to the source; these neutrons in excess must be slowed down to the lower energies of the asymptotic spectrum; and this slowing-down process delays, to a considerable extent, the establishment of a complete

---

\*That is,  $> 1.0$  MeV.



equilibrium. This is much more an energy transfer effect than a classical transport transient phenomenon, and it is likely to have significant importance in dilute fast reactor systems. For instance, we may reasonably conclude that high-energy slowing-down transient modes are primarily responsible for the almost certain lack of equilibrium in exponential experiments performed on insufficiently large natural uranium systems.

#### 6.4.5. The Behavior of Slowing-Down Transients in the Low-Energy Range

Let us consider the results for system 3 outlined in Fig. 23; this system is the least enriched of all, with a considerably degraded asymptotic spectrum (Fig. 20(c)) and slowing-down transients take on already a significant importance. We realize that  $\rho(x,E)$  behaves in a totally different way for  $E = 1.5$  MeV and  $E = 0.4$  MeV. Specifically, for the low-energy 0.4 MeV,  $\rho$  starts with a value very close to the unit, then decreases and has a pronounced minimum, before increasing again asymptotically toward the unit value. The least that one could say, this isn't the classical shape for well-behaved transport transients to which we are accustomed from every day transport theory. Yet this phenomenon—the existence of a minimum for  $\rho(x,E)$ —appears in a more or less marked extent in all systems—Fig. 22(c).

The physical explanation is of utmost interest: at distances of 2 m.f.p., transport transients are damped out; however, the energy spectrum of the neutron distribution presents a considerable deficit of low-energy neutrons ( $E < 0.4$  MeV). This deficit stems from the fact that, the initial source spectrum is much higher than the final asymptotic spectrum and in this case,

slowing-down transients act as negative transients which yield abnormally high and unstable values for  $\rho(x,E)$  at distances close to the source. The further spatial decrease of  $\rho$  corresponds to the spatial appearance of a wave of slowed-down neutrons, which "feed in" the spectrum at low energies. The effect can be of importance in very dilute systems where, by measuring the distribution of low-energy neutrons, one could get the erroneous impression of a pseudoequilibrium.

Such a pseudoequilibrium would only be due to the uncoupling of transport spatial transients from the slowing-down transients, and it would be destroyed by an incoming wave of slowed-down neutrons which would appear at rather large distances from the source. We suspect that such a pseudoequilibrium at low energies could be also responsible for the broad spread of values measured in natural uranium exponential systems (where equilibrium has certainly not been reached). However, such effects have not been demonstrated explicitly in experiments up to now, since low-energy neutrons were detected by continuous "thermal" fission chambers sensitive in fact to the complete energy spectrum; nevertheless, we think that more refined proton recoil spectrometry in the low-energy range ( $< 0.4$  MeV) could evidence such a pseudoequilibrium.

In conclusion, the following numerical work showed the autonomy of spatial slowing-down transient modes, which act as a positive source of excess neutrons in the high-energy domain, and a negative-sink of deficit neutrons in the low-energy range; therefore, they delay the approach to equilibrium in dilute fast-reactor media.

## CHAPTER VII

### CONCLUSIONS AND DIRECTIONS OF FURTHER WORK

The preceding work has covered some aspects of the energy-dependent neutron transport equation, with emphasis on conditions of interest for the high-energy domain. This included detailed consideration of both fission, inelastic and elastic slowing-down phenomena. At this point, we may now draw three essential conclusions.

First of all, we have shown the feasibility and usefulness of a continuous energy formulation in dealing with inelastic, spatial, slowing-down problems. Synthetic slowing-down kernels have been fashionable for a long time in both thermalization (degenerate kernels) and elastic slowing-down theories (Greuling-Goertzel). The introduction of a synthetic (separable, but not degenerate) inelastic scattering operator enables us to get a similar wealth of information for problems in the fast domain. The mathematical methods involved in the solution of the corresponding spatial Boltzmann equation are often complex and unconventional; they imply the definition of a new functional transform, the investigation of the associated inversion formulae, and unusual asymptotic evaluation of the corresponding solutions. The final results, however, reach far beyond the "academism" of most analytical formulae; we have obtained an expression of the Green's function for the spatial, inelastic slowing-down problem, which is valid for all energies and large distances.

Thus, the systematical use of a continuous energy formulation and a synthetic inelastic scattering kernel, seems to be very promising in obtaining much deeper understanding of neutron transport problems in the fast domain. We can gather consistent information for both transient and asymptotic aspects of neutron inelastic slowing down. For, multigroup methods (associated with a multigroup inelastic scattering matrix) yield coherent information about the asymptotic behavior of neutrons; yet, they are implicitly associated with asymptotic transport theory, and therefore completely blue and distort the picture of the transient behavior (into both energy and space). Thus far, we have been dealing with static (time-independent) situations. We believe that a similar wealth of information could be obtained by introducing a continuous energy formulation and a synthetic inelastic slowing-down operator in the solution of time dependent problems. There, one could restrict the investigation to a spatially asymptotic behavior\* (use of asymptotic transport theory) and concentrate on the detailed study of time and energy transients, which multigroup methods are unable to clarify.

The second conclusion concerns the relative importance of the fission and the slowing-down operator in the global neutron transport equation representing a fast multiplying medium. As we have realized, the fission regeneration is responsible for those normal modes (solution of the global

---

\*But such a restriction would allow the practical consideration of arbitrarily varying cross-sections.

equation) which are separable into space and energy. Such fundamental modes reflect the multiplicative process in the fast medium and are associated with integral constants of the system; they are the asymptotically dominant solutions far from sources and boundaries. We have shown, however, that such modes do not form a complete set; in order to achieve completeness one must also consider nonseparable normal modes, which are the solution of a plain slowing-down equation,\* and are submitted to further mathematical restrictions. The existence of such nonseparable "slowing-down transient" modes has been rigorously proved in the case of simple cross-sections for both isotropic inelastic, and anisotropic elastic scattering. It is quite remarkable that such "slowing-down transients" are found in the complex situation of anisotropic elastic scattering where energy exchange occurs between different angular harmonics. Therefore, we believe that the solution of the most general Boltzmann equation involving both fission regeneration and slowing-down, requires the introduction of "slowing-down transients", solution of a plain slowing-down equation, in order to achieve overall completeness for the normal modes. Such "slowing-down transients", although nonseparable into space and energy, are not classical transport transients, to the extent that they may be regular, and not singular normal modes.\*\*

---

\*i.e., the initial equation, where the fission operator has been omitted.  
 \*\*i.e., they may decay more slowly than  $e^{-\Sigma_{Tmin}|x|}$ , where  $\Sigma_{Tmin}$  is the minimum value of the total cross-section.

Physically, they characterize a spatial adjustment of the neutron distribution from the initial high-energy source to the final degraded asymptotic energy spectrum. An interesting extension would be to consider the integral form of the most general Boltzmann equation with fission, slowing-down, and arbitrary cross-sections, and to prove the existence of a fundamental, asymptotic, space-energy separable mode. Such a fundamental mode is closely related to the positivity\* of the transport operator, but it has never been proven that it always exists; we suspect that it could disappear in very dilute fast neutron multiplying media; in this case, one would be very close to a pure "slowing-down" situation, since the regular normal modes involved in the complete solution, would be only "nonseparable slowing-down transients" (the fission regeneration would influence only the singular normal modes, i.e., the classical spatial transport transients). Such a situation would correspond, in the fast domain, to Corngold's findings for the exponential experiment on a thermal moderator: there, too much absorption could oblivate the effects of thermalization up-scattering and lead to the disappearance of space-energy separable modes.

The third conclusion concerns the relative importance of slowing-down transients and asymptotic separable modes in experimental situations. Integral experiments on fast neutron multiplying media are devised to yield information about integral constants, while still using a limited amount of nuclear fuel in the overall system. Such is the purpose of classical expo-

---

\*Reference 51.

nential devices and more recent multizone experiments. In the latter case, one tries to get integral constants for a fuel of given isotopic composition, by inserting a rather thin layer in a much larger critical fast assembly. In both cases, the energy spectrum of the source or the incoming neutron distribution, is quite different from the asymptotic spectrum of the studied fuel. This raises the question of knowing whether an actual equilibrium is reached in the system, and to what extent one can measure accurately a dominating asymptotic separable mode. For "slowing-down transients" are responsible for the adjustment of the neutron distribution from the initial incoming energy spectrum to the final asymptotic distribution.

From the results of our work, it seems that there is a remarkable spatial uncoupling between the effects of slowing-down transients and classical transport transients: while the latter damp out very quickly from system boundaries, the former further delay the approach to equilibrium. Such effects are especially marked in dilute fast media; there, the asymptotic spectrum is quite degraded in energy, which increases the importance of slowing-down transients and considerably delays the approach to equilibrium, especially if the incoming neutron distribution has a high-energy spectrum. Computations point out that high-energy slowing-down transients act as a positive source of excess neutrons in the upper energy domain, while low-energy slowing-down transients act as a negative sink of deficit neutrons in the lower energy range. The latter may also cause a metastable "pseudo-equilibrium" for the spatial neutron distribution in dilute fast media.

Finally, our work strongly outlines the limitations of the validity of asymptotic transport theory for insufficiently large and too subcritical experimental fast systems; this is especially true for integral experiments on fast dilute multiplying media. Asymptotic transport theory involves space-energy separability and therefore implies consideration of the sole asymptotic fundamental mode; this in turn, requires that the fundamental mode should be dominant in the experimental system. This is generally fulfilled for systems made of very enriched fuel, but in many cases, experimentalists keep the same assembly size for a sequence of experiments on much less enriched media. Then, it is unavoidable that discrepancies should appear between experimentally measured values and results from calculations using asymptotic transport theory. In other words, in order to be sure to reach asymptotic equilibrium, and be allowed to use multigroup diffusion theories, one must make the size of a system strongly dependent upon the enrichment of the nuclear fuel studied in an integral experiment.

It is well known that multigroup methods are totally inadequate to represent pure slowing-down situations.<sup>30</sup> Therefore, in fast neutron multiplying media, the inadequacy of these methods is strictly proportional to the spatial importance of slowing-down transients.

An interesting extension of our work would be to consider kinetic (pulsed and modulated) experiments on fast neutron multiplying media. One would use a continuous energy formulation together with asymptotic transport theory, only to the extent that the experimental system would be sufficiently



large (and this, in turn, depends upon the enrichment of the medium). It is suspected that fundamental time-decay constants calculated by multigroup methods have strictly no meaning when they are related to a fast system which is too dilute, too small, and too subcritical. It is probable that the fundamental time-decaying constant disappears into the continuum for such systems. The same limitations would apply to calculations using a continuous energy formulation, together with an oversimplified spatial representation. Quite generally, one may use diffusion and asymptotic transport theories to describe a dominant fundamental mode, but one should be very suspicious about using such simplifications to describe the continuum part of the spectrum.

Finally, the purpose of our work has not been to solve formally the energy-dependent Boltzmann equation, for the sake of surmounting formidable analytical difficulties; but rather, we tried to point out the interest of a continuous energy formulation, to define much more precisely the domain of validity of multigroup asymptotic transport theory applied to fast systems.

APPENDIX A - TO CHAPTER II

EXTENSIONS OF THEOREMS 2.3.1 AND 2.3.4 TO A FUNCTIONAL SPACE  $L'$

We wish to prove that Theorems 2.3.1 and 2.3.4 concerning the spectral properties of  $\sigma_E$  (synthetic inelastic transfer kernel) are still true if we consider functions such that:

$$\begin{aligned}\Phi(E) &\in L' [E_T, \infty] \\ \|\Phi\| &= \int_{E_T}^{\infty} |\Phi(E')| dE' \quad (A.1)\end{aligned}$$

(which correspond to the extension of the upper energy bound to infinity).

Theorem 2.3.1. As an operator acting in the space  $L'$ ,  $\sigma_E$  is linear and continuous.

Proof:

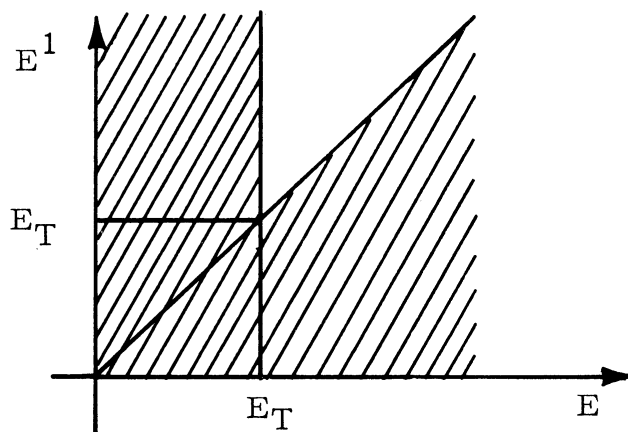
Let

$$\Phi(E) = \sigma_E \otimes \Phi(E) = g(E) \int_E^{\infty} \frac{\Phi(E') dE'}{h(E')}$$

Then

$$\begin{aligned}\|\Phi\| &= \int_{E_T}^{\infty} |\Phi(E')| dE' \\ \|\Phi\| &\leq \int_{E_T}^{\infty} |g(E)| \int_E^{\infty} \frac{|\Phi(E')| dE'}{|h(E')|}\end{aligned}$$

Then, the domain of integration being defined by the adjacent figure, we may invert the order of integration.



$$\|\Phi\| \leq \int_{E_T}^{\infty} \frac{|\phi(E)|}{|h(E)|} \int_{E_T}^{E'} |g(E)| dE$$

$$\|\Phi\| \leq \int_{E_T}^{\infty} \frac{|\phi(E')|}{|h(E')|} \cdot [h(E') - h(E_T)] dE'$$

(Since  $|g(E)| \equiv g(E)$ ,  $|h(E)| \equiv h(E)$ )

$$\|\Phi\| \leq \frac{\sup h(E) - h(E_T)}{\inf h(E)} \cdot \|\phi\|$$

$$\|\Phi\| \leq M \|\phi\| \quad \text{since } \inf h(E) \neq 0 \text{ for } E \in [E_T, \infty)$$

Where  $M$  is some constant, Q.E.D.

Theorem 2.3.4. The whole spectrum (continuous, point, residual) of  $\Theta_E$  is empty, except for the point at infinity.

Proof:

Let us show that the operator  $(I - \lambda \sigma_E)^{-1}$  exists for  $\forall \lambda, \lambda \neq \infty$ .

Given  $S(E)$  arbitrary,  $S(E) \in L'[E_T, \infty]$ , the existence of  $(I - \lambda \sigma_E)^{-1}$  is equivalent to the existence of a solution  $\phi(E) \in L'[E_T, \infty]$  to the equation:

$$(I - \lambda \sigma_E) \phi(E) = S(E) \quad (\text{A.2})$$

But we know that a formal solution to Eq. (A.2) is, from Eq. (2.26b):

$$\phi(E) = S(E) + \lambda g(E) h(E)^{-\lambda} \int_E^{\infty} \frac{S(E')}{h(E')^{1-\lambda}} dE' \quad (\text{A.3})$$

So  $(I - \lambda \sigma_E)^{-1}$  exists, but we have to show furthermore, that it is continuous; that is,

$$\|\phi\| \leq M \|S\| \quad (\text{A.4})$$

This is true, since:

$$\|\phi\| \leq \|S\| + |\lambda| \cdot \int_{E_T}^{\infty} |g(E) h(E)^{-\lambda}| dE \int_E^{\infty} \frac{|S(E')|}{|h(E')^{1-\lambda}|} dE'$$

$$\|\phi\| \leq \|S\| + \frac{|\lambda|}{\inf |h(E)^{1-\lambda}|} \cdot \|S\| \cdot \int_{E_T}^{\infty} |g(E) h(E)^{-\lambda}| dE$$

but  $\inf |h(E)^{1-\lambda}| \neq 0$  for fixed  $\lambda, E \in [E_T, \infty]$ .  $\int_{E_T}^{\infty} |g(E) h(E)^{-\lambda}| dE$  is bounded for fixed  $\lambda, E \in [E_T, \infty]$ . So,

$$\|\Phi(E)\| \leq M \cdot \|S(E)\| \quad (\text{A.4})$$

Q.E.D.

Relation (A.4) shows that  $\forall \lambda \neq \infty$  belongs to the resolvent set of  $\mathcal{O}_E$ . Q.E.D.

Of course, all the preceding results rely heavily upon the fact that  $1/h(E)$  is bounded in the domain of definition of  $\mathcal{O}_E$ . If we were to consider a Banach space  $L'[0, \infty]$ , then the operator  $\mathcal{O}_E$  would be unbounded; however the point-spectrum would still be empty.

APPENDIX B

HALF-RANGE COMPLETENESS THEOREM IN THE ANISOTROPIC CASE

(Section 4.5 in Chapter IV)

APPENDIX C - TO CHAPTER VI

ABOUT THE REDUCTION OF THE THREE-DIMENSIONAL TRANSPORT EQUATION  
TO A SINGLE-DIMENSIONAL ONE

We wish to prove the following relation for some domain of the complex variable  $k$ :

$$\begin{aligned} & \frac{1}{4\pi} \int_{-1}^{+1} d\mu \int_0^{2\pi} \frac{d\eta}{1 + ik\mu - iB_L \sqrt{1-\mu^2} \cdot \cos(\eta - \Delta)} \\ &= S(k^2) = \frac{1}{\sqrt{k^2 + B_L^2}} \cdot \arctan \sqrt{k^2 + B_L^2} \end{aligned} \quad (C.1)$$

Use the following quadrature formula\*:

$$\int \frac{d\eta}{a + b \cdot \cos \eta} = \frac{2}{\sqrt{a^2 - b^2}} \arctan \left\{ \sqrt{a^2 - b^2} \cdot \tan \eta/2 \right\} \quad (C.2a)$$

Comparing with the first term of (C.1), we see that:

$$a = 1 + ik\mu \quad (C.2b)$$

$$b = -i B_L \sqrt{1-\mu^2} \quad (C.2c)$$

$$a^2 - b^2 = 1 + B_L^2 + 2ik\mu - (k^2 + B_L^2)\mu^2 \quad (C.2d)$$

\*See "Tables of Integrals, Series, Products" by Gradshteyn and Ryzhik, Academic Press (1965).

The quadrature formula (C.2a) is valid only if the integration path is contained in a domain of analyticity of the integral. This requires:

$$a + b \cos \eta \neq 0$$

The line of singularities is defined by

$$a + b \cos \eta = 0$$

That is, by the following hyperbola in the  $k$ -complex plane:

$$\{\operatorname{Re} k\}^2 = B_L^2 \cdot \cos^2 \eta \cdot (\{Y_m k\}^2 - 1).$$

The domain of analyticity is exterior to this hyperbola (domain including the asymptotes); in particular, it includes the strip:

$$-1 < Y_m k < +1$$

In particular (C.1), will be correct for those poles  $k$  of the Green's function such that:

$$|k| < 1.$$

For such poles, one is entitled to use formula (C.1) and obtain the corresponding asymptotic solutions. Then Eq. (C.1) becomes, after integration over  $\eta$ :

$$S(k^2) = \frac{1}{2} \int_{-1}^{+1} \frac{d\mu}{\sqrt{1 + B_L^2 + 2ik\mu - (B_L^2 + k^2)\mu^2}} \quad (\text{C.3})$$



Then, rewrite Eq. (C.3) as:

$$S(k^2) = \frac{1}{2} \frac{\sqrt{B_L^2 + k^2}}{B_L \sqrt{1 + B_L^2 + k^2}} \int_{-1}^{+1} \frac{d\mu}{\sqrt{1 - \left\{ \frac{(B_L^2 + k^2)\mu}{B_L \sqrt{1 + B_L^2 + k^2}} - \frac{ik}{B_L \sqrt{1 + B_L^2 + k^2}} \right\}^2}} \quad (C.4)$$

Equation (C.4) can be reduced through the use of a classical quadrature formula:

$$S(k^2) = \frac{1}{2\sqrt{B_L^2 + k^2}} \left\{ \text{Arcsin} \frac{B_L^2 + k^2 - ik}{B_L \sqrt{1 + B_L^2 + k^2}} + \text{Arcsin} \frac{B_L^2 + k^2 + ik}{B_L \sqrt{1 + B_L^2 + k^2}} \right\} \quad (C.5)$$

Using the sine addition theorem, Eq. (C.5) becomes:

$$S(k^2) = \frac{1}{2\sqrt{B_L^2 + k^2}} \text{Arcsin} \Phi(k^2) \quad (C.6a)$$

where  $\Phi(k^2)$  is:

$$\begin{aligned} \Phi(k^2) = & \frac{B_L^2 + k^2 + ik}{B_L \sqrt{1 + B_L^2 + k^2}} \sqrt{1 - \frac{(B_L^2 + k^2 - ik)^2}{B_L^2 (1 + B_L^2 + k^2)}} \\ & + \frac{B_L^2 + k^2 - ik}{B_L \sqrt{1 + B_L^2 + k^2}} \sqrt{1 - \frac{(B_L^2 + k^2 + ik)^2}{B_L^2 (1 + B_L^2 + k^2)}} \end{aligned} \quad (C.6b)$$

Next calculations intend to simplify  $\phi(k^2)$ :

$$\phi(k^2) = \left[ (B_L^2 + k^2 + ik) \sqrt{B_L^2(1+B_L^2+k^2) - (B_L^2+k^2-ik)^2} \right. \\ \left. + (B_L^2+k^2-ik) \sqrt{B_L^2(1+B_L^2+k^2) - (B_L^2+k^2+ik)^2} \right]$$

$$(x) \frac{1}{B_L^2(1+B_L^2+k^2)} \quad (C.7)$$

It can be easily\* shown that:

$$\sqrt{B_L^2(1+B_L^2+k^2) - (B_L^2+k^2-ik)^2} = \sqrt{B_L^2+k^2}(1+ik) \quad (C.8a)$$

and

$$\sqrt{B_L^2(1+B_L^2+k^2) - (B_L^2+k^2+ik)^2} = \sqrt{B_L^2+k^2}(1-ik) \quad (C.8b)$$

Then  $\phi(k^2)$  given in Eq. (C.7) becomes:

$$\phi(k^2) = \frac{1}{B_L^2} \cdot \frac{\sqrt{B_L^2+k^2}}{1+B_L^2+k^2} \left\{ (B_L^2+k^2+ik)(1+ik) + (B_L^2+k^2-ik)(1-ik) \right\} \\ = \frac{1}{B_L^2} \frac{\sqrt{B_L^2+k^2}}{1+B_L^2+k^2} \cdot 2B_L^2 \quad (C.9)$$

And finally,  $\phi(k^2)$  becomes:

\*Simply, systematically isolate  $(B_L^2 + k^2)$  in the development of Eq. (C.8a).

$$\Phi(k^2) = \frac{2\sqrt{B_L^2 + k^2}}{(1 + B_L^2 + k^2)} \quad (\text{C.10})$$

Then, coming back to Eq. (C.6a):

$$S(k^2) = \frac{1}{2\sqrt{B_L^2 + k^2}} \text{Arcsin } \Phi(k^2) \quad (\text{C.6a})$$

We get:

$$S(k^2) = \frac{1}{2\sqrt{B_L^2 + k^2}} \text{Arcsin } \frac{2\sqrt{B_L^2 + k^2}}{(1 + B_L^2 + k^2)} \quad (\text{C.11a})$$

And, through the use of elementary trigonometric formulae, we obtain:

$$S(k^2) = \frac{1}{\sqrt{B_L^2 + k^2}} \text{Arcsin } \frac{\sqrt{B_L^2 + k^2}}{\sqrt{1 + B_L^2 + k^2}} \quad (\text{C.11b})$$

$$S(k^2) = \frac{1}{\sqrt{B_L^2 + k^2}} \text{Arctan } \sqrt{B_L^2 + k^2} \quad (\text{C.11c})$$

Q.E.D.

APPENDIX D - TO CHAPTER VI

ON AN IMPROVED THEORETICAL FORMULA FOR THE ASYMPTOTIC ENERGY SPECTRUM

In Section 6.3.3, it was pointed out that the adjustment of the theoretical curve for the asymptotic energy-spectrum with the "experimental" one, required some modification of the theoretical formula (3.29):

$$H(E) = \frac{c_F}{c_F + c_i} \chi(E) + \frac{c_i}{c_F + c_i} \cdot g(E) \cdot h(E) \frac{-c_i}{c_F + c_i} \int_E^{\infty} \frac{\frac{c_F}{c_F + c_i} \chi(E') dE'}{h(E') \left\{ 1 - \frac{c_i}{c_F + c_i} \right\}} \quad (3.29)$$

Indeed, computations showed that the adjustment to the "experimental" curves (Fig. 20) could be obtained only for highly unphysical values of  $c_i$  (namely, very small ones). This difficulty was lifted through the following observation:

if we consider the experimental asymptotic spectra for natural uranium (Fig. 14) and ZPR-IV (Fig. 20) we realize that the position of the peak is independent from the concentration in  $U^{235}$ ; in all cases, the maximum of  $H(E)$  occurs around 0.125-0.150 MeV; the fuel concentration influences only the sharpness of the peak: the less enriched is the medium, the more numerous are degraded low-energy neutrons, and the more peaked is the asymptotic spectrum. But the position of the maximum has little correlation with the enrichment of the medium: it must be suspected that it is in fact closely correlated to the inelastic threshold energy. This assumption was verified

through the introduction of an effective inelastic-threshold energy  $\textcircled{H}$ , with the prescription that  $\textcircled{H}$  should be equal to the energy for which the experimental  $\mathcal{H}(E)$  presents a maximum.

We can, then, easily modify the theoretical expression for  $\mathcal{H}(E)$ , taking into account this effective inelastic threshold-energy  $\textcircled{H}$ .

The eigenvalue problem introduced in Section 3.3 becomes:

$$\lambda \mathcal{H}(E) = c_F \chi(E) + c_i g(E) \int_E^{\infty} \frac{\mathcal{H}(E') dE'}{h(E')} \quad \text{for } E \geq \textcircled{H} \quad (\text{D.1a})$$

and

$$\lambda \mathcal{H}(E) = c_F \chi(E) + c_i g(E) \int_{\textcircled{H}}^{\infty} \frac{\mathcal{H}(E') dE'}{h(E')} \quad \text{for } E < \textcircled{H} \quad (\text{D.1b})$$

with the normalization:

$$\int_0^{\infty} \mathcal{H}(E) dE = 1 \quad (\text{D.1c})$$

The eigenfunction solution of Eq. (D.1) is closely related\* to the previous one defined in (3.29); it can be easily verified that:

$$\mathcal{H}(E) = \frac{c_F}{\lambda} \chi(E) + \frac{c_i}{\lambda} g(E) \cdot h(E)^{-\frac{c_i}{\lambda}} \int_E^{\infty} \frac{\frac{c_F}{\lambda} \chi(E') dE'}{h(E')^{\{1 - \frac{c_i}{\lambda}\}}} \quad \text{for } E \geq \textcircled{H} \quad (\text{D.2a})$$

\*There is no difference between  $\mathcal{H}(E)$  defined in Eq. (D.2) and the previous  $\mathcal{H}(E)$  defined in Eq. (3.29), for all energies  $\geq \textcircled{H}$ .

And:

$$\mathcal{H}(E) = \frac{c_F}{\lambda} \chi(E) + \frac{c_i}{\lambda} g(E) h(\Theta) \int_{\Theta}^{\infty} \frac{\frac{c_F}{\lambda} \chi(E') dE'}{h(E') \left\{ 1 - \frac{c_i}{\lambda} \right\}}$$

for

$$E < \Theta \quad (\text{D.2b})$$

However, the eigenvalue  $\lambda$  is not any more equal to  $c_F + c_i$ ; integrating the eigenfunction given in Eq. (D.2) over the whole energy range, and using the normalization (D.1c), we find the following eigenvalue equation:

$$\left( 1 - \frac{c_i}{\lambda} \right) = \frac{c_F}{\lambda} \left\{ 1 - \frac{c_i}{\lambda} + \frac{c_i}{\lambda} \int_{\Theta}^{\infty} \chi(E') dE' - \left( \frac{c_i}{\lambda} \right)^2 \cdot h(\Theta) \left\{ 1 - \frac{c_i}{\lambda} \right\} \int_{\Theta}^{\infty} \frac{\chi(E') dE'}{h(E') \left\{ 1 - \frac{c_i}{\lambda} \right\}} \right\} \quad (\text{D.3})$$

Equation (D.3) is a relation between the new eigenvalue  $\lambda$ ,  $c_F$  and  $c_i$ ; we verify that if we shift the effective inelastic threshold energy  $\Theta$  to zero, we find back the classical eigenvalue  $\lambda = c_F + c_i$ . But in the present case,  $\lambda$  is different from  $c_F + c_i$ .

So, in our further calculations, we consider the modified eigenfunction  $\mathcal{H}(E)$ ,\* defined in Eq. (D.2), and the eigenvalue equation (D.3).

The problem is now to determine the parameters  $\lambda$ ,  $c_i$ , and  $T$ .

The eigenvalue  $\lambda$  is in fact already known, since:

---

\*Which is in fact strictly equal to the classical one for values of  $E \geq \Theta$ .

$$c = \lambda + c_e \quad (D.4)$$

Relation (D.4) replaces the classical relation  $c = c_F + c_i + c_e$  from the previously adjusted values of  $c$ ,  $c_F$ , and  $c_e$  (see Section 6.3.3, Eqs. (6.40), (6.41), and (6.43b)), we immediately deduce the corresponding values of  $\lambda$  (through Eq. (D.4)) and  $c_F/\lambda$ .

A computer program was written, for the calculation of  $\mathcal{H}(E)$  through Eq. (D.2), and for the evaluation of the eigenvalue Eq. (D.3). The input parameters were  $c_i/\lambda$  and  $T$  (all other parameters,\* that is,  $c_F$ ,  $\lambda$ , and  $\textcircled{H}$  being known data). The optimal values for  $c_i/\lambda$  and  $T$  were determined the following ways:

the value of  $c_F/\lambda$  yielded by the eigenvalue equation (D.3), in which  $c_i/\lambda$  and  $T$  are input parameters, should coincide with the previously known value of  $c_F/\lambda$ .

the theoretical curve for  $\mathcal{H}(E)$  (from Eq. (D.2)) should reasonably coincide with the corresponding experimental curve.

It was out of question to write a least-squares fitting program for  $\mathcal{H}(E)$ , since the corresponding formula is highly nonlinear in  $c_i/\lambda$  and  $T$ . However, successive empirical adjustments worked remarkably well, as it can be concluded from Figs. 20. The following table presents the resulting values for  $c_i$  and  $T$ .

---

\*The fission spectrum was computed with the help of:  $X(E) = 0.771343 \sqrt{E} e^{-0.776E}$

TABLE D.I

Adjusted Values for  $c_i$  and T

System Designation (See Table VI)	1	2	3
$U^{238}:U^{235}$ ratio	3.13:1	5.0:1	6.82:1
$\lambda$ (from: $c - c_e = \lambda$ )	0.174	0.183	0.139
$c_F/\lambda$	0.473	0.395	0.322
$c_i/\lambda$ (from the curve-fitting)	0.60	0.70	0.81
$c_i = (c_i/\lambda) \cdot \lambda$	0.104	0.128	0.113
T (MeV) (from the curve-fitting)	0.34	0.41	0.36
$\textcircled{H}$ (MeV) (effective inelastic threshold, set equal to the position of the maximum of $\chi(E)$ )	0.125	0.150	0.125



APPENDIX E - TO CHAPTER VI

TABLES OF CALCULATED VALUES OF  $\rho(x, E)$  IN SYSTEM 1 ( $U^{238}:U^{235} = 3.13:1$ )

TABLE A

E Variable, x = 5 m.f.p.

E (MeV)	3	2	1.5	1	0.8	0.6	0.4
$\rho_{AS}$	.971	.971	.972	.974	.977	.981	.990
$\rho$	.971	.971	.972	.974	.977	.981	.990

TABLE B

E = 1.5 MeV, x Variable

x (m.f.p.)	2	3	4	5	6	8	10	15
$\rho_{AS}$	.907	.937	.958	.972	.981	.992	.996	.999
$\rho$	.899	.934	.957	.972	.981	.992	.996	.999

TABLE C

E = 0.8 MeV, x Variable

x (m.f.p.)	2	3	4	5	6	8	10	15
$\rho_{AS}$	.951	.961	.969	.977	.983	.991	.995	.999
$\rho$	.948	.959	.969	.977	.983	.991	.995	.999

TABLE D

E = 0.4 MeV, x Variable

x (m.f.p.)	2	3	4	5	6	8	10	15
$\rho_{AS}$	1.017	1.000	.993	.990	.990	.993	.995	.999
$\rho$	1.015	1.000	.993	.990	.990	.993	.995	.999

SYSTEM 2 ( $U^{238}:U^{235} = 5.0:1$ )

TABLE A

E Variable,  $x = 5$  m.f.p.

E (MeV)	3	2	1.5	1	0.8	0.6	0.4
$\rho_{AS}$	.971	.971	.971	.972	.974	.978	.986
$\rho$	.970	.970	.970	.972	.974	.978	.986

TABLE B

E = 1.5 MeV, x Variable

x (m.f.p.)	2	3	4	5	6	8	10	15
$\rho_{AS}$	.902	.933	.955	.971	.981	.992	.997	.999
$\rho$	.895	.931	.955	.971	.981	.992	.997	.999

TABLE C

E = 0.8 MeV, x Variable

x (m.f.p.)	2	3	4	5	6	8	10	15
$\rho_{AS}$	.945	.955	.965	.974	.981	.990	.995	.999
$\rho$	.942	.954	.965	.974	.981	.990	.995	.999

TABLE D

E = 0.4 MeV, x Variable

x (m.f.p.)	2	3	4	5	6	8	10	15
$\rho_{AS}$	1.008	.993	.987	.986	.987	.991	.994	.999
$\rho$	1.007	.993	.987	.986	.987	.991	.994	.999

SYSTEM 3 ( $U^{238}:U^{235} = 6.83:1$ )

TABLE A

E Variable,  $x = 5$  m.f.p.

E (MeV)	3	2	1.5	1	0.8	0.6	0.4
$\rho_{AS}$	.949	.949	.949	.950	.952	.957	.969
$\rho$	.949	.949	.949	.950	.952	.957	.969

TABLE B

E = 1.5 MeV, x Variable

x (m.f.p.)	2	3	4	5	6	8	10	15
$\rho_{AS}$	.852	.894	.926	.949	.965	.984	.993	.999
$\rho$	.846	.893	.925	.949	.965	.984	.993	.999

TABLE C

E = 0.4 MeV, x Variable

x (m.f.p.)	2	3	4	5	6	8	10	15
$\rho_{AS}$	.988	.973	.968	.969	.971	.980	.987	.997
$\rho$	.987	.973	.968	.969	.971	.980	.987	.997

## APPENDIX F

### ON A COMPLETENESS THEOREM BY R. J. BEDNARZ AND J. R. MIKA

In Ref. 13, Bednarz and Mika presented a general method for solving the energy-dependent transport equation. The main feature was the introduction of a change of variables, which allowed the consideration of arbitrarily varying cross-sections. Completeness was proved only for the full-range expansion, extending Case's method.

Unfortunately, their completeness theorem is erroneous: in their proof, they consider an integral equation, the kernel of which is a sectionally holomorphic operator; completeness is strictly equivalent to the solubility of this integral equation. They make explicit use of the Fredholm alternative: "the condition of the solubility of the integral equation is that the inhomogeneous term be orthogonal to the eigenfunctions of the adjoint homogeneous equation" (Ref. 13, page 1288). Unfortunately, the Fredholm alternative holds only for compact operators, and it collapses for operators which are neither compact, nor bounded; this is indeed the case for a Boltzmann equation where energy-transfer occurs only through slowing-down. Similarly, they claim: "It is evident that the spectra of the operator...and [its adjoint] are identical" (Ref. 13, page 1287). This statement is incorrect, if one deals with unbounded and noncompact operators, like those found in pure slowing-down situations.

Rather than going into purely theoretical arguments, we will present a counter-example, following step by step their argumentation. We will point out a case where:

A) The direct operator has no eigenfunctions and eigenvalues (empty point spectrum).

B) Its adjoint has a set of regular eigenfunctions and eigenvalues.

C) A necessary condition of solubility of the integral equation involved in the completeness proof is still that: the inhomogeneous term should be orthogonal to the eigenfunctions of the adjoint homogeneous equation.

D) There are no discrete modes of the direct operator, with the help of which one could make the inhomogeneous term of the integral equation satisfy the above condition.

E) Therefore, the modes of the transport equation, as defined by Mika and Bednarz, are incomplete.

We will consider an energy-dependent Boltzmann equation where energy transfer occurs only through inelastic scattering and slowing-down. We will use the synthetic inelastic scattering kernel introduced in Section 2.2. Since the main features are similar for both variable and constant cross-sections cases, a fast outline can be given, using the constant cross-sections model.

The starting equation is:

$$\mu \frac{\partial}{\partial x} \psi(x, \mu, E) + \psi(x, \mu, E) = \frac{c_i}{2} g(E) \int_{-1}^{+1} d\mu' \int_E^{\infty} \frac{\psi(x, \mu', E')}{h(E')} dE' + S(x, \mu, E) \quad (\text{F.1a})$$

Since we are in a constant cross-section situation, the angular variable  $\mu$  is identical to the auxiliary variable  $v$  of Ref. 13:

$$\mu = v \quad (\text{F.1b})$$

Then, the homogeneous equation (F.1a) becomes:

$$v \frac{\partial}{\partial x} \psi(x, v, E) + \psi(x, v, E) = \frac{c_i}{2} g(E) \int_{-1}^{+1} dv' \int_E^{\infty} \frac{\psi(x, v', E')}{h(E')} dE' \quad (\text{F.2})$$

Introduce the Ansatz:

$$\psi(x, v, E) = e^{-x/t} \cdot \phi(t, v, E) \quad (\text{F.3})$$

Then:

$$(t - v) \phi(t, v, E) = \frac{t}{2} \int_{-1}^{+1} dv' c_i g(E) \int_E^{\infty} \frac{\phi(t, v', E')}{h(E')} dE' \quad (\text{F.4})$$

Put:

$$H(t, v, E) = \int_{-1}^{+1} dv' c_i g(E) \int_E^{\infty} \frac{\phi(t, v', E')}{h(E')} dE' \quad (\text{F.5})$$

Then:

$$\phi(t, v, E) = (t/2) \frac{H(t, v, E)}{t - v} + \lambda(t, E) \cdot \delta(t - v) \quad (\text{F.6a})$$

In fact,  $H(t, v, E)$  does not depend upon  $v$ :

$$H(t, v, E) \equiv H(t, E) \quad (\text{F.6b})$$

To the normal mode  $\phi(t, v, E)$  defined in Eq. (F.6a), apply the following operator:

$$\int_{-1}^{+1} dv' c_i g(E) \int_E^{\infty} \frac{\phi(t, v', E')}{h(E')} dE' \quad (\text{F.7a})$$

And obtain:

$$\begin{aligned} H(t, E) &= \left\{ \left[ \frac{t}{2} \int_{-1}^{+1} \frac{dv}{t-v} \right] \cdot c_i g(E) \int_E^{\infty} \frac{H(t, E')}{h(E')} dE' \right\} \\ &= c_i g(E) \int_E^{\infty} \frac{\lambda(t, E')}{h(E')} dE' \end{aligned} \quad (\text{F.7b})$$

At this point, we can define the sectionally holomorphic operator  $\Omega(z, E)$ , following the pattern of Ref. 13:

$$\Omega(z, E) \boxtimes H(z, E) = H(z, E) - (z \operatorname{argth} \frac{1}{z}) c_i g(E) \int_E^{\infty} \frac{H(z, E')}{h(E')} dE' \quad (\text{F.8})$$

The operator  $\Omega(z, E)$  will be essential in the tentative proof of the completeness theorem. Its eigenfunctions correspond to the discrete solutions of the Boltzmann equation. Unfortunately,  $\Omega(z, E)$  has no discrete eigenvalues. For, calling the hypothetical eigenfunctions  $H(L_i, E)$ , we would have:

$$\Omega(L_i, E) \boxtimes H(L_i, E) = 0 \quad (\text{F.9a})$$

That is:

$$H(L_i, E) = \lambda_i g(E) \int_E^{\infty} \frac{H(L_i, E')}{h(E')} dE' \quad (\text{F.9b})$$

where we defined:

$$\lambda_i = c_i L_i \operatorname{argth} \frac{1}{L_i} \quad (\text{F.9c})$$

But Eq. (F.9b) is nothing but the eigenvalue problem for the operator  $\Theta_E$ , as studied in Section 2.3. There, we proved in detail that the point spectrum is empty.

So, Eq. (F.9b) has no solutions; the point spectrum of  $\Omega(z,E)$  is empty, and the associated Boltzmann equation has no discrete normal modes.

Things are quite different for the operator adjoint to  $\Omega(z,E)$ ; call this adjoint  $\Omega^+(z,E)$ :

$$\Omega^+(z,E) \otimes H(z,E) = H(z,E) - (z \operatorname{argth} \frac{1}{z}) c_i \frac{1}{h(E)} \int_0^E g(E') \cdot H(z,E') dE' \quad (\text{F.10a})$$

The adjoint eigenvalue problem becomes:

$$\Omega^+(L_i,E) \otimes H^+(L_i,E) = 0 \quad (\text{F.10b})$$

That is:

$$H^+(L_i,E) = \lambda_i \frac{1}{h(E)} \int_0^E g(E') H^+(L_i,E') de' \quad (\text{F.10c})$$

where we defined:

$$\lambda_i = c_i L_i \operatorname{argth} \frac{1}{L_i} \quad (\text{F.10d})$$

Equation (F.10c) has the obvious solution:

$$H^+(L_i,E) = h(E)^{\lambda_i - 1} \quad (\text{F.11a})$$

(just remember that  $\frac{dh}{dE} = g(E)$ ).



Therefore, the adjoint to the Boltzmann equation (F.2) has the following set of discrete regular normal modes:

$$\phi^+(L_i, v, E) = \frac{L_i}{L_i - v} \cdot h(E)^{\lambda_i - 1} \quad (\text{F.11b})$$

where  $L_i$  is defined by Eq. (F.10d).

The point spectrum of  $\Omega(z, E)$  is empty, while its adjoint has eigenfunctions; this is not surprising mathematically, since we are considering operators which are neither self-adjoint, nor compact, nor bounded.\*

Let us now turn our attention to the proof of the completeness theorem, as established in Ref. 13. Following their pattern, the crux of the full-range completeness lies in the inversion of the following operator equation:

$$\Omega(z, E) \otimes N(z, E) = F(z, E) \quad (\text{F.12})$$

where  $\Omega(z, E)$  is defined in Eq. (F.8);  $F(z, E)$  is a known function, stemming from the source term of Eq. (F.1);  $N(z, E)$  includes the unknown expansion coefficients for the set of singular normal modes.

Let us now show that  $F(z, E)$  must be orthogonal to the eigenfunctions  $\phi^+(L_i, v, E)$  of the adjoint equation, as defined in Eq. (F.11b). Suppose that the source term is separable in the energy variable:

$$F(z, E) = F(z) \cdot S(E) \quad (\text{F.13a})$$

---

\*Term  $1/h(E)$  in the scattering kernel, unbounded for  $E = 0$ .

Take  $S(E)$  such that, everywhere:

$$S(E) > 0 \quad (\text{F.13b})$$

Then, obviously, for every  $\lambda$  real and positive:

$$\int_0^{\infty} S(E) h(E)^{\lambda-1} dE > 0 \quad (\text{F.14})$$

But:

$$S(E) F(z) = N(z, E) - c_i \left( z \operatorname{argth} \frac{1}{z} \right) g(E) \int_E^{\infty} \frac{N(z, E')}{h(E')} dE' \quad (\text{F.12})$$

Then multiply both terms of Eq. (F.12) by  $h(E)^{\lambda-1}$ , integrate over the whole energy range, from zero to infinity, invert the order of integrations in the right term of Eq. (F.12), and get:

$$F(z) \int_0^{\infty} S(E) h(E)^{\lambda-1} dE = \left\{ 1 - \frac{c_i}{\lambda} z \operatorname{argth} \frac{1}{z} \right\} \int_0^{\infty} N(z, E) h(E)^{\lambda-1} dE \quad (\text{F.15})$$

However, for values of  $z$  such that:

$$\lambda = c_i z \operatorname{argth} \frac{1}{z} \quad (\text{F.16})$$

the right term of Eq. (F.15) becomes identically null, which is in contradiction with the condition (F.14). Therefore, we must have:

$$\int_0^{\infty} S(E) h(E)^{\lambda-1} dE \equiv 0 \quad (\text{F.17})$$

This is strictly equivalent to the condition of orthogonality of  $F(z,E)$  to the adjoint eigenfunctions defined in Eq. (F.11b).\*

But we cannot satisfy this orthogonality condition for an arbitrary source term  $F(z,E)$ , since we do not have any available set of discrete modes for the direct Boltzmann equation. Therefore, the normal modes such as defined by Mika and Bednarz, are incomplete.

We know, of course, that we have to work with a transformed energy-variable ( $\mathcal{M}$ -transformation defined in Section 2.4). The completeness proof by Mika and Bednarz is, of course, valid whenever one considers bounded and compact operators: this is the case for finite dimensional matrix operators, for degenerate projection kernels, and for compact thermalization kernels. It fails for noncompact operators found in slowing-down situations; without or with fission regeneration.

---

\*We only proved that this condition is necessary.

## REFERENCES

1. R. E. Marshak, Rev. Mod. Phys., 19, 185 (1947).
2. M. Verde and G. C. Wick, Phys. Rev., 71, 852 (1947).
3. G. C. Wick, Phys. Rev., 75, 738 (1949).
4. G. Hölte, Arkiv Fysik, Band 2, Nr. 48 (1950).
5. G. Hölte, Arkiv Fysik, Band 2, Nr. 14 (1951).
6. H. Hejtmanek, Atomkernenergie, 6, 350 (1961).
7. H. Hejtmanek, Atomkernenergie, 7, 359 (1962).
8. R. Bednarz, "Green's function of the transport equation with a synthetic Shirkov kernel," Poland, PAN 284/IX (1962).
9. H. Hejtmanek, A/conf 28/P/401, Geneva (1964).
10. N. Pappmehl, Nucl. Sci. Eng., 22, 451 (1965).
11. J. J. MacInerney, Nucl. Sci. Eng., 22, 215 (1965).
12. N. Corngold, P. Michael, and W. Wollmann, Nucl. Sci. Eng., 15, 13 (1963).
13. R. J. Bednarz and J. R. Mika, J. Math. Phys., 4, Nr. 9, 1285 (1963).
14. J. R. Mika, Nucl. Sci. Eng., 22, 235 (1965).
15. M. C. Stewart, I. Kuscer, and N. J. MacCormick, Ann Phys. (N.Y.), 40, 321 (1966).
16. M. M. R. Williams, Nucl. Sci. Eng., 18, 260 (1964).
17. J. Arkuszewski, Nucl. Sci. Eng., 27, 104 (1967).
18. M. M. R. Williams, Nucl. Sci. Eng., 27, 511 (1967).
19. A. Leonard, "Energy dependent transport theory," Thesis, Stanford (1963).
20. J. Ferziger and A. Leonard, Ann. Phys. (N.Y.), 22, 192 (1963).

## REFERENCES (Continued)

21. G. C. Summerfield and P. F. Zweifel, "On the energy-dependent transport equation," Nucl. Sci. Eng., 15, 476 (1963).
22. R. Zelazny and A. Kuszell, "Multigroup neutron transport theory," Proc. Int. Symp. on "Physics of fast and intermediate reactors," Vol. 2, 55-71 (Vienna 1962).
23. P. P. Abatti Marescotti, "On the transport of neutrons in many-group theory," A.E.C. Tr. 6332 (1964).
24. K. Zumbrunn, "Exact and approximate solutions of many-group transport equations in plane geometry," (Thesis) - Eidgenoesische Technische Hochschule, Zurich, Switzerland, EIR-72 (1966).
25. C. E. Siewert and P. F. Zweifel, Ann. Phys. (N.Y.), 36, 61-85 (1966).
26. A. Leonard and J. Ferziger, Nucl. Sci. Eng., 26, 170 (1966).
27. A. Leonard and J. Ferziger, Nucl. Sci. Eng., 26, 181 (1966).
28. D. Okrent, R. Avery, and H. H. Hummel, Geneva 5, 357 (1955).
29. M. Cadilhac and M. Pujol, J. Nucl. Energy, 21, Nr. 1, 58-63 (1967).
30. B. Davidson, Neutron Transport Theory, Oxford Univ. Press (1957).
31. M. M. R. Williams, The Slowing-Down and Thermalization of Neutrons, Interscience Publishers, John Wiley (1966).
32. N. Corngold, Theoretical interpretation of pulsed neutron phenomena," I.A.E.A. Symposium on "Pulsed Neutron Methods," Karlsruhe (1965).
33. K. M. Case and P. F. Zweifel, Linear Transport Theory, Addison-Wesley, Reading, Mass. (1967).
34. J. H. Ferziger and P. F. Zweifel, The Slowing-Down of Neutrons in Nuclear Reactors, Pergamon Press (1966).
35. F. Storrer and J. Govaerts, "Contribution to the theory of exponential experiments with fast neutrons," I.A.E.A. Symposium on "Exponential Experiments," vol. I, p. 197, Amsterdam (1963).
36. F. C. Beyer, et al., "The fast exponential experiment," Geneva, 5, 342 (1955).
37. D. Okrent, Lowenstein, "The physics of fast power reactors," Geneva, 12, 13 (1958).

## REFERENCES (Concluded)

38. A. I. Leipunsky, "Fast reactor physics," Geneva, 12, 3 (1958).
39. Campan, Clauzon, Zaleski, "Etude du flux de neutrons à l'équilibre dans l'Uranium naturel," I.A.E.A. Symposium on "Fast and Intermediate Reactor Physics," Vienna, p. 345 (1961).
40. \_\_\_\_\_, "Propagation à longue distance du flux de neutrons dans les réacteurs à neutrons rapides," I.A.E.A. Symposium on "Fast and Intermediate Reactor Physics," Vienna, p. 387 (1961).
41. \_\_\_\_\_, "Propagation des neutrons dans des massifs d'Uranium naturel et Uranium naturel-Acier," I.A.E.A. Symposium on "Exponential Experiments," Amsterdam, 1, 277 (1963).
42. A. I. Leipunsky, "Experimental research on fast neutron reactors," Geneva, 6, 153 (1964).
43. A. E. Taylor, Introduction to Functional Analysis, John Wiley (1958).
44. H. Bateman and A. Erdélyi, Bateman Manuscript Project, Table of Integral Transforms, Vol. I, p. 305, McGraw-Hill (1954).
45. F. C. Beyer, et al., "The fast exponential experiment," Report ANL-5379 (1956).
46. C. G. Chezem, "Neutron flux parameters of an uranium metal exponential experiment," Thesis submitted to Oregon State College (1954).
47. J. R. Brolley, et al., "Neutron multiplication in a massif of uranium metal," Report LA
48. J. J. Never and C. R. Stewart, Report LA-2023.
49. M. M. R. Williams, Nukleonik, Band 9, Nr. 7 (1967).
50. J. R. Mika, Nucl. Sci. Eng., 11, 415 (1961).
51. G. Birkhoff, "Positivity and criticality," "Nuclear Reactor Theory: Proceedings of Symposia in Applied Mathematics, Vol. XI," Am. Math. Soc., Providence (1961).
52. L. Schwartz, Théorie des distributions, Hermann, Paris (1966).



UNIVERSITY OF MICHIGAN



3 9015 03483 4138